73-3892

HIRANUMA, Hiroshi, 1939-
ANALYSIS OF RADIATION FROM A LINE SOURCE
USING THE TRANSMISSION MATRIX METHOD.

Iowa State University, Ph.D., 1972
Engineering, nuclear

Analysis of radiation from a line source using the transmission matrix method

by

Hiroshi Hiranuma

A Dissertation Submitted to the
Graduate Faculty in Partial Fulfillment of
The Requirements for the Degree of
DOCTOR OF PHILOSOPHY

Major: Nuclear Engineering

Approved:

Signature was redacted for privacy.

In Charge of Major Work

Signature was redacted for privacy.

For the Major Department

Signature was redacted for privacy.

For the Graduate College

Iowa State University
Ames, Iowa

1972

TABLE OF CONTENTS

LIST OF SYMBOLS

a_i = fraction of slab thickness to total

AUX = summation of power series of x^{-i}

b_i = coefficient of expansion of exp(- t)

B_j = buildup factor of functional of flux

$\underline{B}_{+i}^{-1}$ = matrix related to transmission operator matrix $\underline{T}_i$

C = coefficient of the Berger's form of a buildup factor

C_j = conversion constant

$\underline{C}_{+1}^{-1}$ = matrix related to transmission operator matrix $\underline{T}_i$

D = coefficient of the Berger's form of a buildup factor

$\underline{D}$ = diagonal matrix

E_n = error estimated by the Lanczos's method

$E_n(x)$ = nth order exponential integral

$F(x, \theta_o)$ = modified secant integral

$F(\underline{\Lambda}z)$ = matrix dependent on $\underline{\Lambda}z$

$f(x, \theta)$ = function of x and θ

$f^{(4)}(x, \theta)$ = fourth derivative of $f(x, \theta)$

$G(\theta^2)$ = function of θ^2

$G_1(\theta^2)$ = polynomial expansion of $\exp[-x(\frac{5}{24}\theta^4 + \frac{61}{720}\theta^6 + \frac{277}{8064}\theta^8 + \frac{50521}{3628800}\theta^{10} + \cdots)]$

$\overline{I}(x, \theta_o)$ = numerical integration value of function $F(x, \theta_o)$

$I_o(r, E)$ = differential energy spectrum

$\underline{K}$ = matrix

$K(r', r)$ = point kernel at r to a point source at r'

$\underline{K}_{n,1}(x)$ = point matrix kernel for n multi-layered slab

$K_p(\mu, r)$ = extended point kernel

L = length of a line source

$L(x)$ = function of x

$\underline{M}(r)$ = matrix of function of r

N = integer

$\underline{P}$ = matrix for similarity transformation

$Q_m(t)$ = mth order canonical polynomial function

$R(x)$ = function of x

$\underline{R}_i(x)$ = reflection operator matrix of layer i

$\underline{R}_{1,n}(x)$ = reflection operator matrix from layer 1 to layer n

$\underline{R}_\infty$ = infinite medium reflection operator matrix

r = spatial variable

r_i = vector position of ith region of shield

$\underline{S}$ = isotropic radiation source matrix

$S(r)$ = radiation source distribution

$\underline{T}_i(x)$ = transmission operator matrix of layer i

$\underline{T}_{n,1}(x)$ = transmission operator matrix for n multi-layered slab

$\underline{T}_\infty(x)$ = infinite medium transmission operator matrix

t = independent variable

$U(x)$ = function of x

$W(x)$ = function of x

w_i = weights of Gaussian quadrature

x = independent variable

$y_n(t)$ = nth order approximation to function y(t)

z = thickness of slab

z_i = zeros of Gaussian quadrature

$\Gamma(\mu_o r, E)$ = $4\pi r^2 \exp(\mu_o r) I_o(r, E)$

η_{max} = maximum possible error

θ = angle

θ_o = maximum value of angle θ

$\underline{\Lambda}_i$ = diagonal matrix related to transmission operator matrix $\underline{T}_i(x)$

Λ_{ij} = jth row diagonal element of matrix Λ_i

μ = linear attenuation coefficient

τ = constant determined by the tau method

$\phi(r)$ = response to a detector at spatial r

$\underline{\phi}_f(z)$ = flux at slab thickness z for finite medium

$\underline{\phi}_{f\infty}(z)$ = flux at slab thickness z for infinite reflection medium

$\phi_u(z)$ = uncollided flux at slab thickness z

$\phi_c(z)$ = collided flux at slab thickness z

I. INTRODUCTION

Since nuclear reactors are increasingly being constructed with a viewpoint from competitive economic consideration, optimum dimensions are also becoming more important for reactor shielding. The overdesigned radiation shields and hence overdimensioned reactor buildings can be reduced. However, since safety concern must be always a prime consideration in radiation shielding, this can only be accomplished if an accurate computing method of the external radiation is available. Therefore, one is required to search for new computing techniques which will satisfy more stringent requirements.

For shielding design purposes, the transmission of radiation through material layers must be rapidly, accurately and systematically determinable. For the construction of useful shields and for experiments with material layers, however, the transmitted and reflected radiation is of primary interest because only these are directly responsible for radiation damage outside shields, and they are relatively easily accessible to measurement.

The great advantage of the transmission matrix method consists of the fact that it contains a formulation of radiation transport which is particularly well adapted to the layer problem. Reactor shields consist of material layers of neutron and gamma-ray absorbers. A shielding calculation must establish the optimum sequence of the material layers and determine the necessary layer thicknesses.

The transmission matrix method is particularly attractive for this purpose. In a first computing cycle the integral intermediate

results are obtained in the form of the space independent matrices for all material layers in question. These intermediate data can be stored in the form either of cards, disk, or tape for digital computation.

Every desired layer combination can be then calculated from the intermediate data in a simple matrix operation in the following cycle. When the layer combination is changed, the entire calculation need not be started anew. The space independent matrices require only one determination.

The transmission and reflection operators can also be determined experimentally. In the formulation of radiation transport by means of the transmission and reflection operators it is possible to compare theory and experiments with intermediate data already calculated.

Thus, the transmission matrix method can become a useful engineering method, particularly because of their favorable characteristics for the construction of layer shields. This permits a sufficiently precise calculation of radiation shields without an extensive investment of experimental facilities.

It is also valuable if those intermediate results can be used for other source geometries. Recently, Rohach [34] has developed the concept of a point kernel from the transmission matrix for plane geometry. As originally developed, this transmission matrix method was applied for plane geometry problems. There are a lot of possibilities for application of the point matrix kernel for analyses of other geometries combining the extended point kernel method conception [18].

In this investigation the radiation from a line source is investigated. Little work on the line source radiation has been done because of the lack of suitable methods of attack. The extended point kernel method gives the analytical expression only for uncollided flux calculation, and can analyze the radiation with the aid of appropriate buildup factors only if they are available.

Thus, the purposes of this investigation are:

(1) to show availability of the point matrix kernel for line sources, and

(2) to analyze radiation from line sources including evaluation of a special secant integral which is called the modified secant integral.

II. LITERATURE REVIEW

There are several analytical methods of radiation attenuation.

As a result of modern computers, an enormous number of Monte Carlo programs have been developed. Basic principles of the Monte Carlo methods are available in a number of books and articles [7, 13, 21]. All these methods make use of the idea of "random walk", and the theory of probability. In order to obtain good statistical results very many trials are required and the computer economy is important.

Point kernel methods are also used for relatively simple calculations [4]. All extended sources of radiation may be considered to be composed of differential sources. The response of a detector due to any extended source results from superposition of point sources. This is the essence of the point kernel method. By response is meant the flux or some functional of the flux, such as dose rate, energy fluence or energy deposition. There are two distinct problems in point kernel methods. The first, and the most difficult is to find a suitable response point kernel. The second is the performance of the integration over the extended point sources.

The transport methods are one which are based on the integro-differential form of the linear, time-independent Boltzmann equation. The transport methods comprise the various methods of solutions. Some rigorous solutions of the one-velocity transport problems are treated in Refs. [6, 23, 39]. The moment method [8, 13, 16, 19] is usually considered as one of a few rigorous methods for the solution. A direct numerical integration is also used [33]. Among other numerical

solution methods the special harmonics expansion [12, 13, 28, 31, 39] and the discrete ordinate method, in particular S_n approximation [5] are suited for use on high speed digital computers. The invariant imbedding method [2, 10, 23, 26, 29] is also applied to solve transport problems.

A unique approach to the solution of the radiation problems is the transmission matrix method. Peebles and Plesset [32] computed the transmission operator for thin slab by order of scattering, doing the spatial integrations analytically and angle-energy integrations numerically. A second approach, in which transmission and reflection operators for a thin slab were computed by Monte Carlo method, has been developed by Kataoka [22]. Aronson, Yarmush and Zell [1, 40] have proceeded from a formal solution of the transport equation for the transmission matrix as a function of slab thickness. Maute [27] also calculated the transmission and reflection operators with polynomial expansion for the transmission operator starting from the transport equation, and obtained the results for the gamma rays from plane geometry up to 8 mean free path (mfp) slab thickness. Rohach [34] recently developed the point matrix kernel based on Ref. [1, 40] and applied it for the point source analysis.

None of the methods above mentioned except the extended point kernel method have been applied for the line source analyses. The extended point kernel method is also limited only for simple analyses because of the nature of the point kernel.

III. GENERAL THEORY

A. Point Kernel Method

All extended sources of radiation may be considered to be composed of differential point sources. The response of a detector from any extended radiation sources may be obtained by summing or integrating the responses from the point sources of which the extended source consists. This is the essence of the point kernel method [4, 18]. Symbolically,

$$\phi(r) = \int S(r')K(r', r)dr', \tag{1}$$

where $\phi(r)$ is the response of a point isotropic detector at spatial point r. By the response is meant the flux or some functional of the flux, such as the biological dose rate, the energy fluence or the energy deposition rate. $S(r')dr'$ is the source strength, measured in particles per unit time, in the spatial element dr' about r'. The differential element dr' is either an increment of length, area or volume depending on the source geometry. The dimension of $S(r')$ is either particles per unit length, area or volume, per unit time.

$K(r', r)$ is the response of a detector at r to a unit point source located at r'. This point response kernel depends on the type of particles, their energy, and the composition of materials between the source and the detector. The point kernel is usually assumed to depend on the material composition of the regions in the direct path between the point source and the detector point, but not on the composition off the direct path. This assumption may not be

good for the case of the predominant scattering in the medium unless the point kernel has a character to take care of this consideration.

In photon attenuation analyses the contribution of scattered radiation to the functional ϕ_j is accounted for, at least formally, by multiplying the uncollided point kernel by an appropriate buildup factor B_j, where the uncollided flux means the flux of particles which traverses the path between the source and the detector points without suffering any interaction, either scattering or absorption

$$\phi_j = \frac{C_j B_j}{4\pi x^2} \exp(-\sum_i \mu_i x_i) \tag{2}$$

where

C_j = the constant which converts the uncollided number of the flux to the functional ϕ_j

μ_i = total macroscopic cross section of the ith attenuating medium

x_i = thickness of the ith medium along the path between the source and the detector points

x = total thickness along the path between the source and detector points.

$\phi_j(r)$ is obtained by integrating Eq. (2) over the extended sources and over the energy of the emitted photons (Fig. 1).

$$\phi_j(r) = \int_r \int_E \frac{S(r', E) C_j(E) B_j(E, \mu_i(E)) |r_i - r_{i+1}|}{4\pi |r_n - r'|^2} \exp(-\sum_i \mu_i(E) |r_i - r_{i+1}|) dr' dE. \tag{3}$$

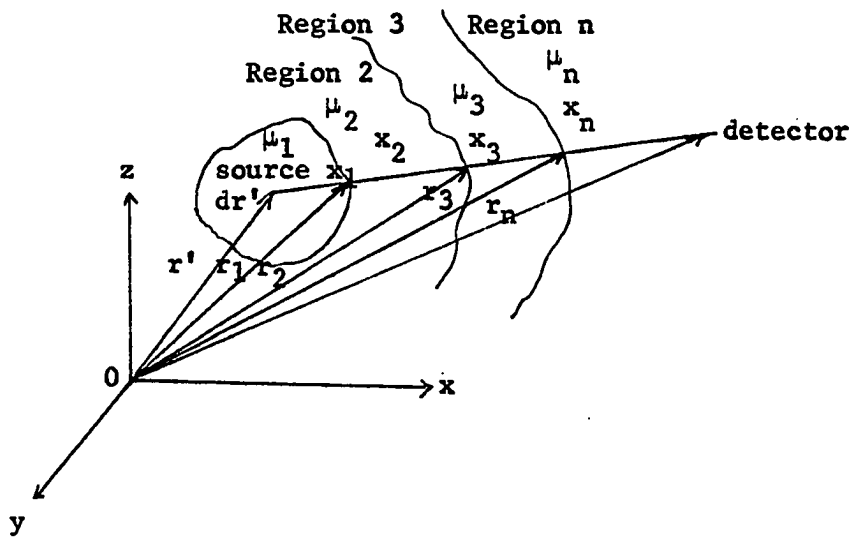

Fig. 1. Integration of point kernel over extended source.

$S(r', E)dr'dE$ is the number of photons emitted per unit time in the spatial range dr' about r' and in the energy range dE about E. r_i is the vector position of the ith region boundary along the path between the source and detector, r' is a variable in the integration, and r_n is the vector position of the detector.

Outside of the mathematical difficulty of the integration, the ordinary point kernel is limited to calculation of the total effects of the uncollided flux and collided flux because buildup factors for layered shields have not been extensively developed. When one can use a point kernel which is able to take care of the uncollided flux, the buildup factor method can be more extensively used.

B. Point Matrix Kernels

Rohach [34] developed a point matrix kernel from the transmission matrix under the condition that a source vector is isotropic and uniform

$$\underline{K}(x) = -\frac{1}{2\pi x}\underline{T}'(x), \tag{4}$$

where

$\underline{K}(x)$ = point matrix kernel at a distance x from a point source

$\underline{T}'(x)$ = derivative of the transmission operator matrix for a plane source at a distance x

x = distance between a differential point source and a detector point.

For a single layer the transmission operator matrix, $\underline{T}(x)$ and the reflection operator matrix $\underline{R}(x)$ are given by the following asymptotic forms [34]:

$$\underline{T}_{\infty}(x) = 4\underline{C}_{+}^{-1}\exp(-\underline{\Lambda}x)\underline{B}_{+}^{-1} \tag{5}$$

and

$$\underline{R}_{\infty}(x) = \underline{B}_{-}\underline{B}_{+}^{-1} \tag{6}$$

where $\underline{C}_{+}^{-1}$, $\underline{B}_{+}^{-1}$, $\underline{B}_{-}$ and $\underline{\Lambda}$ are matrices independent of distance x.

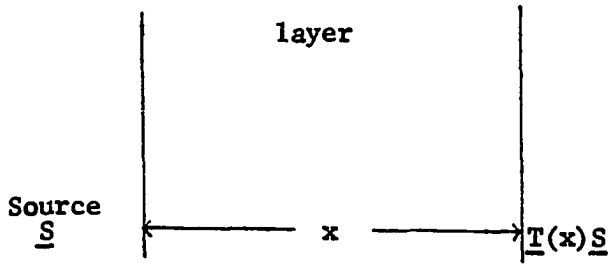

Fig. 2. A single layered slab.

One can consider a transmission operator matrix, $\underline{T}_{n,1}(x)$ for multi-layered slab. For a two-layered slab

$$\underline{T}_{2,1}(x) = \underline{T}_2(a_2x)[\underline{I} - \underline{R}_1(a_1x)\underline{R}_2(a_2x)]^{-1}\underline{T}_1(a_1x) \tag{7}$$

where

$\underline{T}_{2,1}(x)$ = transmission operator matrix through layer 1 and layer 2

$\underline{T}_1(x)$ = transmission operator matrix through layer 1

$\underline{T}_2(x)$ = transmission operator matrix through layer 2

$\underline{R}_1(x)$ = reflection operator matrix from layer 1

$\underline{R}_2(x)$ = reflection operator matrix from layer 2

a_1 and a_2 = fractions of thicknesses of layer 1 and layer 2 respectively.

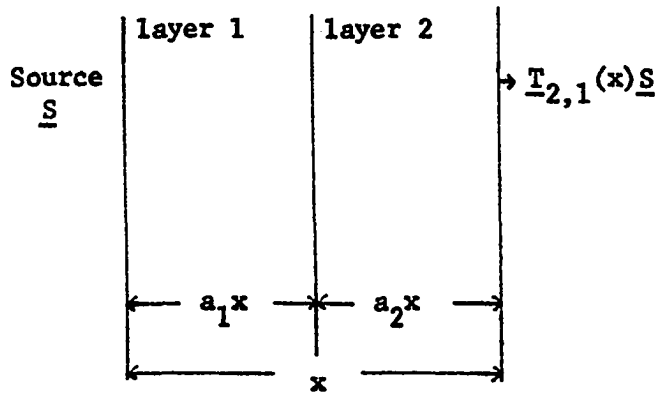

Fig. 3. Two-layered slab $a_1 + a_2 = 1.0$.

For a two-layered slab the point matrix kernel, $\underline{K}_{2,1}(x)$ becomes

$$\begin{aligned}
\underline{K}_{2,1}(x) &= -\frac{1}{2\pi x}\,\underline{T}'_{2,1}(x) \\
&= -\frac{1}{2\pi x}\frac{d}{dx}\left\{\underline{T}_2(a_2x)[\underline{I} - \underline{R}_1(a_1x)\underline{R}_2(a_2x)]^{-1}\underline{T}_1(a_1x)\right\} \\
&= -\frac{1}{2\pi x}\left\{\underline{T}'_2(a_2x)[\underline{I} - \underline{R}_1(a_1x)\underline{R}_2(a_2x)]^{-1}\underline{T}_1(a_1x)\right. \\
&\quad + \underline{T}_2(a_2x)[\underline{I} - \underline{R}_1(a_1x)\underline{R}_2(a_2x)]^{-1}\underline{T}'_1(a_1x) \\
&\quad \left. + \underline{T}_2(a_2x)([\underline{I} - \underline{R}_1(a_1x)\underline{R}_2(a_2x)]^{-1})'\underline{T}_1(a_1x)\right\} \qquad (8)
\end{aligned}$$

where it has been assumed that this operation will only operate on an isotropic source vector. For n multi-layered slab, the transmission operator matrix becomes

$$\begin{aligned}
&\underline{T}_{n,1}(a_1, a_2, \ldots a_n, x) \\
&\quad = \underline{T}_n(a_nx)[\underline{I} - \underline{R}_{1,n-1}(a_1, a_2, \ldots a_{n-1}, x)\underline{R}_n(a_nx)] \\
&\quad \underline{T}_{n-1,1}(a_1, a_2, \ldots a_{n-1}, x) \qquad (9)
\end{aligned}$$

where

$\underline{T}_{n,1}(a_1, a_2, \ldots a_n, x)$ = transmission operator matrix through layer 1 to layer n

$\underline{T}_{n-1,1}(a_1, a_2, \ldots a_{n-1}, x)$ = transmission operator matrix through layer 1 to layer n - 1

$\underline{T}_n(a_n x)$ = transmission operator matrix solely through layer n

$\underline{R}_{1,n-1}(a_1, a_2, \ldots a_n, x)$ = reflection operator matrix from layer 1 to layer n - 1

$\underline{R}_n(a_n x)$ = reflection operator matrix solely from layer n

x = total thickness of slab

a_i = fraction of thickness of layer i to total thickness, x

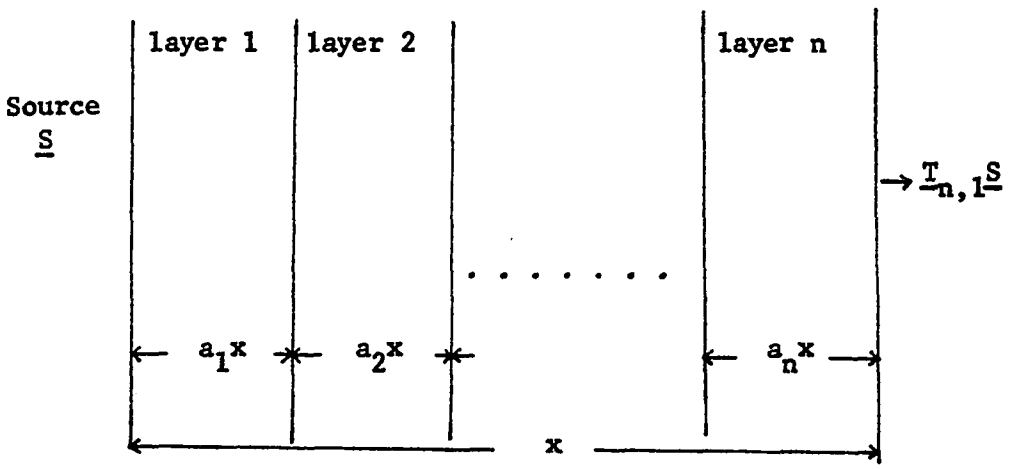

Fig. 4. n multi-layered slab.

Under the condition that a source vector is isotropic and uniform using the asymptotic forms of the transmission and reflection operator matrices, one has:

for a single-layered slab from Eqs. (4), (5) and (6)

$$\underline{K}(x) = \frac{4}{2\pi x} \underline{C}_{+}^{-1} \underline{\Lambda} \exp(-\underline{\Lambda} x) \underline{B}_{+}^{-1} \tag{10}$$

for a two-layered slab neglecting the double reflection term in Eq. (8)

$$\underline{K}_{2,1}(x) = \frac{16}{2\pi x} \underline{C}_{+2}^{-1} \exp(-\underline{\Lambda}_2' x)[\underline{\Lambda}_2' \underline{B}_{+2}^{-1} \underline{C}_{+1}^{-1} + \underline{B}_{+2}^{-1} \underline{C}_{+1}^{-1} \underline{\Lambda}_1'] \exp(-\underline{\Lambda}_1' x) \underline{B}_{+1}^{-1} \tag{11}$$

where subscripts indicate layer identifications,

$$\underline{\Lambda}_1' = a_1 \underline{\Lambda}_1$$

$$\underline{\Lambda}_2' = a_2 \underline{\Lambda}_2 ,$$

and only exponential terms are functions of x and other are independent of x. The assumption of negligence of the double reflection may not be too bad for gamma ray analysis especially if one of materials of a slab has a high atomic number with a large photoelectric cross section.

One can also obtain an expression of the point matrix kernel for n multi-layered slab. In Eq. (9) the double reflection terms are neglected, then Eq. (9) becomes

$$\underline{T}_{n,1}(a_1, a_2, \ldots a_n, x) = \underline{T}_n(a_n x) \underline{T}_{n-1}(a_{n-1} x) \ldots\ldots \underline{T}_2(a_2 x) \underline{T}_1(a_1 x) \tag{12}$$

The differentiation of Eq. (12) results in

$$\underline{T}'_{n,1}(a_1, a_2, \ldots a_n, x) = \underline{T}'_n(a_n x)\underline{T}_{n-1}(a_{n-1}x) \ldots \underline{T}_2(a_2 x)\underline{T}_1(a_1 x)$$

$$+ \underline{T}_n(a_n x)\underline{T}'_{n-1}(a_{n-1}x) \ldots \underline{T}_2(a_2 x)\underline{T}_1(a_1 x)$$

$$\ldots\ldots\ldots\ldots\ldots$$

$$\ldots\ldots\ldots\ldots\ldots$$

$$+ \underline{T}_n(a_n x) \ldots\ldots\ldots \underline{T}_2(a_2 x)\underline{T}'_1(a_1 x)$$

$$= \sum_{i=0}^{n-1} \underline{T}_n(a_n x) \ldots \frac{d}{dx}\left\{\underline{T}_{n-i}(a_{n-i}x)\right\} \ldots\ldots$$

$$\underline{T}_1(a_1 x). \qquad (13)$$

Substituting the asymptotic transmission functions one has

$$\underline{T}'_{n,1}(x) = \frac{-4^n}{2\pi x}\sum_{i=0}^{n-1} \left\{\underline{C}_{+n}^{-1} \exp(-\underline{\Lambda}'_n x)\underline{B}_{+n}^{-1}\underline{C}_{+n-1}^{-1} \exp(-\underline{\Lambda}'_{n-1}x) \ldots\right.$$

$$\ldots \underline{C}_{+n-i}^{-1}\left[\frac{d}{dx}\exp(-\underline{\Lambda}'_{n-i}x)\right]\underline{B}_{+n-i}^{-1} \ldots$$

$$\left.\ldots \underline{C}_{+1}^{-1} \exp(-\underline{\Lambda}'_1 x)\underline{B}_{+1}^{-1}\right\}, \qquad (14)$$

where

$$\underline{\Lambda}'_i = a_i\underline{\Lambda}_i .$$

The point matrix kernel for n multi-layered slab becomes

$$\underline{K}_{n,1}(x) = -\frac{4^n}{2\pi x}\sum_{i=0}^{n-1} \left\{\underline{C}_{+n}^{-1} \exp(-\underline{\Lambda}'_n x)\underline{B}_{+n}^{-1} \ldots\right.$$

$$\ldots \underline{C}_{+n-1}^{-1}\left[\frac{d}{dx}\exp(-\underline{\Lambda}'_{n-i}x)\right]\underline{B}_{+n-i}^{-1} \ldots$$

$$\left.\ldots \underline{C}_{+1}^{-1} \exp(-\underline{\Lambda}'_1 x)\underline{B}_{+1}^{-1}\right\} \qquad (15)$$

As a result of the negligence of double reflections for multi-layered slab, the point matrix kernel may have tendency to underestimate collided flux densities to some extent depending on magnitudes of reflections.

C. Formulation of Line Source Analysis

Combining the extended point kernel conception to the point matrix kernel one will be able to analyze radiation from a line source.

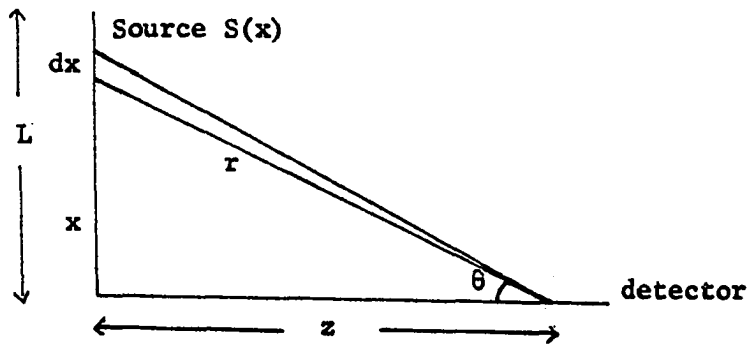

Fig. 5. Radiation from line source.

The flux or functional, $\phi_f(z)$ from a line source is given by

$$\phi_f(z) = \int_0^L K(r)S(x)dx, \tag{16}$$

where

$K(r)$ = a point kernel

$S(x)$ = a distribution of line source along the edge of the slab at $z = 0$

L = length of line source

z = thickness of the slab

r = distance between differential length dx and detector point.

1. One homogeneous layer

If one considers the uniformly distributed isotropic line source and a homogeneous slab material, then the point matrix kernel is

$$\underline{K}(r) = -\frac{1}{2\pi r}\,\underline{T}'(r)$$

$$\doteq \frac{4}{2\pi}\,\underline{C}_+^{-1}\underline{\Lambda}\,\exp(-\underline{\Lambda}r)/r\;\underline{B}_+^{-1} \tag{17}$$

and a source vector is

$$\underline{S}(s) = \underline{S}. \tag{18}$$

Substituting Eqs. (17) and (18) for Eq. (16), one obtains

$$\phi_{\underline{f}}(z) = \int_0^L \frac{4}{2\pi}\,\underline{C}_+^{-1}\underline{\Lambda}\,\exp(-\underline{\Lambda}r)/r\;\underline{B}_+^{-1}\underline{S}dx$$

$$= \frac{4}{2\pi z}\,\underline{C}_+^{-1}\underline{\Lambda}z\int_0^{\theta_1} \sec\theta\,\exp(-\underline{\Lambda}z\sec\theta)d\theta\;\underline{B}_+^{-1}\underline{S} \tag{19}$$

where

$$\theta = \arctan\,(L/z)$$

$$r = z\sec\theta$$

$$dx = z\sec^2\theta\,d\theta.$$

If one considers an infinite medium reflection for both source and boundary [34], Eq. (19) becomes

$$\phi_{\underline{f}\infty}(z) = \frac{4}{2\pi z}\,(\underline{I} - \underline{R}_\infty)^{-1}\underline{C}_+^{-1}\underline{\Lambda}z\int_0^{\theta_1} \sec\theta\,\exp(-\underline{\Lambda}z\sec\theta)d\theta\,\underline{B}_+^{-1}(\underline{I} - \underline{R}_\infty)^{-1}\underline{S} \tag{20}$$

where $\int_0^{\theta_1} \sec\theta\,\exp(-y\sec\theta)d\theta$ has been defined as the modified secant integral.

2. Two layered slab

Now consider a two layered slab (Fig. 6).

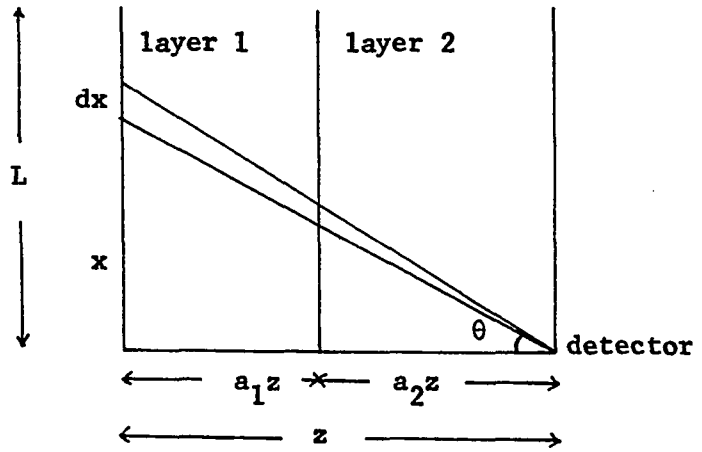

Fig. 6. Two layered slab.

The asymptotic point matrix kernel with negligence of the double reflection term is obtained from Eq. (11).

$$\underline{K}_{2,1}(r) = -\frac{1}{2\pi r}\,\underline{T}'_{2,1}(r)$$

$$= \frac{16}{2\pi r}\,\underline{C}_{+2}^{-1}\exp(-\underline{\Lambda}'_2 r)[\underline{\Lambda}'_2\underline{B}_{+2}^{-1}\underline{C}_{+1}^{-1} + \underline{B}_{+2}^{-1}\underline{C}_{+1}^{-1}\underline{\Lambda}'_1]\exp(-\underline{\Lambda}'_1 r)\underline{B}_{+1}^{-1} \tag{21}$$

where

$$\underline{\Lambda}'_1 = a_1\underline{\Lambda}_1$$

$$\underline{\Lambda}'_2 = a_2\underline{\Lambda}_2 \ .$$

Substituting Eq. (21) in Eq. (16), one obtains

$$\underline{\phi}_{21f}(z) = \frac{16}{2\pi}\,\underline{C}_{+2}^{-1}\int_0^{\theta_1}\sec\theta[F(\underline{\Lambda}z)]d\theta\,\underline{B}_{+1}^{-1}\underline{S}, \tag{22}$$

where

$$[F(\underline{\Lambda}z)] =$$

$$\begin{bmatrix} a_{11}\exp(-\Lambda'_{21}-\Lambda'_{11})z\sec\theta & a_{12}\exp(-\Lambda'_{21}-\Lambda'_{12})z\sec\theta & \cdots & a_{1n}\exp(-\Lambda'_{21}-\Lambda'_{1n})z\sec\theta \\ a_{21}\exp(-\Lambda'_{22}-\Lambda'_{11})z\sec\theta & \cdots & & \vdots \\ \vdots & & & \vdots \\ a_{n1}\exp(-\Lambda'_{2n}-\Lambda'_{11})z\sec\theta & \cdots & & a_{nn}\exp(-\Lambda'_{2n}-\Lambda'_{1n})z\sec\theta \end{bmatrix}$$

$$a_{ij} = a'_{ij} + a''_{ij}$$

$$\Lambda'_{1k} = a\Lambda$$

where a is the fraction of each layer, subscript 1 or 2 indicates layer 1 or 2, subscript k indicates the diagonal element of kth row of diagonal matrix, $\underline{\Lambda}$. a'_{ij} and a''_{ij} are elements of ith row and jth column of the matrices, $[\underline{\Lambda}'_2\underline{B}^{-1}_{+2}\underline{C}^{-1}_{+1}]$ and $[\underline{B}^{-1}_{+2}\underline{C}^{-1}_{+1}\underline{\Lambda}'_1]$ respectively. If infinite medium reflections are considered, then the same idea of source and boundary backing as a single layer can be applied and Eq. (22) becomes

$$\underline{\phi}_{21f\infty}(z) = \frac{16}{2\pi}(\underline{I} - \underline{R}'_\infty)^{-1}\underline{C}^{-1}_{+2}\int_0^{\theta_1}\sec\theta[F(\underline{\Lambda}z)]d\theta\,\underline{B}^{-1}_{+1}(\underline{I} - \underline{R}''_\infty)^{-1}\underline{S} \tag{23}$$

where R'_∞ is the reflection from boundary side and R''_∞ is the reflection for source side.

Consider

$$\exp(-\underline{\Lambda}_2' r)[\underline{\Lambda}_2' \underline{B}_{+2}^{-1} \underline{C}_{+1}^{-1} + \underline{B}_{+2}^{-1} \underline{C}_{+1}^{-1} \underline{\Lambda}_1'] \exp(-\underline{\Lambda}_1' r) \tag{24}$$

where $\underline{\Lambda}_1'$ and $\underline{\Lambda}_2'$ are diagonal matrices.

If one can use the array multiplication rule that multiplication should be made only between two entries which are located at the same position in their arrays and that the product should be stored as the entry at the same position of a new array or a matrix, then Eq. (24) becomes

$$([BC])_{array} \times ([\exp(-\underline{\Lambda}_2' r)]_{col} [\exp(-\underline{\Lambda}_1' r)]_{row})_{array} \tag{25}$$

where

$$[BC] = [\underline{\Lambda}_2' \underline{B}_{+2}^{-1} \underline{C}_{+2}^{-1} + \underline{B}_{+2}^{-1} \underline{C}_{+1}^{-1} \underline{\Lambda}_1']$$

$[\exp(-\underline{\Lambda}_2' r)]_{col}$ = a column vector matrix which has entries of diagonal entries of $\exp(-\underline{\Lambda}_2' r)$

$[\exp(-\underline{\Lambda}_1' r)]_{row}$ = a row vector matrix which has entries of diagonal entries of $\exp(-\underline{\Lambda}_1' r)$.

In the second array of Eq. (25), one can write

$$[\exp(-\underline{\Lambda}_2' r)]_{col} [\exp(-\underline{\Lambda}_1' r)]_{row} = \exp(-\underline{K} r) = \underline{M}(r), \tag{26}$$

where

$$\underline{K} = \begin{bmatrix} \Lambda_{21}' + \Lambda_{11}' & \Lambda_{21}' + \Lambda_{12}' & \cdots & \Lambda_{21}' + \Lambda_{1n}' \\ \Lambda_{22}' + \Lambda_{11}' & \Lambda_{22}' + \Lambda_{12}' & \cdots & \cdots \\ \vdots & & & \cdots \\ \Lambda_{2n}' + \Lambda_{11}' & \cdots & \cdots & \Lambda_{2n}' + \Lambda_{1n}' \end{bmatrix} \tag{27}$$

which is independent of r.

It is convenient if the matrix, $\underline{M}(r)$ is diagonalized. In this procedure one defines a similarity transformation $\underline{P}$ on $\underline{M}(r)$ that diagonalizes $\underline{M}(r)$. Therefore,

$$\underline{PM}(r)\underline{P}^{-1} = \underline{P}\left\{\exp\ (-\ \underline{K}r)\right\}\underline{P}^{-1} = \exp(-\ \underline{PKP}^{-1})r \tag{28}$$

or

$$\underline{M}(r) = \underline{P}^{-1}\left\{\exp(-\ \underline{PKP}^{-1})r\right\}\underline{P} \tag{29}$$

It can be seen that one needs only to diagonalize $\underline{K}$, a matrix independent of r. Therefore

$$\int_0^{\theta_1} \sec\theta\ \exp(-\ \underline{\Lambda}_2' z \sec\theta)[BC]\exp(-\ \underline{\Lambda}_1' z \sec\theta)d\theta$$

$$= ([BC])_{array} \times \left(\underline{P}^{-1}\int_0^{\theta_1} \sec\theta\ \exp(-\ \underline{D}z \sec\theta)d\theta\ \underline{P}\right)_{array} \tag{30}$$

where

$$\underline{D} = \underline{PKP}^{-1} \text{ (diagonal matrix).}$$

One can now define Eq. (30) as a matrix, $\underline{G}$ and obtain the expression of the flux from the line source where photons pass through a two layered slab.

$$\underline{\phi}_{21f}(z) = \frac{16}{2\pi}\ \underline{C}_{+2}^{-1}\underline{GB}_{+1}^{-1}\underline{S}. \tag{31}$$

For an infinite medium reflection one has

$$\underline{\phi}_{21f\infty}(z) = \frac{16}{2\pi}\ (\underline{I} - \underline{R}_{2\infty})^{-1}\underline{C}_{+2}^{-1}\underline{GB}_{+1}^{-1}(\underline{I} - \underline{R}_{1\infty})^{-1}\underline{S}. \tag{32}$$

By diagonalization of the matrix, $\underline{K}$, one can reduce the number of the integration of the modified secant integral by factor N which is the size of the square matrix of $\underline{\Lambda}$.

3. N multi-layered slab

One can consider a general, n multi-layered slab. The point matrix kernel with asymptotic form and with negligence of the double reflection terms is

$$\underline{K}_{n,1}(r) = -\frac{1}{2\pi r}\underline{T}'_{n,1}(r)$$

$$\doteq -\frac{4^n}{2\pi r}\sum_{i=1}^{n-1} \underline{C}_{+n}^{-1}\exp(-\underline{\Lambda}'_n r)\underline{B}_{+n}^{-1}\cdots\cdot\underline{C}_{+i}^{-1}\frac{d}{dr}[\exp(-\underline{\Lambda}'_i r)]$$

$$\cdots\underline{C}_{+1}^{-1}\exp(-\underline{\Lambda}'_1 r)\underline{B}_{+1}^{-1} \tag{33}$$

where

$$\underline{\Lambda}'_i = a_i\underline{\Lambda}_i \ .$$

Thus, one obtains

$$\underline{\phi}_{n1f}(z) = \int_0^{\theta_1}\underline{K}_{n,1}(z,\ \theta)z\ \sec^2\theta d\theta\ \underline{S}. \tag{34}$$

IV. EVALUATION OF THE MODIFIED SECANT INTEGRAL

A. Numerical Integration of the Modified Secant Integral by Use of Gaussian Quadrature

In order to calculate the radiation from a line source one needs to evaluate the modified secant integral,

$$F(x, \theta_o) = \int_0^{\theta_o} \sec\theta \exp(-x \sec\theta) d\theta. \tag{35}$$

In recent years Gaussian quadrature has been recognized as a useful numerical integration technique in computer calculations. Gaussian rules are simple and economical since a N-point integration formula is exact for polynomials up to degree 2N - 1. However, it is rather difficult to check the errors as a result of the application of the method.

The order N approximation of $F(x, \theta_o)$ by Gaussian quadrature is given [24]

$$\bar{I}(x, \theta_o) = \frac{b - a}{2} \sum_{i=1}^{N} w_i f(x, \theta_i) \tag{36}$$

where

$$f(x, \theta) = \sec\theta \exp(-x \sec\theta)$$

$$\theta_i = [(b - a)z_i + (b + a)]/2$$

$$b = \theta_o$$

$$a = 0$$

where z_i's are the zeros of the order N Gaussian quadrature and w_i's are the associated weights.

The error E_n of the Nth order approximation can be calculated from the formula [24]

$$E_n = \frac{1}{2N+1}\left\{\frac{b-a}{2}\left[f(x, 0) + f(x, \theta_o)\right] - \bar{I}(x, \theta_o) - \left(\frac{b-a}{2}\right)^2 \sum_{i=1}^{N} w_i z_i f'(x, \theta_i)\right\} \tag{37}$$

where

$$f'(x, \theta) = \tan\theta(1 - x\sec\theta)f(x, \theta).$$

B. Asymptotic Approximation to the Modified Secant Integral

In order to check the results of the application of Gaussian quadrature, one can use asymptotic approximations. Divide the integral range into two parts

$$F(x, \theta_o) = \int_0^{\theta_o} f(x, \theta)d\theta$$

$$= \int_0^{\theta_1} \sec\theta \exp(-x\sec\theta)d\theta + \int_{\theta_1}^{\theta_o} \sec\theta \exp(-x\sec\theta)d\theta$$

$$0 < \theta_1 < \theta_o . \tag{38}$$

For the special case $x = 0$

$$F(x, \theta_o) = \int_0^{\theta_o} \sec\theta\, d\theta = \log_e(\sec\theta_o + \tan\theta_o). \tag{39}$$

For the first integral in Eq. (38) one can use the polynomial expansion for $\exp(-x\sec\theta)$

$$\exp(-x\sec\theta) = \sum_{i=0}^{\infty} (-1)^i \frac{x^i}{i!} (\sec\theta)^i . \tag{40}$$

Then,

$$\int_0^{\theta_1} \sec\theta \exp(-x\sec\theta)\,d\theta = \sum_{i=0}^{\infty} (-1)^i \frac{x^i}{i!} \int_0^{\theta_1} (\sec\theta)^{i+1} d\theta$$

$$= \sin\theta_1 \left\{ \sum_{i=0}^{\infty} \frac{x^{2i}}{(2i)!} \left(\frac{1}{2i} \sec^{2i}\theta_1 + \frac{2i-1}{2i(2i-2)} \sec^{2i-1}\theta_1 + \cdots \right.\right.$$

$$\cdots + \frac{(2i-1)(2i-3)\cdots 5.3}{2i(2i-2)\cdots\cdots\cdots 4.2} [\sec^2\theta_1$$

$$\left. + \frac{1}{\sin\theta_1} \log_e(\sec\theta_1 + \tan\theta_1)] \right)$$

$$- \sum_{i=1}^{\infty} \frac{x^{2i-1}}{(2i-1)!} \left(\frac{1}{2i-1} \sec^{2i-1}\theta_1 + \frac{2i-2}{(2i-1)(2i-3)} \sec^{2i-3}\theta_1 + \cdots \right.$$

$$\left.\left. + \frac{(2i-2)(2i-4)\cdots 4\cdot 2}{(2i-1)(2i-3)\cdots\cdots\cdots 5.3} \sec\theta_1 \right) \right\}, \qquad (41)$$

where any term is zero if any numerator or denominator of any term is not positive, and the coefficient of the term of $\log_e(\sec\theta_1 + \tan\theta_1)$ should be the same as the coefficient of the term of $(\sec^2\theta_1)$ with the exception that the coefficient is 1.0 at $i = 0$. For large x Eq. (41) is slowly convergent, therefore one can use the following expansion:

$$\sec\theta \exp(-x\sec\theta) = \exp(-x)\exp(-x\theta^2/2)G(\theta^2) \qquad (42)$$

where

$$\sec\theta = 1 + \frac{1}{2}\theta^2 + \frac{5}{24}\theta^4 + \frac{61}{720}\theta^6 + \cdots\cdots \qquad [14]$$

$$\exp(-x\sec\theta) = \exp[(-x)(1 + \frac{1}{2}\theta^2 + \frac{5}{24}\theta^4 + \frac{61}{720}\theta^6 + \cdots)]$$

$$= \exp(-x)\exp(-x\theta^2/2)\exp[(-x)(\frac{5}{24}\theta^4 + \frac{61}{720}\theta^6 + \cdots)]$$

$$= \exp(-x)\exp(-x\theta^2/2)G_1(\theta^2)$$

$$G(\theta^2) = G_1(\theta^2)(1 + \frac{1}{2}\theta^2 + \frac{5}{24}\theta^4 + \cdots)$$

$$G_1(\theta^2) = \text{polynomial expansion of } \exp[(-x)(\frac{5}{24}\theta^4 + \frac{61}{720}\theta^6 + \cdots)]$$

Then,

$$F(x, \theta_1) = \exp(-x)\int_0^{\theta_1} \exp(-x\theta^2/2)G(\theta^2)d\theta. \tag{43}$$

One can easily treat the second integral of Eq. (38). Let $u = \sec\theta$, then

$$\int_{\theta_1}^{\theta_o} \sec\theta \exp(-x\sec\theta)d\theta = \int_{u_1}^{u_o} \frac{\exp(-xu)}{u\sqrt{1-u^{-2}}}du$$

$$= \int_{u_1}^{\infty} \frac{\exp(-xu)}{u\sqrt{1-u^{-2}}}du - \int_{u_o}^{\infty} \frac{\exp(-xu)}{u\sqrt{1-u^{-2}}}du$$

$$= E_1(xu_1) - E_1(xu_o) + \frac{1}{2u_1^2}E_3(xu_1) - \frac{1}{2u_o^2}E_3(xu_o) + \cdots$$

$$+ \frac{1\cdot 3\cdot \cdots (2n-1)}{2\cdot 4 \cdots 2n}(E_{2n+1}(xu_1)/u_1^{2n} - E_{2n+1}(xu_o)/u_o^{2n}) + \cdots \tag{44}$$

where

$$u_1 = \sec\theta_1$$

$$u_o = \sec\theta_o$$

$$E_n(xu) = u^{n-1}\int_u^{\infty} t^{-n}\exp(-xt)dt,$$

where $E_n(xu)$ is nth order exponential integral [4],

$$\left(u\sqrt{1-u^{-2}}\right)^{-1} = u^{-1} + \frac{1}{2}u^{-3} + \frac{3}{2.4}u^{-5} + \cdots\cdots .$$

In particular for $\theta_o = \pi/2$

$$\int_{\theta_1}^{\pi/2} \sec\theta \exp(-x\sec\theta)\,d\theta = E_1(xu_1) + \sum_{n=1}^{\infty} \left\{ \prod_{i=1}^{n} \left(\frac{2i-1}{2i}\right) \right\} E_{2n+1}(xu_1)/u_1^{2n} . \tag{45}$$

since

$$E_{2n+1}(xu_o) = 0 \text{ as } u_o = \infty.$$

1. Approximation of exp(- t)

In order to take only a few polynomial terms for approximation of exp(- t) one can derive a suitable polynomial expansion formula.

Consider the differential equation

$$y'(t) + y(t) = 0 \tag{46}$$

with $y(0) = 1$,

so that $y(t) = \exp(-t)$.

One can find the canonical polynomials (definition can be found on page 70 in Ref. [24]) for Eq. (46)

$$Q_o(t) = 1$$

$$Q_1(t) = (-1)1!(1-t)$$

$$Q_2(t) = (-1)^2 2!(1 - t + t^2/2)$$

$$\vdots$$

$$Q_m(t) = (-1)^m m! \sum_{i=0}^{m} (-1)^i t^i/i!. \tag{47}$$

Using Eq. (47) one can write the nth order polynomial approximation to y(t)

$$y_n(t) = \tau \sum_{m=0}^{n} C_n^m Q_m(t) \tag{48}$$

when

$y_n(t)$ = nth order approximation to $y(t)$

C_n^m = coefficient of the mth polynomial of the nth shifted Chebyshev polynomials, T_n^* [24].

τ is given by the condition, $y(0) = 1$

$$\tau = \left\{ \sum_{m=0}^{n} C_n^m Q_m(0) \right\}^{-1} . \tag{49}$$

and the maximum possible error η_{max} is estimated by [24]

$$|\eta_{max}| = \tau/\sqrt{4n^2 + 1} . \tag{50}$$

2. Evaluation of the integral $\int_0^x t^n \exp(-t^2)dt$

In order to calculate Eq. (43) one needs to evaluate the integral

$$L(x) = \int_0^x t^n \exp(-t^2)dt. \tag{51}$$

where n is zero or a positive integer.

One can differentiate both sides of Eq. (51), with respect to x and obtain

$$L'(x) = x^n \exp(-x^2) \tag{52}$$

Now assume a solution such that

$$L(x) = x^n \exp(-x^2)u(x), \tag{53}$$

where

$$u(x) = \sum_{m=1}^{\infty} a_{2m-1} x^{2m-1} \tag{54}$$

which satisfies with condition, $L(0) = 0$.

Therefore a differential equation is obtained from Eqs. (52) and (53)

$$xu'(x) + (n - 2x^2)u(x) = x \tag{55}$$

Substituting Eq. (54) into Eq. (55) results in

$$\sum_{m=1}^{\infty} \left\{(2m + n - 1)a_{2m-1}x^{2m-1} - 2a_{2m-1}x^{2m+1}\right\} = x. \tag{56}$$

Comparing the coefficients on both sides one obtains

$$a_1 = \frac{1}{n+1} = \frac{1}{2}\frac{2}{n+1}$$

and

$$a_{2m-1} = \frac{2}{2m + n - 1} a_{2m-3}$$

$$= \frac{1}{2} \prod_{i=1}^{m} \left(\frac{2}{2i + n - 1}\right). \tag{57}$$

Therefore the solution to $L(x)$ is

$$\int_0^x t^n \exp(-t^2)dt = \frac{1}{2} x^{n+1} \exp(-x^2) \sum_{m=1}^{\infty} \left\{\prod_{i=1}^{m} \left(\frac{2}{2i+n-1}\right)\right\} x^{2(m-1)} . \tag{58}$$

In general

$$\int_0^x t^n \exp(-\gamma^2 t^2)dt = \frac{1}{2\gamma^2} x^{n+1} \exp(-\gamma^2 x^2)$$

$$\times \sum_{m=1}^{\infty} \left\{\prod_{i=1}^{m} \frac{2}{2i + n - 1}\right\} (\gamma x)^{2(m-1)} . \tag{59}$$

In particular, if $\gamma^2 = K/2$

$$\int_0^x t^n \exp(-Kt^2/2)\,dt = \frac{1}{K} x^{n+1} \exp(-Kx^2/2)$$
$$\times \sum_{m=1}^{\infty} \left\{ \prod_{i=1}^{m} \left(\frac{1}{2i+n-1}\right) \right\} (Kx^2)^{m-1} . \tag{60}$$

One may consider the general case

$$W(x) = \int_0^x t^n \exp(-t^m)\,dt, \tag{61}$$

where m and n are nonnegative integers.

Similarly one obtains

$$W(x) = \frac{1}{m} x^{n+1} \exp(-x^m) \sum_{\ell=0}^{\infty} \left\{ \prod_{i=0}^{\ell} \left(\frac{m}{im+n+1}\right) \right\} x^{m\ell} \tag{62}$$

for the case

$$R(x) = \int_0^x t^n \exp(t^m)\,dt, \tag{63}$$

$$R(x) = \frac{1}{m} x^{n+1} \exp(t^m) \sum_{\ell=0}^{\infty} \left\{ \prod_{i=0}^{\ell} \frac{m}{im+n+1} \right\} (-1)^{\ell} x^{m\ell} \tag{64}$$

If m = 0,

$$W(x) = R(x) = \frac{1}{n+1} x^{n+1} . \tag{65}$$

It is noted that n = 0 in Eq. (58) leads to the probability function [14] and that m = 2 and n = 0 in Eq. (64) leads to Sakamoto's function [35].

If one considers

$$(x^n \exp(x^2))' = nx^{n-1} \exp(x^2) + 2x^{n+1} \exp(x^2), \tag{66}$$

$$\int_0^x t^{n+1} \exp(t^2)\,dt = \frac{1}{2} x^n \exp(x^2) - \frac{n}{2} \int_0^x t^{n-1} \exp(t^2)\,dt \tag{67}$$

is obtained.

If $n = 2m$; $m = 0, 1, 2, \ldots,$

$$\int_0^2 t^{2m+1} \exp(t^2)dt = \frac{1}{2} x^{2m} \exp(x^2) - m \int_0^x t^{2m-1} \exp(t^2)dt$$

$$= (-1)^{m+1} \frac{m!}{2} \left\{1 - \exp(x^2) \sum_{i=0}^{m} (-1)^i \frac{x^{2i}}{i!}\right\}. \tag{68}$$

If $n = 2m - 1$; $m = 1, 2, \ldots,$

$$\int_0^x t^{2m} \exp(t^2)dt = \frac{1}{2} x^{2m-1} \exp(x^2) - \frac{1}{2} (2m-1) \int_0^x t^{2m-2} \exp(t^2)dt$$

$$= \exp(x^2) \sum_{i=0}^{m-1} (-1)^i \frac{(m-i)!(2m-1)!}{2^{2i}(m-1)!(2m-2i)!} x^{2m-2i-1}$$

$$+ (-1)^m \frac{(2m-1)!}{2^{2m-1}(m-1)!} \int_0^x \exp(x^2)dt. \tag{69}$$

Similarly the following equation results

$$\int_0^x t^{n+1} \exp(-t^2)dt = -\frac{1}{2} x^n \exp(-x^2) + \frac{1}{2} n \int_0^x t^{n-1} \exp(-t^2)dt. \tag{70}$$

If $n = 2m$; $m = 0, 1, 2, \ldots,$

$$\int_0^x t^{2m+1} \exp(-t^2)dt = \frac{1}{2} m! \left\{1 - \exp(-x^2) \sum_{i=0}^{m} \frac{x^{2i}}{i!}\right\}. \tag{71}$$

If $n = 2m - 1$; $m = 1, 2, \ldots,$

$$\int_0^x t^{2m} \exp(-t^2)dt = \frac{(2m-1)!}{2^{2m-1}(m-1)!} \int_0^x \exp(-t^2)dt$$

$$- \exp(-x^2) \sum_{i=0}^{m-1} \frac{(m-i)!(2m-1)!}{2^{2i}(m-1)!(2m-2i)!} x^{2m-2i-1}. \tag{72}$$

Finally one has the appropriate formulas for the evaluation of Eq. (35)

for small x and small θ, Eq. (41),

for large x and small θ, Eq. (43),

and

for larger angles than θ_1, Eq. (44).

V. RESULTS AND DISCUSSION

A. The Modified Secant Integral

Ten, twenty-two and forty point Gaussian formulas were used numerically to integrate the modified secant integral, and were compared with the checking formulas in Chapter IV. In order to expect five digit accuracy to the checking formulas the following approximations were used:

$$\theta_1 = \sqrt{0.15}$$

$$\sec\theta = 1 + \frac{1}{2}\theta^2 + \frac{5}{24}\theta^4 + \frac{61}{720}\theta^6 + \frac{277}{8064}\theta^8 + \frac{50521}{3628800}\theta^{10} + \Delta E_1 ,$$

$$0 \leq \theta \leq \theta_1$$

with ΔE_1 less than 7.5×10^{-8}

$$x \leq 40.$$

Then the power term of $\exp\left\{(-x)(5/24\ \theta^2 + 61/720\ \theta^2 + \cdots)\right\}$ is less than 0.25 and Eq. (48) can be used for the approximation.

$$\exp(-t) \doteqdot \sum_{i=0}^{4} b_i t^i , \tag{73}$$

$$0 \leq t \leq 0.25$$

where the probable maximum error would be less than 1.4×10^{-7}, and

$$b_o = 1$$

$$b_1 = -\ 889984/889985$$

$$b_2 = 444928/889985$$

$$b_3 = -\ 147456/889985$$

$b_4 = 32768/889985.$

In order to calculate the exponential integral $E_1(x)$ for four different approximation power series were used depending on the magnitude of x.

For $0 \leq x < 1$, and $1 < x \leq 10$ the formulas from Ref. [20], for $x \geq 30$ the formula from Ref. [11] were used.

For $10 < x \leq 30$

$$E_1(x) = x * AUX * \exp(-x)$$

where $E_1(x)$ was derived by use of the tau method [24], * implies multiplication, and

$$AUX = \sum_{i=0}^{11} b_i x^{-i}$$

with

$b_o = 0.99999999999946$

$b_1 = -0.99999999844367$

$b_2 = 1.9999992552944$

$b_3 = -5.9998593351996$

$b_4 = 23.986088667743$

$b_5 = -119.17105216042$

$b_6 = 687.64220683609$

$b_7 = -4163.4990821542$

$b_8 = 23016.383545592$

$b_9 = -\ 99522.781419961$

$b_{10} = 281506.31515822$

$b_{11} = -\ 377630.42277323$

and the probable maximum error less than 5.41×10^{-13} in AUX. Then one can calculate nth order exponential integral using the recurrence relation [6]

$$E_n(x) = \frac{1}{n-1}\left(\exp(-x) - xE_{n-1}(x)\right), \qquad n > 1. \tag{74}$$

The checking formulas were iterated so that the last added term would be less than 1.0×10^{-6} of the partial summations. The results from twenty-two and forty point Gaussian formulas were compared to those from the checking formulas. At least the first four digits agreed. The errors of the Gaussian formulas were also calculated by Lanczos's formula [24] even though they might be overestimated. This indicated that Gaussian formulas (twenty-two and forty points) would be accurate up to the first four digits. Some numerical difficulty occurred for the Lanczos's formula for θ approaching 90° because the error estimation formula for the modified secant integral contains $\sec\theta$, $\tan\theta$ and $\exp(-x\sec\theta)$. As a result of the comparison the estimated errors for $\theta_o = 90^o$ would be almost of the same order as those for $\theta_o = 80^o$.

The twenty-two and forty point Gaussian formulas resulted in some difference in the fifth digit. The ten point formula resulted in

some difference in the third digit. However, it is felt that at least four digit accuracy would be sufficient to use for the shielding design purpose.

Numerical calculation results ($0.1 \leq x \leq 40$) were generated using the forty point Gaussian formulas including errors estimated by the Lanczos's formula in Appendix D. Some of the results ($1 \leq x \leq 20$) are plotted in Figs. 7 to 10.

It was concluded that the twenty-two Gaussian formula could be good enough to be used for the radiation analysis from a line source.

Equations (58) and (64), where $m = 2$, were also evaluated and the results are plotted in Figs. 11, 12, and 13.

B. Radiation from a Line Source

A computer program to obtain the transmission and reflection operator matrices is described in Ref. [34]. The gamma ray source in this investigation consisted of 1 MeV photon and were normalized to 1 MeV/cm/sec. The source was an isotropic uniform line source. The seventeen energy groups were used with variable angular expansions, and six half range Legendre polynomials were fitted for an isotropic ($1/\omega$) input source flux to obtain the transmission and reflection operator matrices. The energy grouping, from the highest group to the lowest was tabulated in Table I. As mentioned in Section A, the twenty-two point Gaussian formulas were used numerically to integrate the modified secant integral.

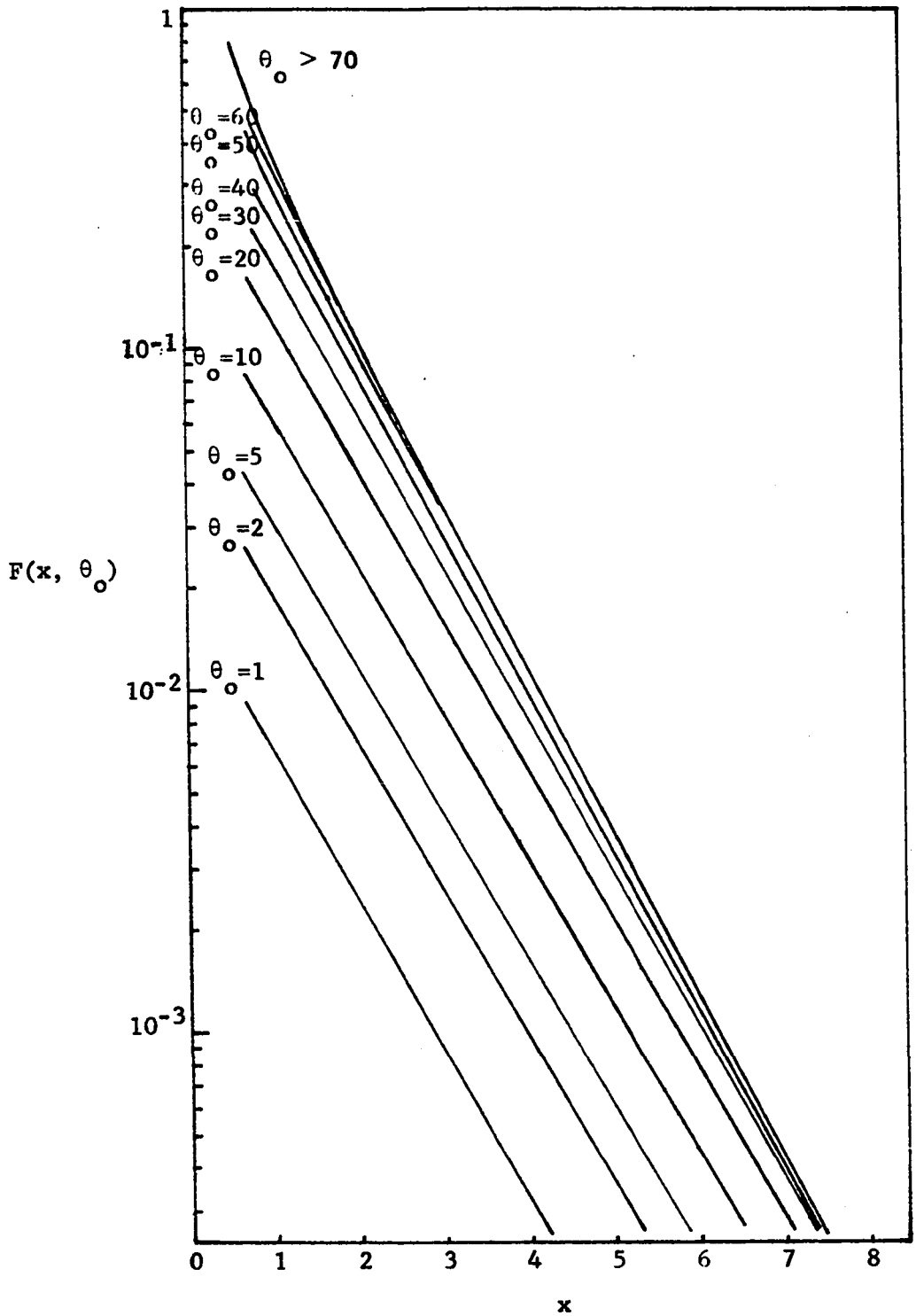

Fig. 7. The function $F(x, \theta_o) = \int_0^{\theta_o} \sec\theta \exp(-x \sec\theta) d\theta$ for x = 1 to 6.

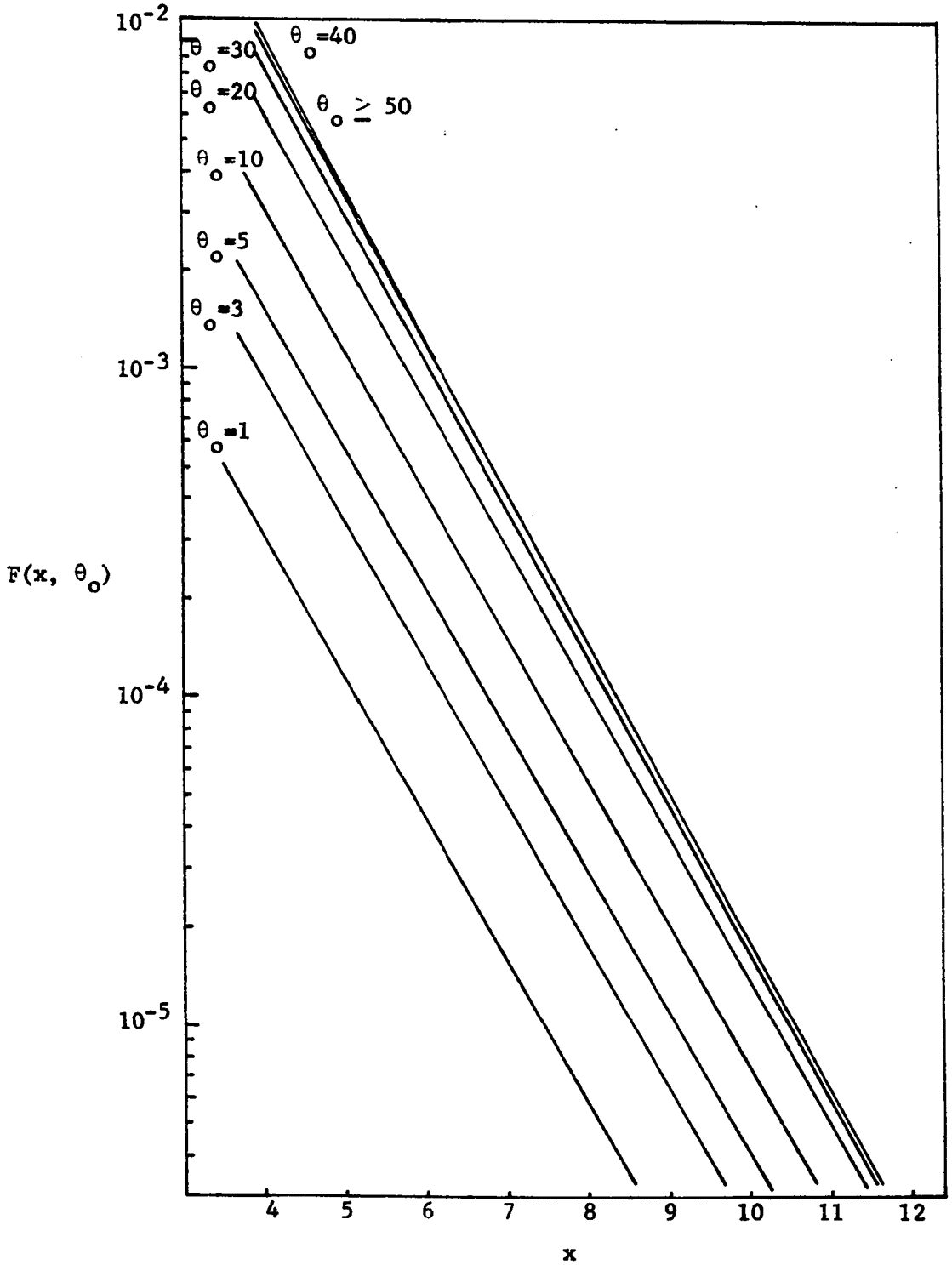

Fig. 8. The function $F(x, \theta_o) = \int_0^{\theta_o} \sec\theta \exp(-x \sec\theta) d\theta$ for x = 4 to 11.

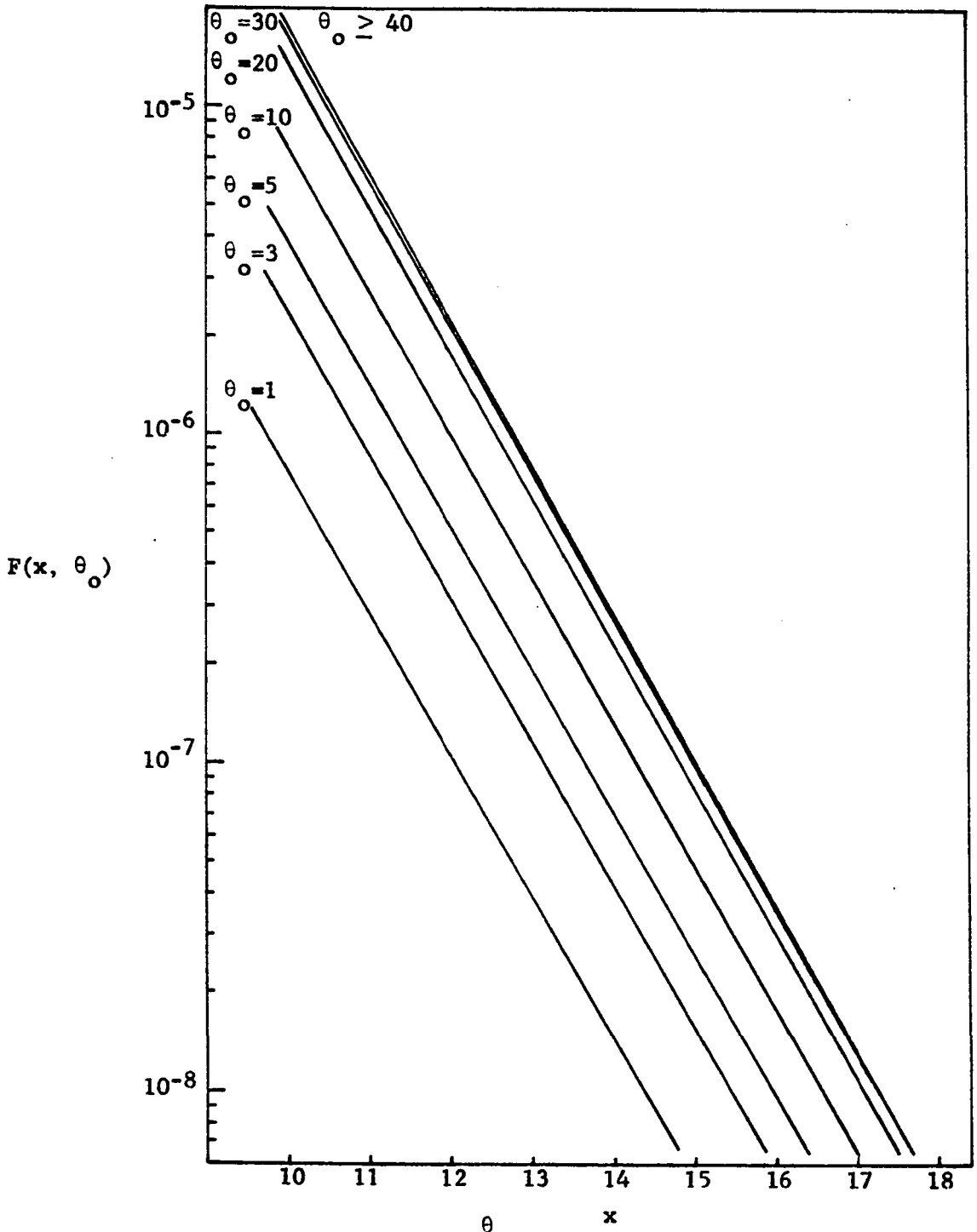

Fig. 9. The function $F(x, \theta_o) = \int_0^{\theta_o} \sec\theta \exp(-x \sec\theta)d\theta$ for $x = 10$ to 17.

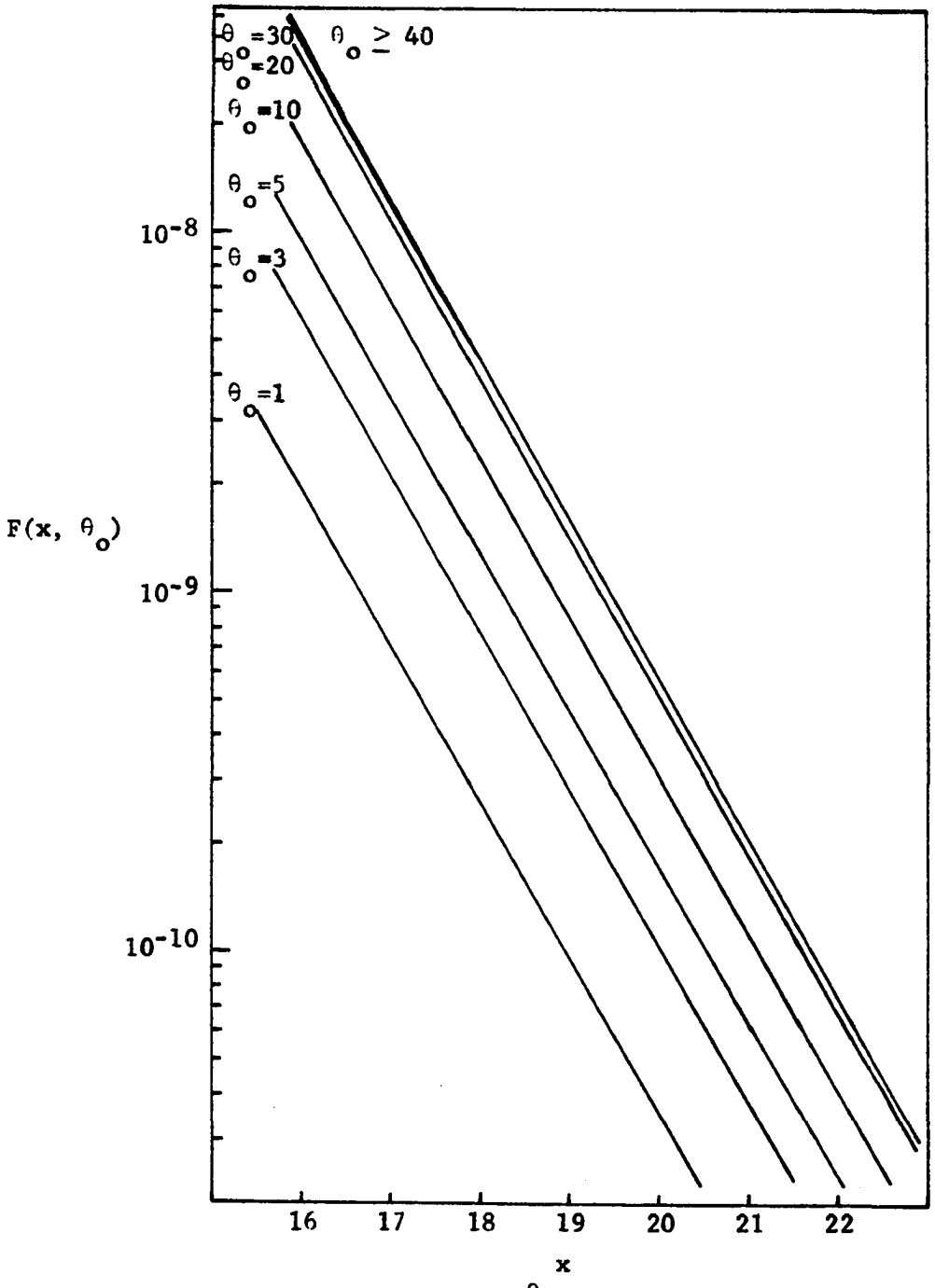

Fig. 10. The function $F(x, \theta_o) = \int_0^{\theta_o} \sec\theta \exp(-x \sec\theta)d\theta$ for x = 16 to 20.

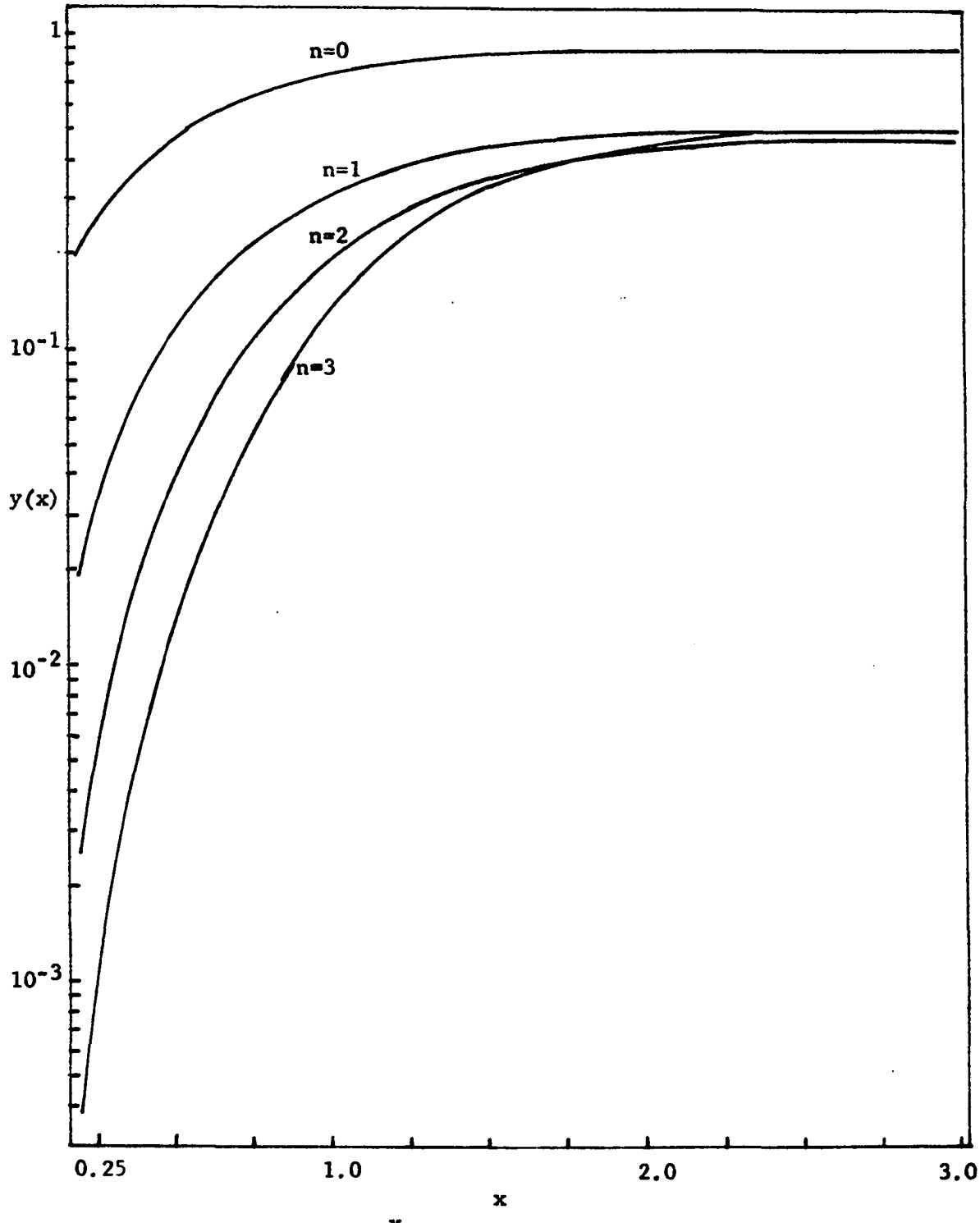

Fig. 11. Function $y(x) = \int_0^x t^n \exp(-t^2)dt$

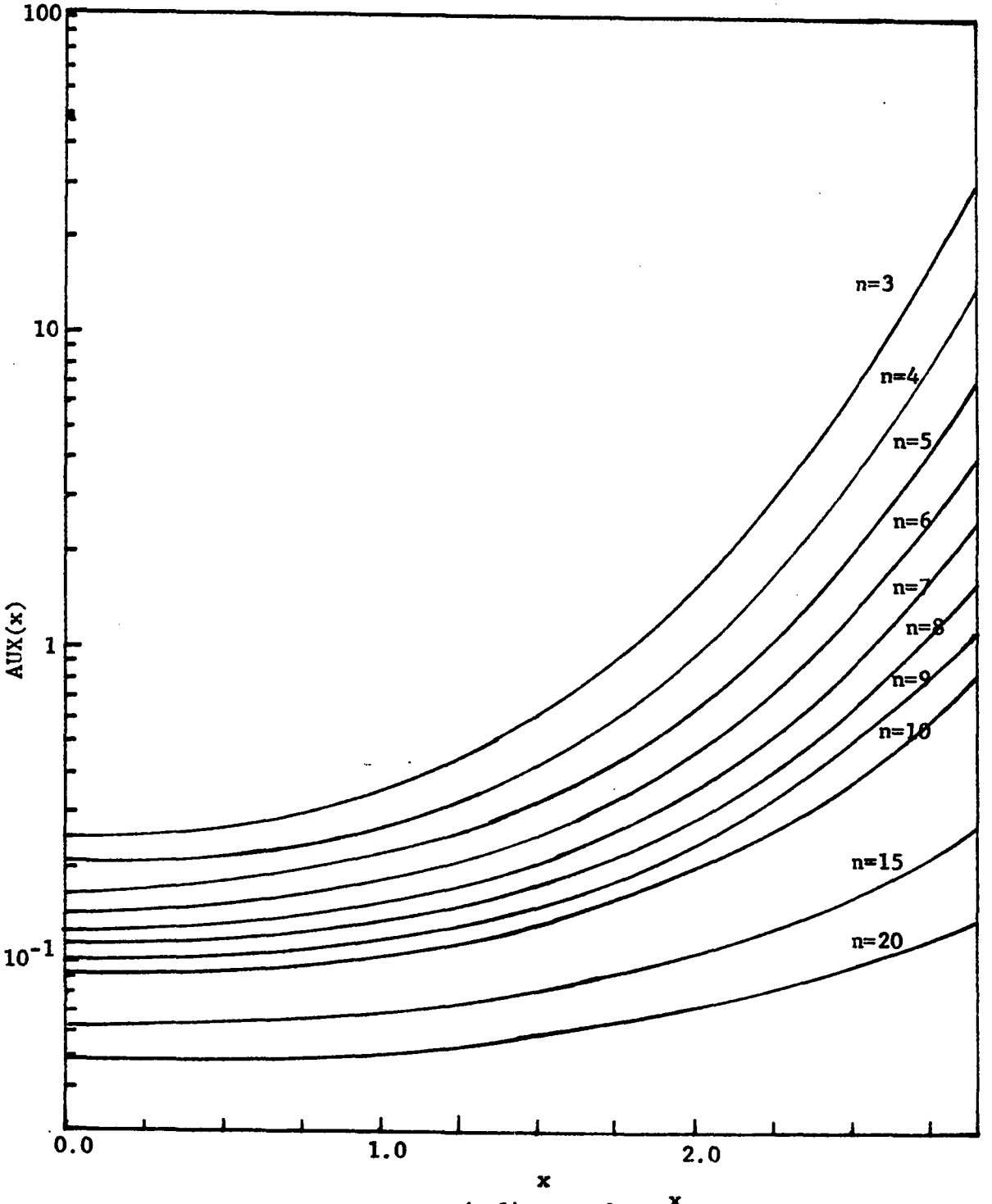

Fig. 12. The function $AUX(x) = x^{-(n+1)} \exp(x^2) \int_0^x t^n \exp(-t^2)dt$.

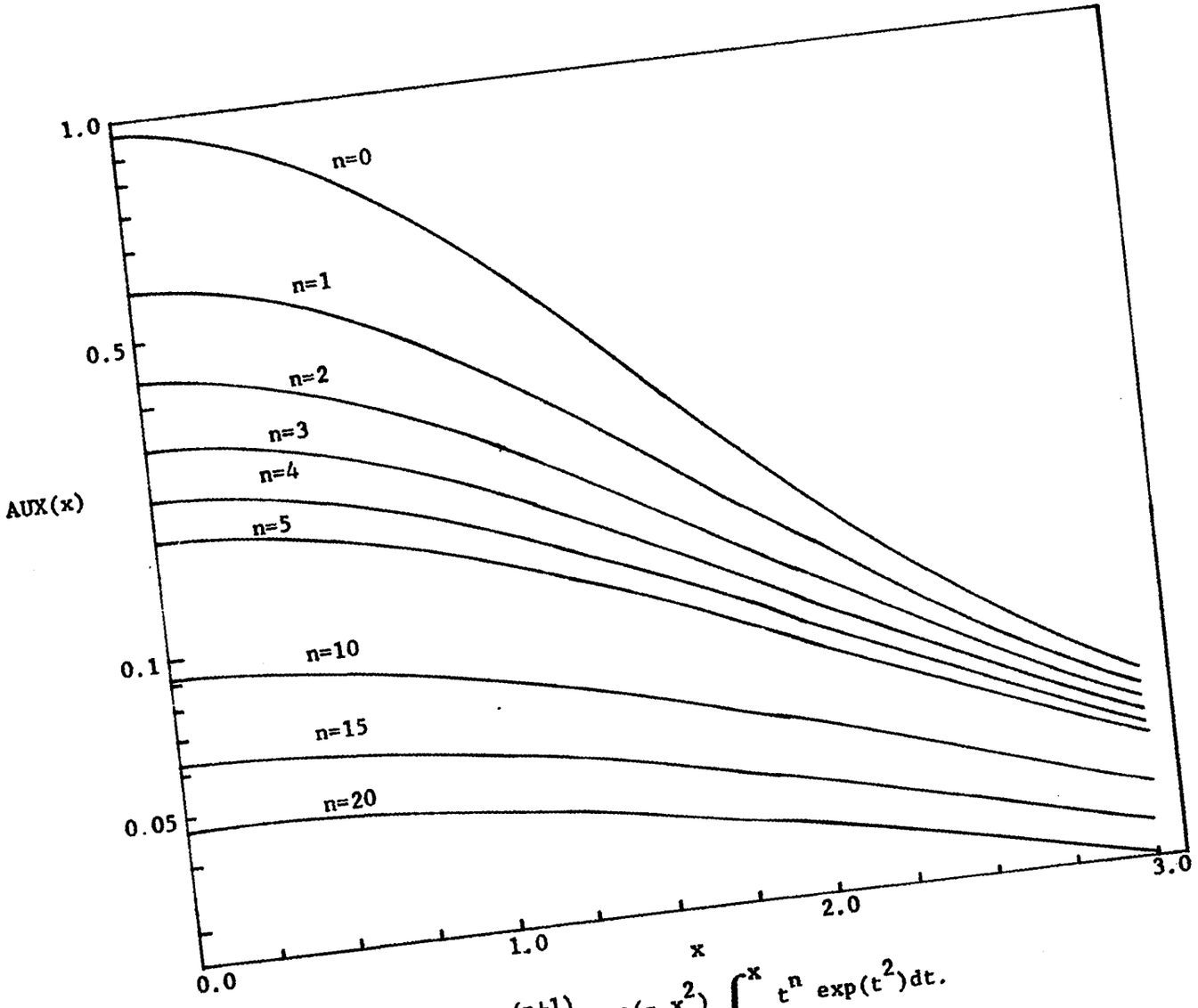

Fig. 13. The function $AUX(x) = x^{-(n+1)} \exp(-x^2) \int_0^x t^n \exp(t^2)dt.$

Table I. Energy grouping

Order of energy group	Energy range (MeV)	Number of angular expansions of the half range Legendre polynomials
First (uncollided source energy)	1.0	6
Second	1.0 – 0.88	5
Third	0.88 – 0.76	5
Fourth	0.76 – 0.64	5
Fifth	0.64 – 0.51	5
Sixth	0.51 – 0.41	5
Seventh	0.41 – 0.31	4
Eighth	0.31 – 0.26	4
Ninth	0.26 – 0.203	4
Tenth	0.203 – 0.173	4
Eleventh	0.173 – 0.143	4
Twelfth	0.143 – 0.113	3
Thirteenth	0.113 – 0.095	3
Fourteenth	0.095 – 0.078	3
Fifteenth	0.078 – 0.060	3
Sixteenth	0.060 – 0.049	3
Seventeenth	0.049 – 0.041	3

Since none of the results of the radiation from line sources could be obtained, in order to check the availability of the point matrix kernel for the line source analysis two comparisons were made.

The first one was the comparison of differential energy spectra from the relative short line sources to those from point sources. It was expected that they would have similar differential energy spectra if the slab thicknesses were very large compared to the short line sources. In Ref. [19] the isotropic point source results were obtained from the moment method originally calculated for the plane problems using the plane-to-point transformation. A special notation was introduced:

$$\Gamma(\mu_o r, E) = 4\pi r^2 \exp(\mu_o r) I_o(r, E), \tag{75}$$

where

r = distance between the source and detector point

μ_o = linear attenuation coefficient of a material in interest at the source energy

$I_o(r, E)$ = differential energy spectrum

$\Gamma(\mu_o r, E)$ = was plotted versus energy.

For comparative purposes the differential energy spectra from the line sources were also multiplied by $4\pi z^2 \exp(\mu_o z)$ where z is the distance normal to a line source from a detector point. These results are plotted in Figs. 14 to 17 for various thicknesses of various materials. As expected, the comparison of differential energy spectra with the moment method calculation were very good for both the spectra shapes and for the magnitudes. When the slab thicknesses were of more than four mean free path while the line source was one mean free path, the results gave essentially point source conditions.

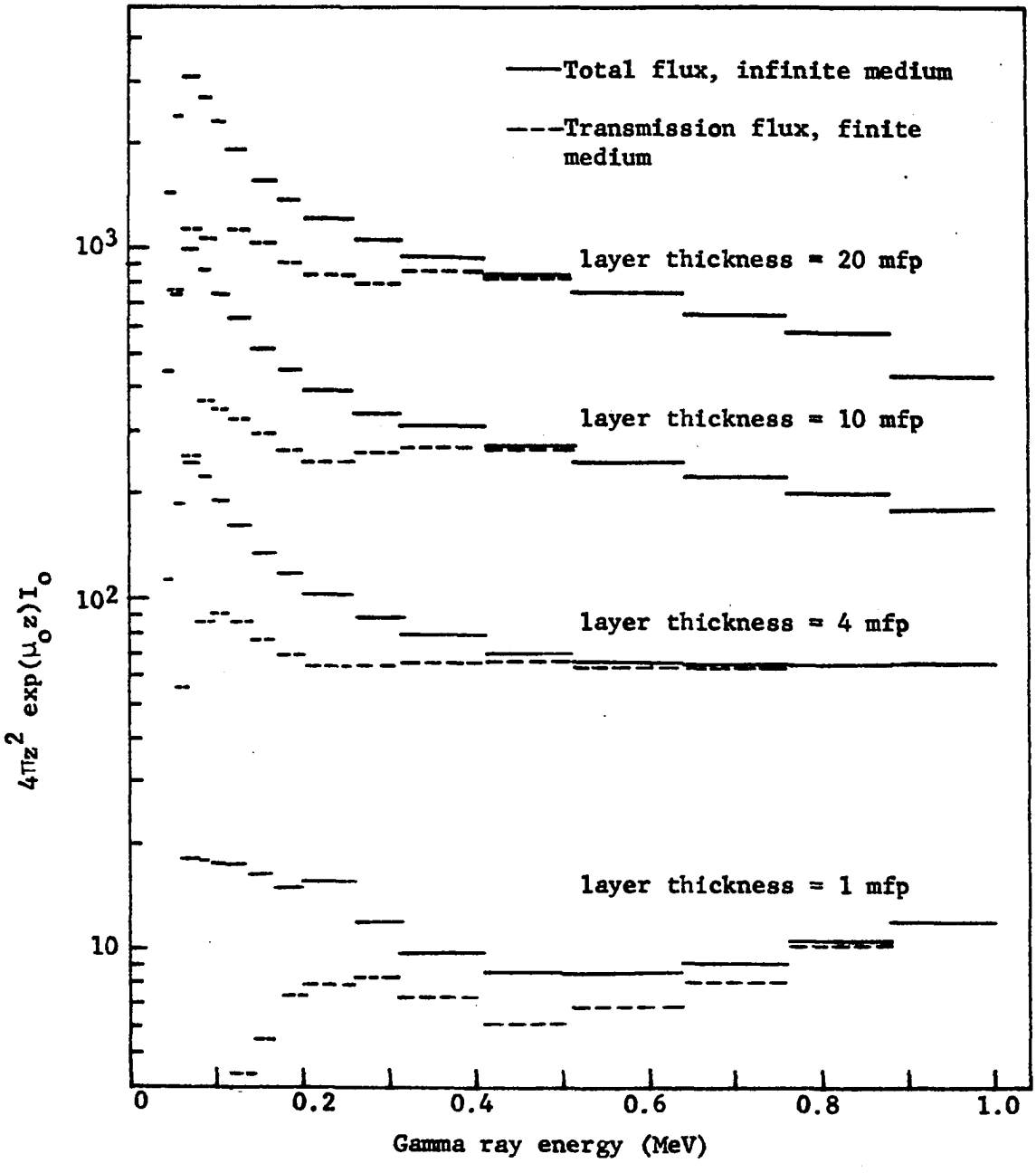

Fig. 14. Differential energy spectrum for medium water. Isotropic source energy = 1 MeV, source strength = 1 MeV/cm/sec, source length = 1 mfp.

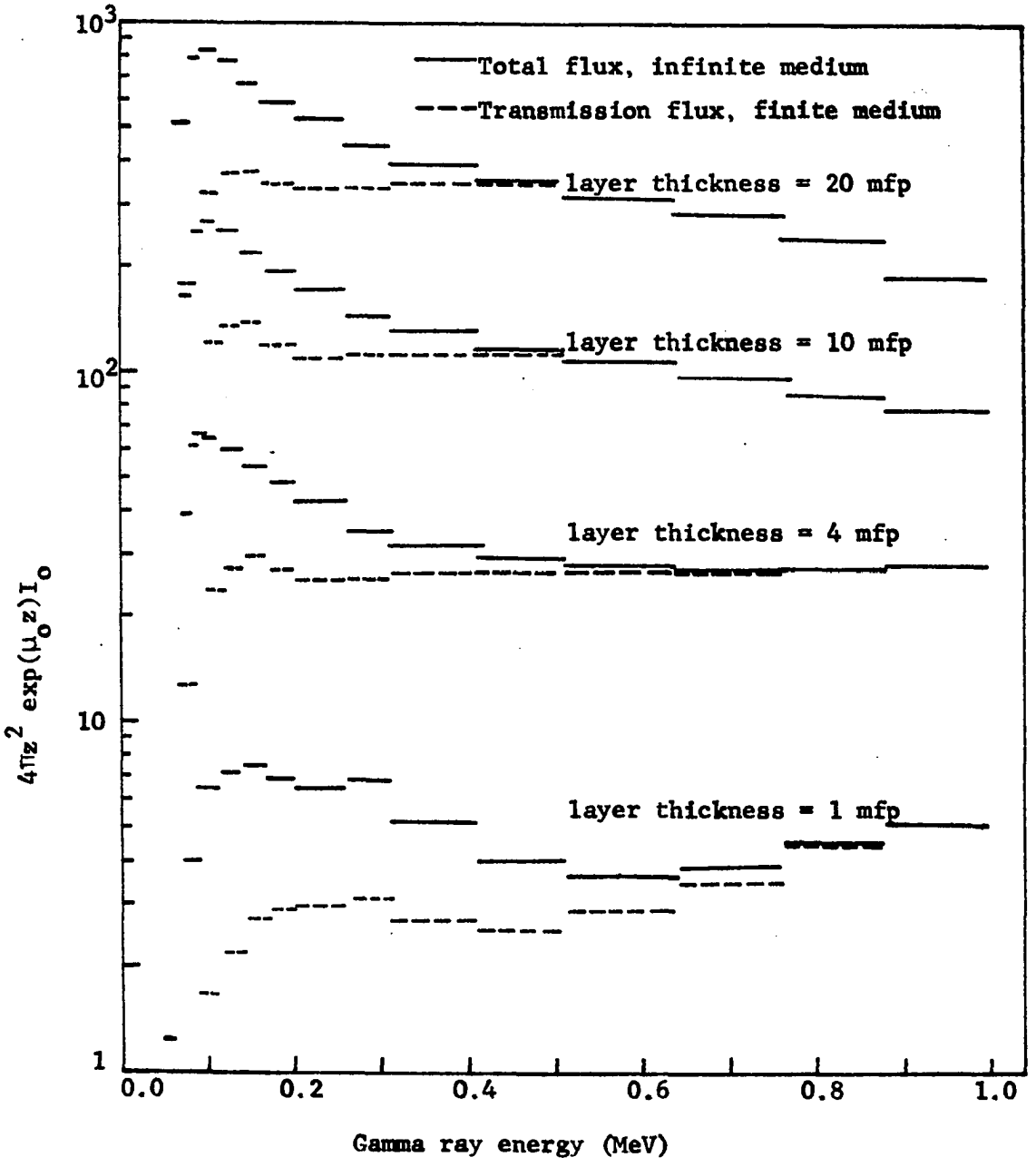

Fig. 15. Differential energy spectrum for medium aluminum. Isotropic source energy = 1 MeV, source strength = 1 MeV/cm/sec, source length = 1 mfp.

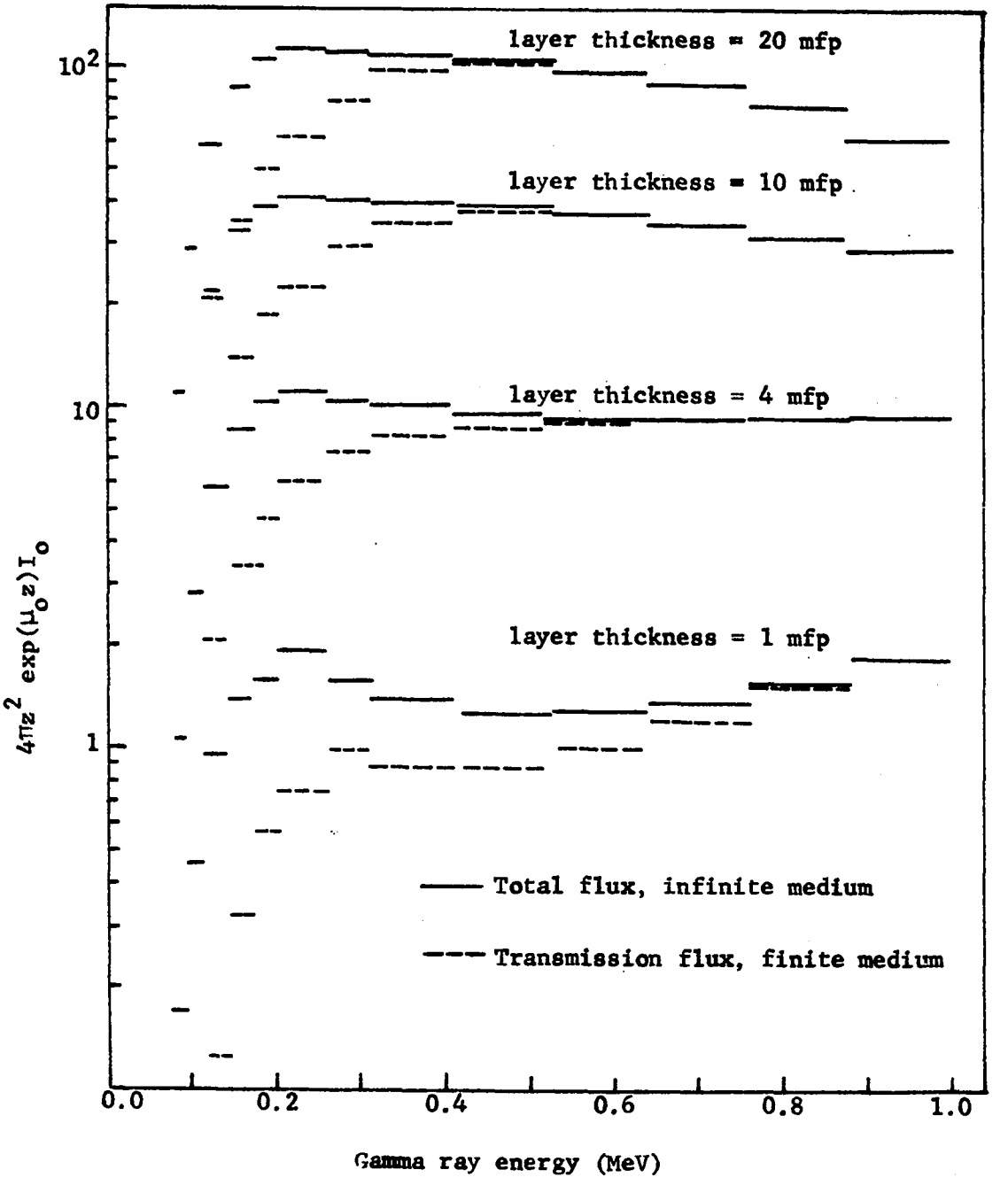

Fig. 16. Differential energy spectrum for medium iron. Isotropic source energy = 1 MeV, source strength = 1 MeV/cm/sec, source length = 1 mfp.

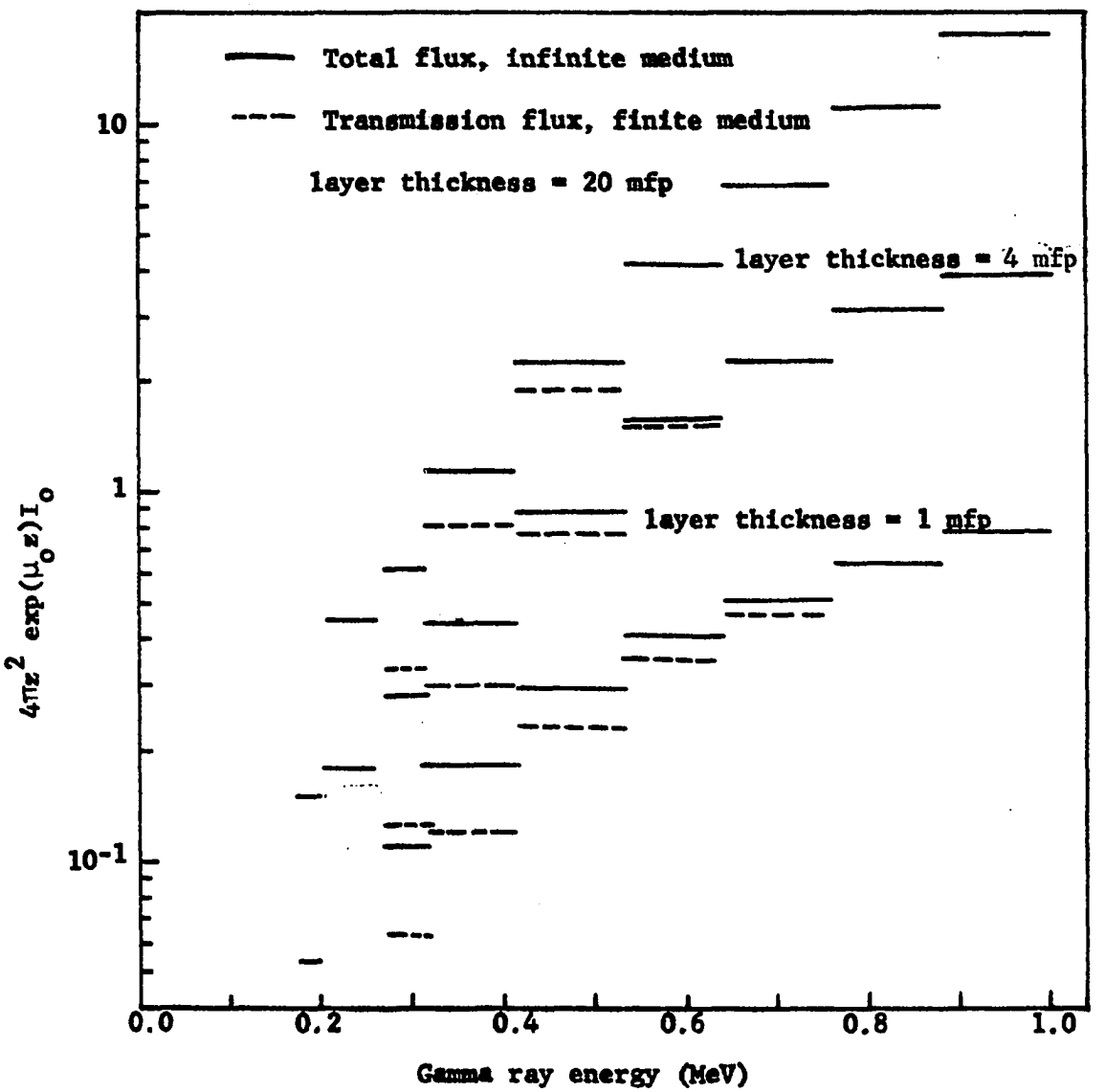

Fig. 17. Differential energy spectrum for medium lead, isotropic source energy = 1 MeV, source strength = 1 MeV/cm/sec, source length = 1 mfp.

The differential energy spectra from one hundred mean free path lengths of line sources (this essentially gave the condition, a half infinite long line source, i.e., $\theta = 0$ to 90°) are plotted in Figs. 18 and 19. The differential energy spectra shapes are similar to those from one mean free path length line sources.

The second comparison method was to use the Berger's form [3, 37] of the buildup factors. One can have the extended point kernel

$$K_p(\mu, r) = (1 + C\mu r \exp(D\mu r))\exp(-\mu r)/(4\pi r^2)$$

$$= \frac{\exp(-\mu r)}{4\pi r^2} + \frac{C\mu r(-(1 - D)\mu r)}{4\pi r^2} \qquad (76)$$

where C and D are the extended fitting coefficients [19, 37] which are dependent on buildup factors in interest. If Eq. (76) is applied to the line source analysis, the first term which is related to uncollided flux leads to the secant integral [36], and the second term which is related to collided flux leads to the modified secant integral. As suggested in Ref. [17] Gaussian quadrature was also used to integrate the secant integral numerically. There was very good agreement in the calculation of the uncollided flux between the point matrix kernel and the extended point kernel methods. There was also fairly good agreement on the buildup factor calculation between both methods for relatively thin thicknesses since the available buildup factor coefficients [19, 37] are good at most only for the range less than twenty mean free path which is the distance between a differential extended source and detector point. The results are shown in Tables II and III as the forms of various buildup factors.

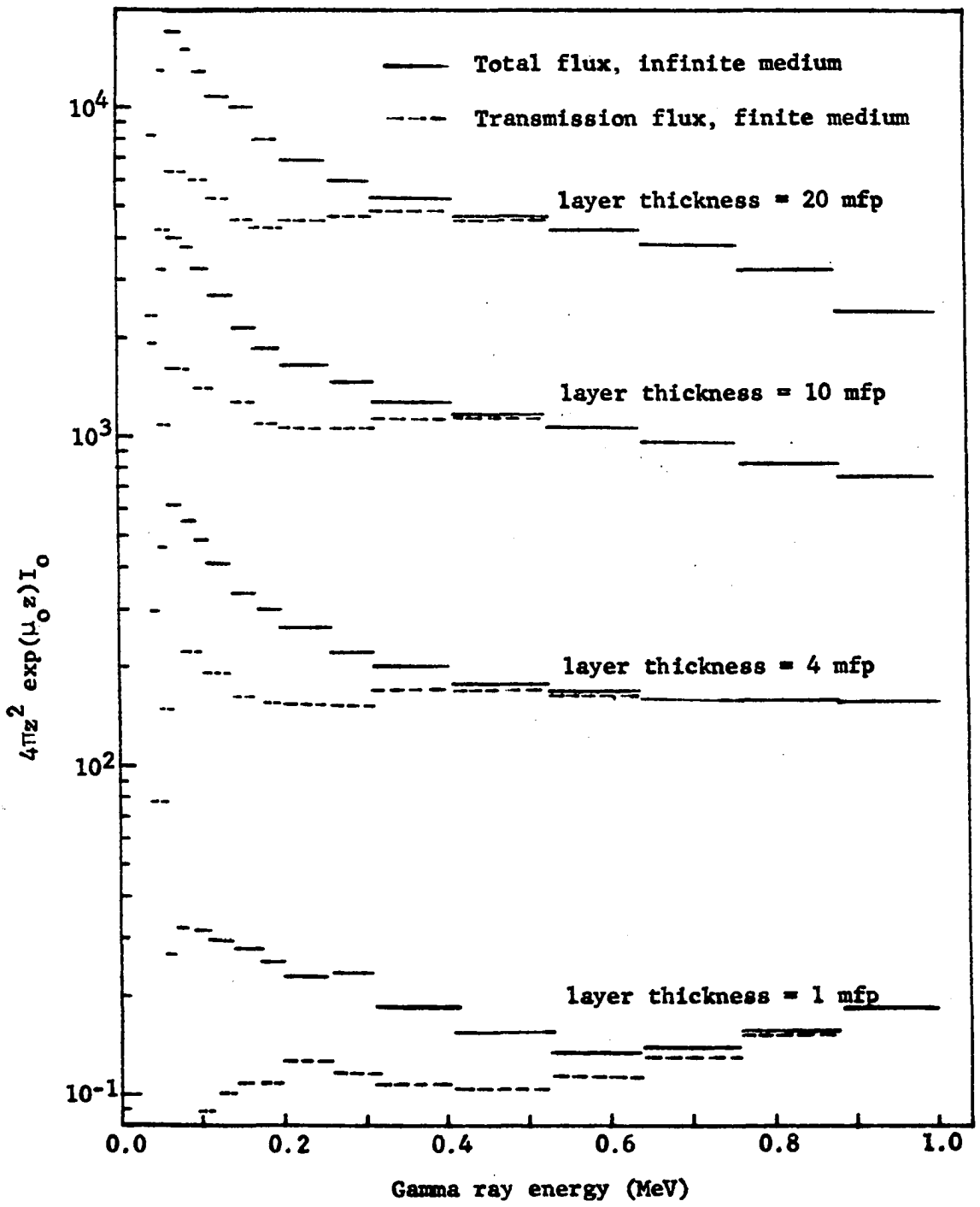

Fig. 18. Differential energy spectrum for medium water. Isotropic source energy = 1 MeV, source strength = 1 MeV/cm/sec, source length = 100 mfp.

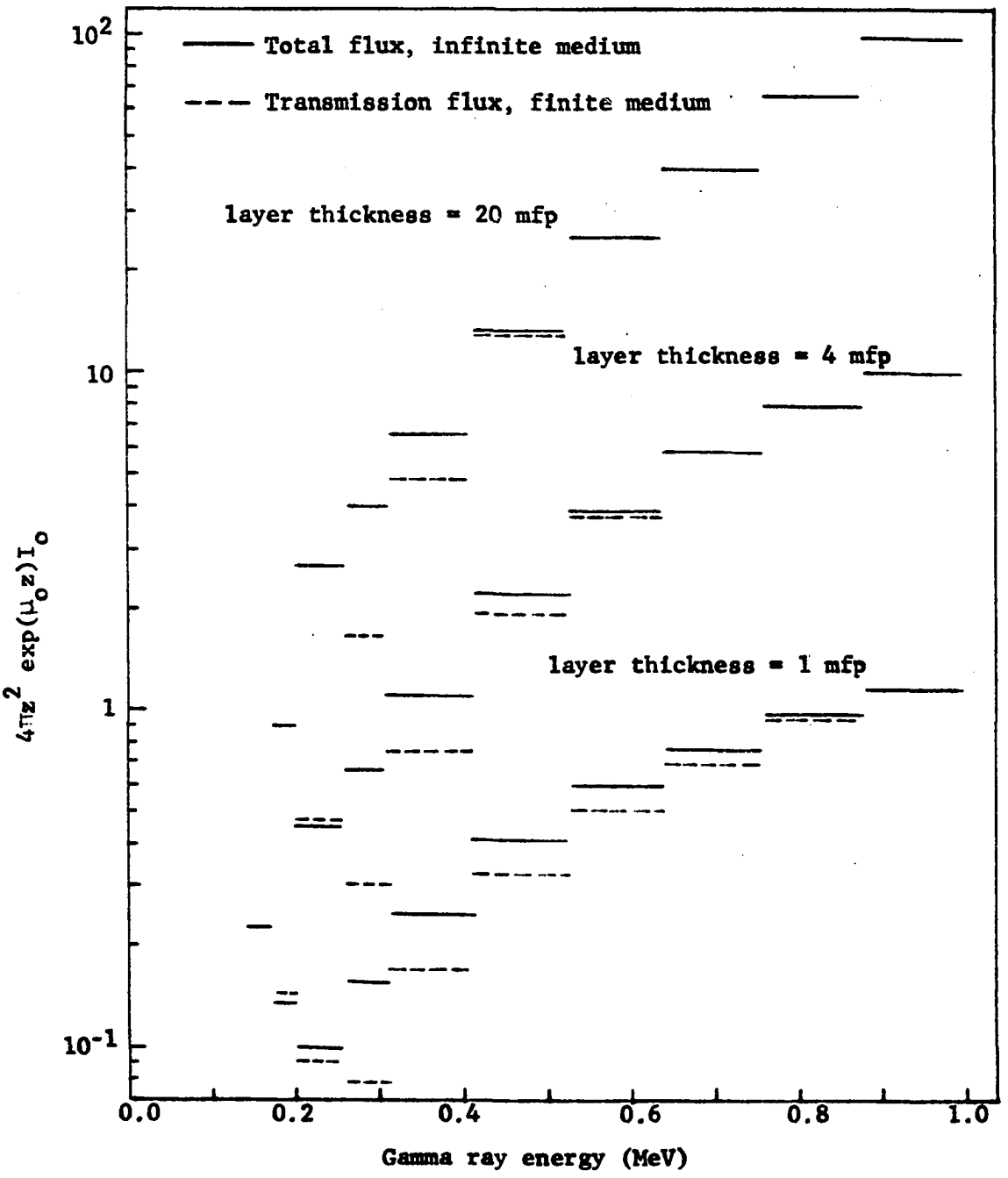

Fig. 19. Differential energy spectrum for medium lead. Isotropic source energy = 1 MeV, source strength = 1 MeV/cm/sec, source length = 100 mfp.

Table II. Buildup factors (1 mfp line source[a] length). Upper row value: point matrix kernel method; lower row value in parentheses: extended point kernel method

Shield material	Buildup factor \ Thickness (mfp)	1.0	2.0	4.0	6.0	8.0	10.0	15.0	20.0
Water	Energy fluence	2.07	3.42	7.02	11.57	16.99	23.20	41.95	64.82
		(2.31)	(3.66)	(7.13)	(11.84)	(18.09)			
	Exposure	2.08	3.45	7.11	11.75	17.26	23.57	42.62	65.85
		(2.33)	(3.74)	(7.56)	(13.07)	(17.58)	(24.57)	(49.84)	(91.04)
	Energy deposition	2.07	3.42	7.03	11.60	17.02	23.23	41.99	64.87
		(2.32)	(3.75)	(7.69)	(13.48)	(17.94)	(25.14)	(51.30)	(94.25)
Aluminum	Energy fluence	2.05	3.27	6.46	10.53	15.38	20.97	37.86	58.51
		(2.18)	(3.37)	(6.36)	(10.27)	(15.33)			
	Exposure	2.06	3.28	6.49	10.57	15.45	21.05	37.99	58.69
		(2.17)	(3.38)	(6.49)	(10.73)	(14.34)	(19.54)	(37.30)	(64.21)
	Energy deposition	2.18	3.61	7.36	12.15	17.89	24.49	44.54	69.08
		(2.30)	(3.61)	(6.87)	(11.12)	(16.25)	(22.27)	(43.02)	(74.83)
Iron	Energy fluence	1.88	2.81	5.14	7.98	11.26	14.90	25.45	37.70
		(1.96)	(2.91)	(5.21)	(8.12)	(11.73)			
	Exposure	1.90	2.86	5.25	8.17	11.53	15.28	26.12	38.70
		(1.98)	(2.96)	(5.37)	(8.48)	(11.36)	(15.18)	(27.75)	(45.86)
	Energy deposition	2.23	3.52	6.75	10.73	15.34	20.48	35.43	52.81
		(2.34)	(3.68)	(6.98)	(11.23)	(15.21)	(20.48)	(37.84)	(62.98)

[a]Isotropic 1 MeV photon; strength: 1 MeV/cm/sec; source length = 1 mfp infinite medium.

Table II. Continued

Shield Material	Thickness (mfp) / Buildup factor	1.0	2.0	4.0	6.0	8.0	10.0	15.0	20.0
Lead	Energy fluence	1.38 (1.38)	1.66 (1.68)	2.17 (2.26)	2.63 (2.76)	3.05 (3.21)	3.44	4.32	5.06
	Exposure	1.39 (1.40)	1.68 (1.72)	2.21 (2.30)	2.68 (2.79)	3.12 (3.39)	3.52 (3.86)	4.42 (4.86)	5.19 (5.63)
	Energy deposition	1.80 (1.81)	2.29 (2.44)	3.14 (3.50)	3.88 (4.33)	4.55 (5.51)	5.17 (6.33)	6.55 (7.95)	7.73 (9.06)

Table III. Buildup factors (100 mfp lines source[a] length). Upper row value: point matrix kernel method; lower row value in parentheses: extended point kernel method

Shield material	Buildup factor \ Thickness (mfp)	1.0	2.0	4.0	6.0	8.0	10.0
Water	Energy fluence	2.32 (2.56)	3.89 (4.11)	7.81 (7.94)	12.63 (13.03)	18.27 (19.75)	24.68
	Exposure	2.33 (2.62)	3.93 (4.24)	7.93 (8.31)	12.82 (13.80)	18.56 (21.17)	25.08 (30.95)
	Energy deposition	2.32 (2.62)	3.90 (4.27)	7.83 (8.45)	12.65 (14.19)	18.30 (21.99)	24.72 (32.49)
Aluminum	Energy fluence	2.27 (2.40)	3.69 (3.77)	7.17 (7.03)	11.47 (11.24)	16.53 (16.63)	22.30
	Exposure	2.28 (2.39)	3.71 (3.79)	7.20 (7.22)	11.52 (11.80)	16.60 (15.40)	22.39 (20.85)
	Energy deposition	2.45 (2.54)	4.10 (4.04)	8.19 (7.60)	13.26 (12.16)	19.25 (17.48)	26.08 (23.79)
Iron	Energy fluence	2.05 (2.14)	3.13 (3.22)	5.64 (5.72)	8.63 (8.81)	12.01 (12.63)	15.75
	Exposure	2.08 (2.16)	3.18 (3.28)	5.77 (5.91)	8.83 (9.23)	12.31 (12.14)	16.15 (16.13)
	Energy deposition	2.47 (2.59)	3.95 (4.12)	7.45 (7.72)	11.63 (12.26)	16.40 (16.29)	21.69 (21.78)

[a]Isotropic 1 MeV photon; strength: 1 MeV/cm/sec; source length = 100 mfp, infinite medium.

Table III. Continued

Shield material	Thickness (mfp) / Buildup factor	1.0	2.0	4.0	6.0	8.0	10.0
Lead	Energy fluence	1.43 (1.43)	1.73 (1.77)	2.26 (2.35)	2.71 (2.85)	3.13 (3.29)	3.52
	Exposure	1.44 (1.46)	1.76 (1.80)	2.30 (2.39)	2.77 (2.87)	3.20 (3.49)	3.60 (3.96)
	Energy deposition	1.89 (1.92)	2.41 (2.59)	3.27 (3.66)	4.01 (4.46)	4.68 (5.69)	5.29 (6.49)

As a result of the differential spectra and the buildup factor comparisons, it is felt that the point matrix kernel could be used for the analysis of the line source radiation. However, in order precisely to evaluate the usage of the point matrix kernel method for the line source analysis some more comparative informations, such as experimental results, are necessary.

The total energy carried by uncollided and collided flux are plotted versus thickness of the layered materials in Figs. 20 to 23.

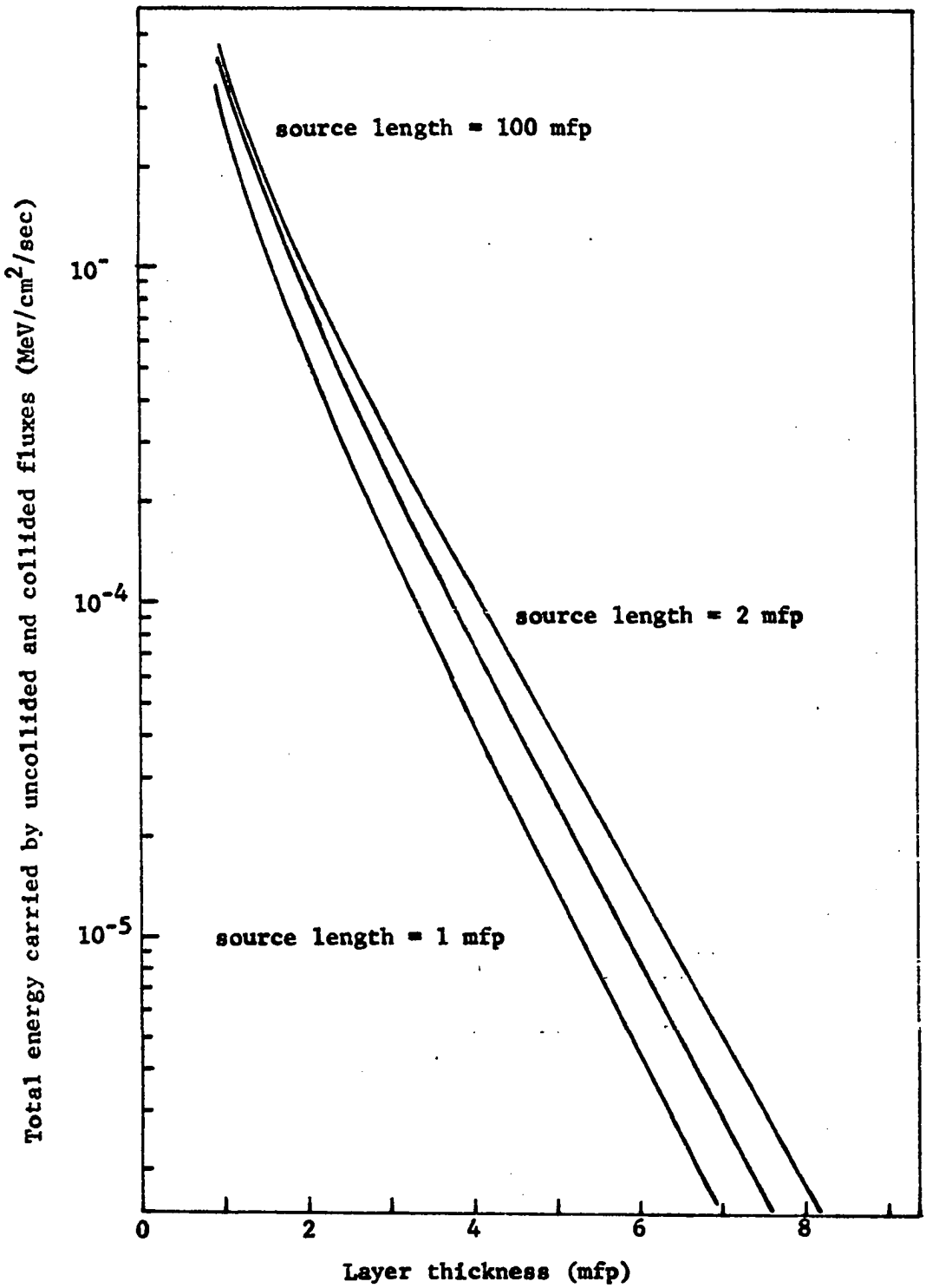

Fig. 20. Total energy carried by uncollided and collided fluxes for various source lengths. Medium: water, isotropic source energy = 1 MeV, source strength = 1 MeV/cm/sec.

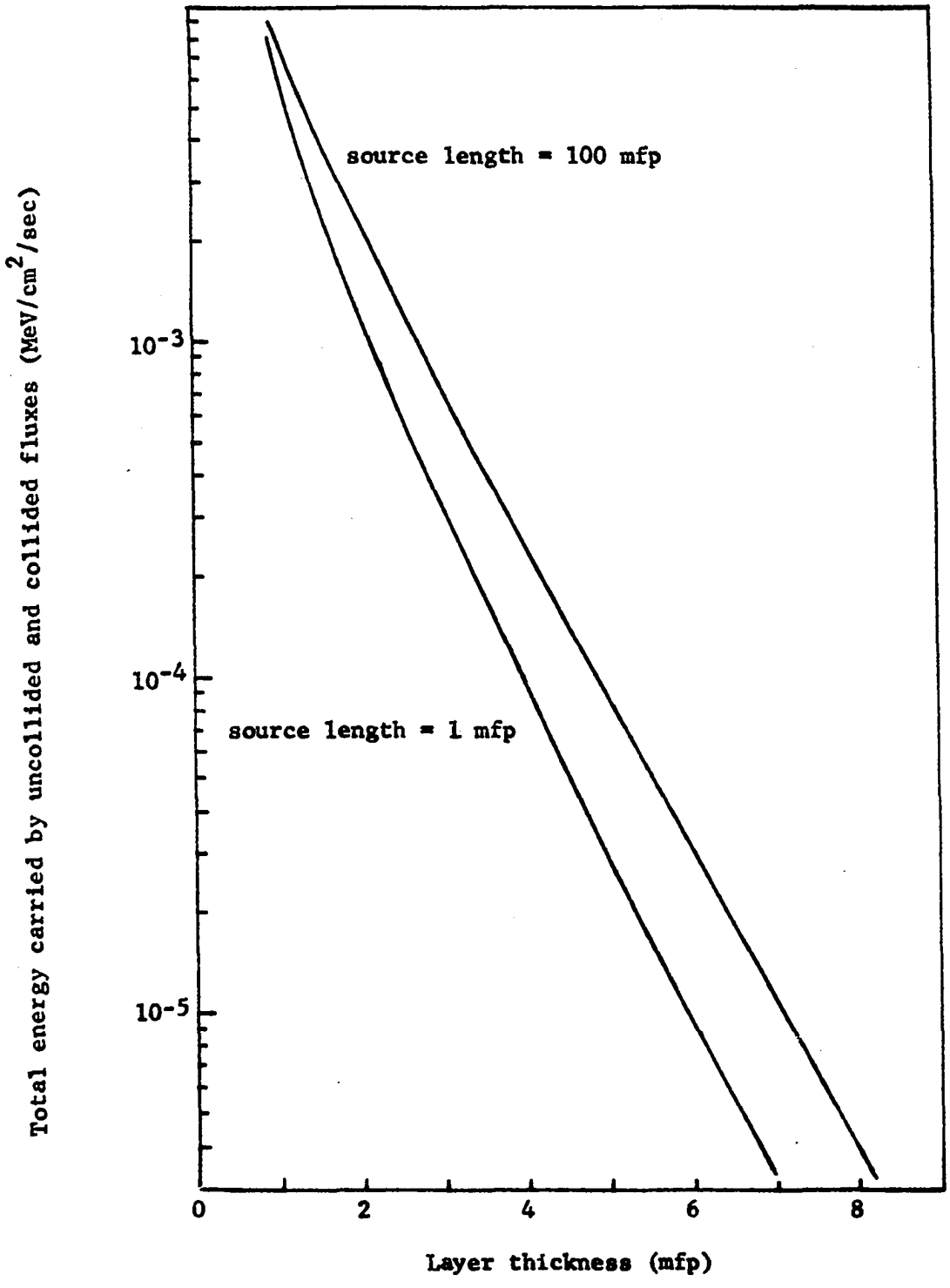

Fig. 21. Total energy carried by uncollided and collided fluxes for various source lengths. Medium: aluminum, isotropic source energy = 1 MeV, source strength = 1 MeV/cm^2/sec.

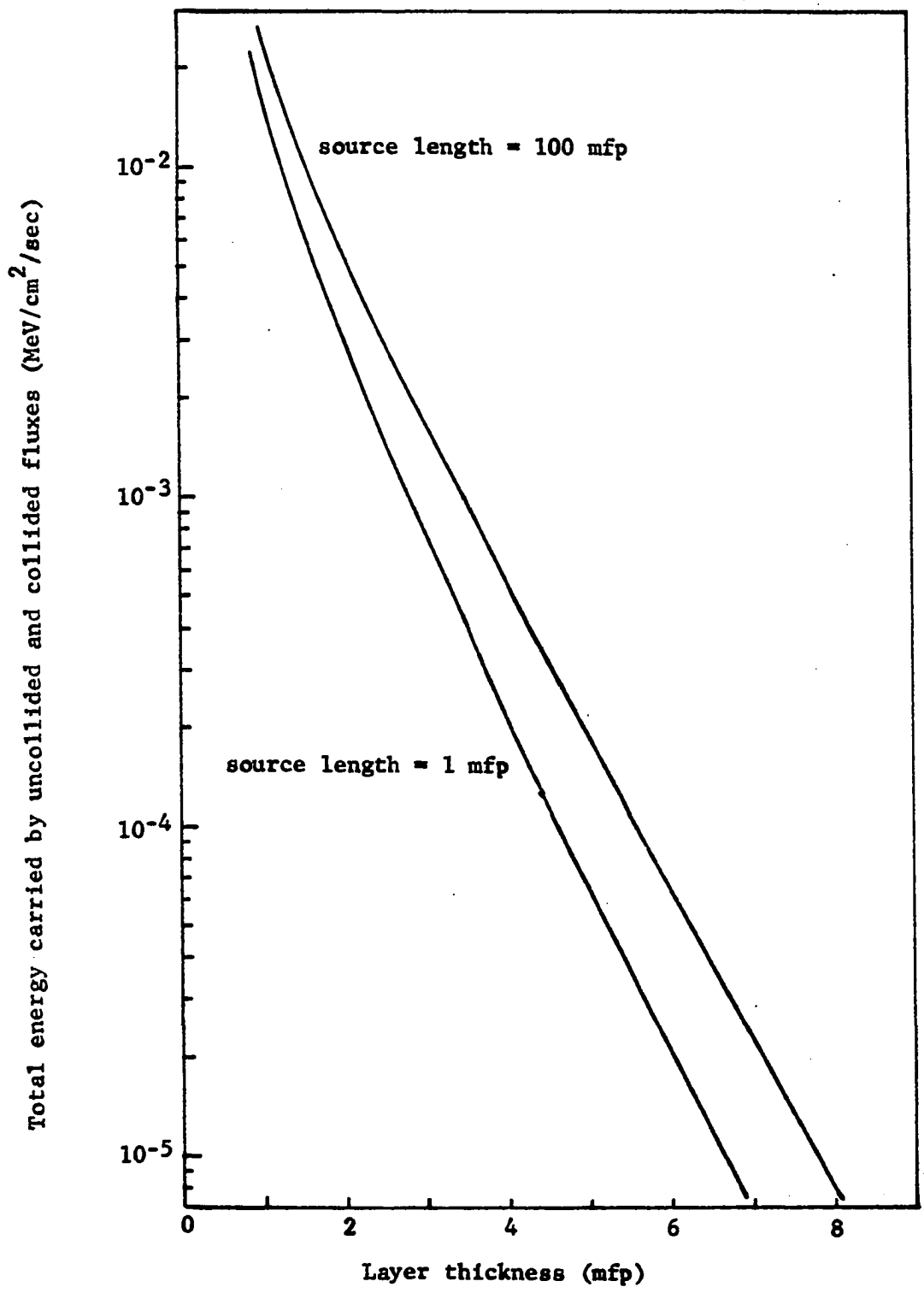

Fig. 22. Total energy carried by uncollided and collided fluxes for various source lengths. Medium: iron, isotropic source energy = 1 MeV, source strength = 1 MeV/cm/sec.

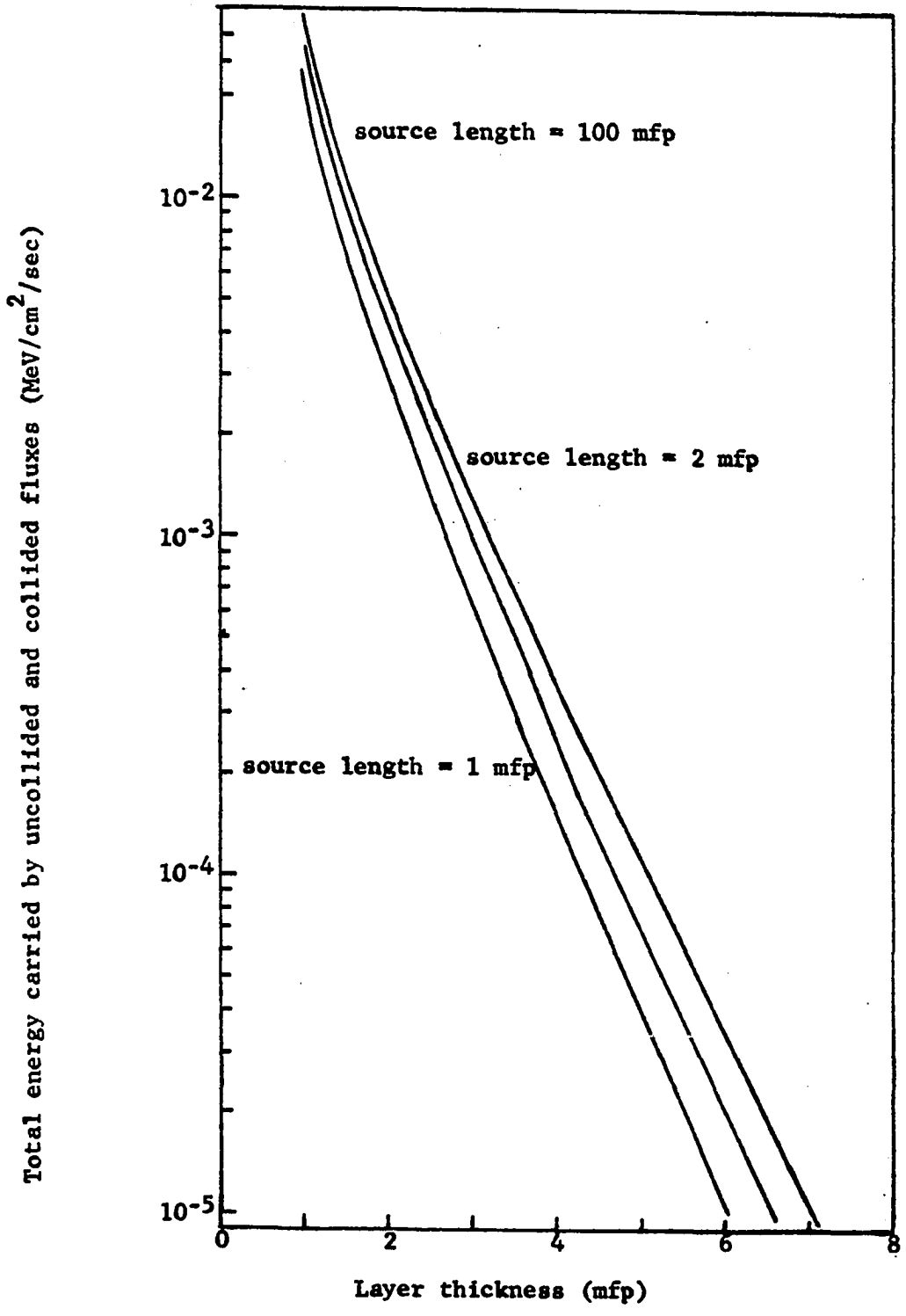

Fig. 23. Total energy carried by uncollided and collided fluxes for various source lengths. Medium: lead, isotropic source energy = 1 MeV, source strength = 1 MeV/cm/sec.

VI. CONCLUSION

Few results have been reported on the line source radiation analyses because of the lack of suitable methods and of the difficulty of mathematics even through the extended point kernel methods give the mathematical expressions for the uncollided flux. The point matrix kernel method has been applied to some gamma ray transport problems from isotropic uniform line sources. The extended point kernel method has shown to be a simple and easy way to calculate radiation from a line source if appropriate buildup factor data are available.

Since the point matrix kernel contains both the uncollided and collided operators, it can calculate total functionals of the flux as a function of energy and thickness of a slab. Therefore, the weakness of the buildup factor concept can be avoided. Since the uncollided flux calculation agrees well with the point matrix kernel and the extended point kernel methods, the extended point kernel method can be used more extensively if the appropriate buildup factors and their coefficients are generated by the point matrix kernel method.

Although the transmission matrix method can be applied for any geometry [1], the present applications have been limited for plane source geometry. The point matrix kernel which has been derived from plane geometry can extend the application of the method not only for point source but also for other source geometries such as line source, and possibly cylindrical volume source and spherical volume source.

All necessary data for the point matrix kernel are the intermediate results of the plane source calculation of the transmission

matrix method. Since the intermediate results are independent of thickness of a slab, they need be calculated only once and can be stored on cards, disk or tape. Using the intermediate results the point kernel method only requires some simple matrix operation, including some integrations depending on source geometry.

The point matrix kernel may be able to be a powerful tool in parametric and optimization studies without any large investment in experimental facilities. Since the transmission and reflection operators can be experimentally measured, both results can easily be compared.

Gaussian quadrature has been shown to be a good, easy and accurate method to integrate the modified secant integral and the Lanczos's error estimation formula has shown reasonable results except near $\theta_o = 90^o$.

VII. SUGGESTIONS FOR FURTHER STUDY

Since point kernel methods can give precise mathematical expressions for problems, they can solve many problems. As has been shown, the point matrix kernel method has been applied only for single layers with isotropic uniform gamma ray line source.

Further work can be done in the following areas:

1. In order to evaluate the point matrix kernel method for the analyses of radiation from a line source, some comparative work, such as experimental work, that would be desirable.
2. Application of the point matrix kernel for multi-layered slabs including the integration method of the modified secant integral for multi-layered. Possibly, Gaussian quadrature can be used.
3. Examination of the effects of double reflections for thick multi-layered slabs.
4. Application of the point matrix kernel to some other geometry such as cylindrical volume source and spherical volume source.
5. Parametric and optimum studies using the point matrix kernel.
6. Application of the point matrix kernel to neutron studies.

VIII. BIBLIOGRAPHY

1. R. ARONSON and D. YARMUSH, J. Math. Phys., 7, 221 (1966).

2. R. E. BELLMAN, R. E. KALABA and G. M. WING, J. Math. Phys., 1, 280 (1960).

3. M. J. BERGER, Proceedings of Shielding Symposium Held at the Naval Radiological Defense Lab., USNRDL Reviews and Lectures No. 29, 47 (1956).

4. E. P. BLIZARD, Reactor Handbook, E. P. Blizard, Ed., Vol. III, Part B, Ch. 11, Interscience Publishers, New York (1962).

5. B. G. CARLSON, "Solution of the Transport Equation by Sn Approximation," LA-1599, Los Alamos Nat. Lab. (1953).

6. K. M. CASE, F. HOFFMAN and G. PLACZEK, Introduction to the Theory of Neutron Diffusion, Vol. 1, Government Printing Office, Washington, D.C. (1953).

7. E. D. CASWELL and C. J. EVERETT, A Practical Manual on the Monte Carlo Method for Random Walk Problems, Pergamon Press, New York (1959).

8. J. CERTAINE, "A Solution of the Neutron Transport Equation," NYO-3081, Nuclear Development Associates (1954).

9. R. L. CHAMBERLAIN and D. JOWETT, The OMNITAB Programming System, Statistical Lab., Iowa State University, Ames, Iowa (1968).

10. S. CHANDRASEKHAR, Radiation Transfer, Oxford University Press, London (1950).

11. F. CLARK, in Reactor Handbook, E. P. Blizard, Ed., Vol. III, Part B, p. 150, Interscience Publishers, New York (1962).

12. M. CLARK and K. F. HANSEN, Numerical Methods of Reactor Analysis, Academic Press, New York (1964).

13. B. DAVISON, Neutron Transport Theory, Oxford University Press, New York (1956).

14. H. B. DWIGHT, Table of Integrals and Other Mathematical Data, Macmillan Co., New York (1968).

15. R. D. EVANS, Atomic Nucleus, McGraw-Hill, New York (1955).

16. U. FANO, L. V. SPENCER and M. J. BERGER, in Encyclopedia of Physics, S. Flügge, Ed., pp. 724-730, Springer, Berlin (1959).

17. C. FARMER, D. S. GOODEN, and J. HOGRTH, Nuc. Eng. Design, 15, 265 (1971).

18. A. FODERARO, in Engineering Compendium on Radiation Shielding, R. G. Jaeger, Ed., Vol. 1, pp. 124-126, IAEA, Vienna (1968).

19. H. GOLDSTEIN and J. E. WILKINS, "Calculation of the Penetration of Gamma Rays," NYO-3075, Nuclear Development Associates (1954).

20. INTERNATIONAL BUSINESS MACHINES CORPORATION, "System/360 Scientific Subroutine Package (360A-CM-03X) Version III," CH20-0166-5, pp. 368-369. International Business Machines Corp., Data Processing Div., White Plains (1970).

21. H. KAHN, Nucleonics, 6, 27 (1950).

22. I. KATAOKA, in Proceedings of the Third International Conference on the Peaceful Uses of Atomic Energy, Vol. 4, pp. 386-394, United Nations, New York (1965).

23. V. KOURGANOFF, Basic Methods in Transport Problems, Oxford University Press, London (1952).

24. C. LANCZOS, Applied Analysis, Prentice-Hall, Englewood Cliffs, N.J. (1956).

25. C. H. LOVE, "Abscissa and Weights for Gaussian Quadrature," Nat. Bur. Stands. Monograph 98 (1966).

26. D. R. MATHEWS, K. F. HANSEN and E. A. MASON, Nuc. Sci. Eng., 27, 263 (1967).

27. A. H. MAUTE, "Direct Determination of Transmission and Reflection Matrix for Gamma Rays," ORNL-Tr-2214, Oak Ridge Nat. Lab. (1968).

28. R. V. MEGHREBLIAN and D. K. HOLMES, Reactor Analysis, McGraw-Hill, New York (1960).

29. J. O. MINGLE, Nuc. Sci. Eng., 28, 177 (1967).

30. E. E. MORRIS and A. B. CHILTON, Nuc. Sci. Eng., 40, 128 (1970).

31. P. M. MORSE and H. FESHBACH, Methods of Theoretical Physics, Vol. II, McGraw-Hill, New York (1953).

32. G. H. PEEBLES and M. S. PLESSET, Phys. Rev., 81, 430 (1951).

33. S. PREISER, G. RABINOWITZ and E. De. DUFOUR, "A Program for the Numerical Integration of the Boltzmann Equation — NIOBE," ARL Technical Report 60-314, Aeronautical Research Lab. (1960).

34. A. F. ROHACH, "Application of the Transmission Matrix to Radiation Shielding," Final Report (ISU-ERI-AMES-72014), Engineering Research Institute, Iowa State University, Ames, Iowa (1972).

35. S. SAKAMOTO, in Reactor Handbook, E. P. Blizard, Ed., Vol. III, Part B, p. 139, Interscience Publishers, New York (1962).

36. R. M. SIEVERT, Acta. Radiol., 1, 89 (1921).

37. D. K. TRUBEY, "A Survey of Empirical Functions Used to Fit Gamma-Ray Buildup Factors," ORNL-RSIC-10, Oak Ridge Nat. Lab. (1966).

38. W. A. WATSON, T. PHILIPSON and P. JOATES, Numerical Analysis, Vol. I & II, American Elsevier Publishing Co., New York (1969).

39. A. M. WEINBERG and E. P. WIGNER, The Physical Theory of Neutron Chain Reactor, University of Chicago Press, Chicago (1958).

40. YARMUSH, J. ZELL and R. ARONSON, "The Transmission Matrix Method for Penetration Problem," Technical Report 57-772, Wright Air Development Center (1956).

IX. ACKNOWLEDGMENT

The author wishes to express his gratitude to Dr. Alfred Rohach for his suggestions, guidance and assistance in this investigation, and to Dr. Glenn Murphy for continuous guidance and encouragement through his entire graduate study.

The author wishes to thank Drs. Harry Hale, Rajbir Singh Dahiya and Michael Ringham who, along with Drs. Rohach and Murphy, formed his graduate committee.

The author extends thanks to the Department of Nuclear Engineering, Iowa State University, which hired him as an assistant and gave him financial support.

Finally the author wishes frankly to thank his wife Tazuko for her continuous understanding and great patience.

X. APPENDIX A:

APPLICATION OF MODIFIED SECANT INTEGRAL FOR SHIELDING CALCULATION

The modified secant integral function defined as

$$F(x, \theta_1) = \int_0^{\theta_1} \sec\theta \exp(-x \sec\theta) d\theta, \qquad \text{(A-1)}$$

where $x \geq 0$ and $0 < \theta_1 < 90^o$, appears in the shielding calculation.

An illustration of the modified secant integral as used in a shielding calculation is shown in Fig. A-1.

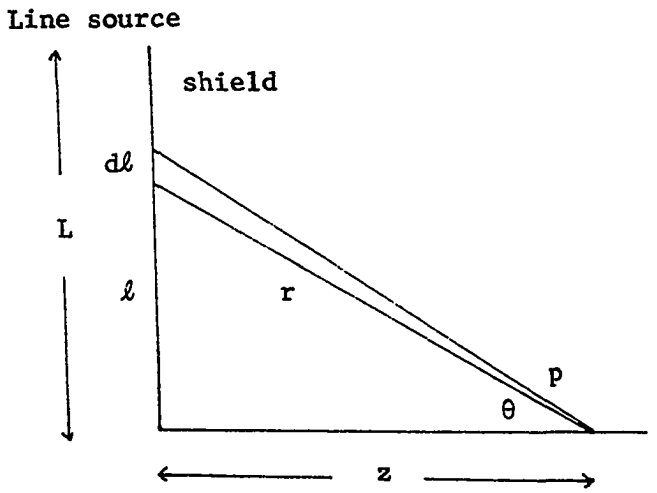

Fig. A-1. Radiation calculation from line source with the Berger's form buildup factors [3].

The monoenergetic uncollided photon flux, $\phi_u(z)$ at the point p due to a small increment of length $d\ell$ is given by

$$d\phi_u(z) = \frac{S d\ell}{4\pi r^2} \exp(-\mu r) \qquad \text{(A-2)}$$

where

S = uniformly distributed isotropic monoenergetic line source per unit length per unit time

μ = linear attenuation coefficient of shielding material.

This expression may be integrated along the line source to obtain

$$\phi_u(z) = \frac{S}{4\pi z}\int_{\theta_1}^{\theta_2} \exp(-\mu z \sec\theta)\,d\theta$$

$$= \frac{S}{4\pi z}\left[\mathrm{SECI}(\mu z, \theta_2) - \mathrm{SECI}(\mu z, \theta_1)\right] \qquad \text{(A-3)}$$

where SECI is the Sievert integral [36] or secant integral. In Fig. A-1 $\theta_1 = \tan^{-1}(L_1/z) = 0$ and $\theta_2 = \tan^{-1}(L_2/z)$ where $L_2 = L$.

In order to calculate the collided photon flux it is usual to use buildup factors. In particular, the Berger's form buildup factors [3] are convenient. Thus, collided flux, $\phi_c(z)$ at the point p due to a small increment of length $d\ell$ is given by

$$d\phi_c(z) = \frac{S\,d\ell}{4\pi r^2} C\mu r \exp(-(1 - D)\mu r) \qquad \text{(A-4)}$$

where C and D are constant coefficients of the Berger's form buildup factor. This expression may again be integrated to obtain

$$\phi_c(z) = \frac{SC\mu z}{4\pi z}\int_{\theta_1}^{\theta_2} \sec\theta \exp(-(1 - D)\mu z \sec\theta)\,d\theta \qquad \text{(A-5)}$$

where μz is the thickness in terms of mean free path lengths and $(1 - D)\mu z$ is replaced by x for the integral part of Eq. (A-5) which can be compared with Eq. (A-1).

XI. APPENDIX B:

INTERPOLATION OF THE TABLE OF THE MODIFIED SECANT INTEGRAL

The modified secant integral has been defined

$$F(x, \theta_o) = \int_0^{\theta_o} \sec\theta \exp(-x \sec\theta) d\theta.$$

There is some merit to a log $F(x, \theta_o)$ versus x representation since an essentially linear interpolation procedure can be applied. To apply a tabulated table for typical shielding calculation one needs the quick evaluation of $F(x + \Delta x, \theta_o + \Delta\theta)$ from the entries in the table. In the first step $F(x, \theta_o + \Delta\theta)$ is approximated by use of Simpson's rule [38] for $h = \Delta\theta/2$. Therefore

$$F(x, \theta_o + \Delta\theta) = F(x, \theta_o) + \frac{\Delta\theta}{6} \left\{ f(x, \theta_o) + 4f(x, \theta_o + \Delta\theta/2) + f(x, \theta_o + \Delta\theta) \right\} + E, \qquad \text{(B-1)}$$

where

$$f(x, \theta) = \sec\theta \exp(-x \sec\theta)$$

$$E = -\frac{(\Delta\theta)^5}{2^5 \cdot 90} f^{(4)}(x, \theta).$$

For sufficiently small $\Delta\theta$

$$F(x, \theta_o + \Delta\theta) \approx F(x, \theta_o) + \Delta\theta \sec\theta_o \exp(-x \sec\theta_o). \qquad \text{(B-2)}$$

The next step in the interpolation procedure involves calculation of the magnitude of $F(x + \Delta x, \theta + \Delta\theta)$ from the values of $F(x, \theta + \Delta\theta)$ and $F(x + 1, \theta + \Delta\theta)$. Fortunately, $\log(F(x + \Delta x, \theta))$ is almost linearly proportional to small variation, Δx with constant θ.

Thus $F(x + \Delta x, \theta + \Delta\theta)$ can be obtained by the following interpolation procedure:

Step 1. Calculate by use of Simpson's rule for $h = \Delta\theta/2$

$F(x, \theta + \Delta\theta)$ and $F(x + 1, \theta + \Delta\theta)$.

Step 2. Calculate

$\log(F(x, \theta + \Delta\theta))$ and $\log(F(x + 1, \theta + \Delta\theta))$.

Step 3. Obtain

$\log(F(x + \Delta x, \theta + \Delta\theta))$

by use of the simple linear interpolation with fixed angle, $\theta + \Delta\theta$, and obtain

$F(x + \Delta x, \theta + \Delta\theta)$.

XII. APPENDIX C:

FITTING FUNCTIONS FOR THE MODIFIED SECANT INTEGRAL WITH $\theta = \pi/2$

The least square fitting technique [9] was used to find the functions to calculate the modified secant integral,

$$F(x, \pi/2) = \int_0^{\pi/2} \sec\theta \exp(-x \sec\theta) d\theta. \qquad \text{(C-1)}$$

The input data were taken from Appendix D. Since the integral values in Appendix D suggest some exponential relations, several polynomial functions were tested using the OMNITAB program [9].

Fitting results are as follows:

for $0.001 \leq x \leq 1.0$

i. $$F(x, \pi/2) = 4.190355 \times 10^{-1} - 1.428022 \log x + 1.007631 (\log x)^2 + 5.669273 \times 10^{-1} (\log x)^3 + 1.543718 \times 10^{-1} (\log x)^4 + 1.623888 \times 10^{-2} (\log x)^5$$

with fitting standard deviation 1.862×10^{-3} in $F(x, \pi/2)$.

ii. $$F(x, \pi/2) = 4.208220 \times 10^{-1} - 1.381036 \log x + 1.196866 (\log x)^2 + 8.394446 \times 10^{-1} (\log x)^3 + 3.305444 \times 10^{-1} (\log x)^4 + 6.862700 \times 10^{-2} (\log x)^5 + 5.837061 \times 10^{-3} (\log x)^6$$

with fitting standard deviation 2.472×10^{-4} in $F(x, \pi/2)$.

for $1.0 \leq x \leq 20.0$

i. $$\log F(x, \pi/2) = 2.149595 \times 10^{-1} - 6.212889 \times 10^{-1}x + 2.744778 \times 10^{-2}x^2 - 2.293096 \times 10^{-3}x^3 + 9.523916 \times 10^{-5}x^4 - 1.532902\ 10^{6}x^5$$

with fitting standard deviation 3.862×10^{-3} in $\log F(x, \pi/2)$.

ii. $$\log F(x, \pi/2) = 2.672359 \times 10^{-1} - 6.975868 \times 10^{-1}x + 6.286472 \times 10^{-2}x^2 - 9.768385 \times 10^{-3}x^3 + 9.153930 \times 10^{-4}x^4 - 5.00050 \times 10^{-5}x^5 + 1.463020 \times 10^{-6}x^6 - 1.768441 \times 10^{-8}x^7$$

with fitting standard deviation 1.028×10^{-3} in $\log F(x, \pi/2)$.

for $10.0 \leq x \leq 40.0$

i. $$\log F(x, \pi/2) = -\ 1.778161 \times 10^{-1} - 4.632313 \times 10^{-1}x + 6.133018 \times 10^{-4}x^2 - 5.491196 \times 10^{-6}x^3$$

with fitting standard deviation 7.414×10^{-4} in $\log F(x, \pi/2)$.

ii. $$\log F(x, \pi/2) = -\ 1.246801 \times 10^{-1} - 4.731684 \times 10^{-1}x + 1.265309 \times 10^{-2}x^2 - 2.341907 \times 10^{-5}x^3 + 1.757636 \times 10^{-7}x^4$$

with fitting standard deviation 1.971×10^{-4} in $\log F(x, \pi/2)$.

XIII. APPENDIX D:

VALUES OF THE MODIFIED SECANT INTEGRAL

MODIFIED SECANT INTEGRAL

X	ANGLE	MSECI VALUE
0.0	1.0	1.74535E-02
0.C	2.0	3.49125E-02
0.0	3.0	5.23833E-02
0.C	4.0	6.98690E-02
0.0	5.0	8.73766E-02
0.0	6.0	1.04910E-01
0.0	7.0	1.22478E-01
0.0	8.0	1.40081E-01
0.0	9.0	1.57729E-01
0.0	10.0	1.75424E-01
0.0	11.0	1.93175E-01
0.0	12.0	2.10986E-01
0.0	13.0	2.28864E-01
C.0	14.0	2.46813E-01
0.0	15.0	2.64841E-01
0.0	16.0	2.82954E-01
0.0	17.0	3.01156E-01
0.0	18.0	3.19457E-01
0.0	19.0	3.37861E-01
0.0	20.0	3.56377E-01
0.0	30.0	5.49305E-01
0.0	40.0	7.62908E-01
0.0	50.0	1.01068E 00
0.0	60.0	1.31695E 00
0.0	70.0	1.73541E 00
0.0	80.0	2.43622E 00

MODIFIED SECANT INTEGRAL

X	ANGLE	MSECI VALUE	ERROR
0.1	1.0	1.57930E-02	1.38E-08
0.1	2.0	3.15903E-02	1.16E-07
0.1	3.0	4.73963E-02	3.97E-07
0.1	4.0	6.32153E-02	9.46E-07
0.1	5.0	7.90517E-02	1.86E-06
0.1	6.0	9.49095E-02	3.21E-06
0.1	7.0	1.10794E-01	5.11E-06
0.1	8.0	1.26709E-01	7.65E-06
0.1	9.0	1.42659E-01	1.09E-05
0.1	10.0	1.58649E-01	1.50E-05
0.1	12.0	1.90766E-01	2.61E-05
0.1	14.0	2.23098E-01	4.16E-05
0.1	16.0	2.55683E-01	6.26E-05
0.1	18.0	2.88562E-01	8.98E-05
0.1	20.0	3.21776E-01	1.24E-04
0.1	30.0	4.94503E-01	4.45E-04
0.1	40.0	6.83471E-01	1.15E-03
0.1	50.0	8.98379E-01	2.56E-03
0.1	60.0	1.15514E 00	5.29E-03
0.1	70.0	1.48355E 00	1.08E-02
0.1	80.0	1.94684E 00	2.31E-02
0.1	90.0	2.42704E 00	9.11E-05
0.2	1.0	1.42900E-02	1.22E-08
0.2	2.0	2.85835E-02	1.05E-07
0.2	3.0	4.28839E-02	3.59E-07
0.2	4.0	5.71949E-02	8.56E-07
0.2	5.0	7.15198E-02	1.68E-06
0.2	6.0	8.58622E-02	2.91E-06
0.2	7.0	1.00226E-01	4.62E-06
0.2	8.0	1.14613E-01	6.91E-06
0.2	9.0	1.29030E-01	9.86E-06
0.2	10.0	1.43478E-01	1.36E-05
0.2	12.0	1.72484E-01	2.35E-05
0.2	14.0	2.01662E-01	3.76E-05
0.2	16.0	2.31042E-01	5.64E-05
0.2	18.0	2.60656E-01	8.08E-05
0.2	20.0	2.90537E-01	1.12E-04
0.2	30.0	4.45180E-01	3.97E-04
0.2	40.0	6.12360E-01	1.01E-03
0.2	50.0	7.98770E-01	2.19E-03
0.2	60.0	1.01406E 00	4.33E-03
0.2	70.0	1.27198E 00	8.08E-03
0.2	80.0	1.58024E 00	1.30E-02
0.2	90.0	1.75269E 00	3.07E-06

MODIFIED SECANT INTEGRAL

X	ANGLE	MSECI VALUE	ERROR
0.4	1.0	1.16996E-02	1.02E-08
0.4	2.0	2.34013E-02	8.65E-08
0.4	3.0	3.51073E-02	2.95E-07
0.4	4.0	4.68196E-02	7.00E-07
0.4	5.0	5.85406E-02	1.37E-06
0.4	6.0	7.02721E-02	2.38E-06
0.4	7.0	8.20167E-02	3.78E-06
0.4	8.0	9.37763E-02	5.65E-06
0.4	9.0	1.05553E-01	8.05E-06
0.4	10.0	1.17349E-01	1.11E-05
0.4	12.0	1.41008E-01	1.92E-05
0.4	14.0	1.64772E-01	3.06E-05
0.4	16.0	1.88657E-01	4.58E-05
0.4	18.0	2.12682E-01	6.55E-05
0.4	20.0	2.36866E-01	9.03E-05
0.4	30.0	3.60825E-01	3.15E-04
0.4	40.0	4.91682E-01	7.81E-04
0.4	50.0	6.31958E-01	1.61E-03
0.4	60.0	7.83392E-01	2.90E-03
0.4	70.0	9.42815E-01	4.50E-03
0.4	80.0	1.08185E 00	4.10E-03
0.4	90.0	1.11452E 00	1.06E-07
0.5	1.0	1.05861E-02	9.15E-09
0.5	2.0	2.11739E-02	7.77E-08
0.5	3.0	3.17649E-02	2.66E-07
0.5	4.0	4.23606E-02	6.33E-07
0.5	5.0	5.29630E-02	1.24E-06
0.5	6.0	6.35732E-02	2.15E-06
0.5	7.0	7.41932E-02	3.42E-06
0.5	8.0	8.48244E-02	5.10E-06
0.5	9.0	9.54686E-02	7.28E-06
0.5	10.0	1.06128E-01	9.99E-06
0.5	12.0	1.27495E-01	1.73E-05
0.5	14.0	1.48941E-01	2.76E-05
0.5	16.0	1.70477E-01	4.13E-05
0.5	18.0	1.92116E-01	5.90E-05
0.5	20.0	2.13872E-01	8.12E-05
0.5	30.0	3.24856E-01	2.81E-04
0.5	40.0	4.40631E-01	6.85E-04
0.5	50.0	5.62326E-01	1.38E-03
0.5	60.0	6.89363E-01	2.38E-03
0.5	70.0	8.14831E-01	3.36E-03
0.5	80.0	9.09032E-01	2.30E-03
0.5	90.0	9.24414E-01	3.68E-08

MODIFIED SECANT INTEGRAL

X	ANGLE	MSECI VALUE	ERROR
0.6	1.0	9.57868E-03	8.19E-09
0.6	2.0	1.91585E-02	7.03E-08
0.6	3.0	2.87407E-02	2.41E-07
0.6	4.0	3.83264E-02	5.73E-07
0.6	5.0	4.79167E-02	1.12E-06
0.6	6.0	5.75129E-02	1.94E-06
0.6	7.0	6.71160E-02	3.09E-06
0.6	8.0	7.67273E-02	4.61E-06
0.6	9.0	8.63479E-02	6.58E-06
0.6	10.0	9.59790E-02	9.03E-06
0.6	12.0	1.15277E-01	1.56E-05
0.6	14.0	1.34630E-01	2.49E-05
0.6	16.0	1.54048E-01	3.72E-05
0.6	18.0	1.73539E-01	5.31E-05
0.6	20.0	1.93112E-01	7.30E-05
0.6	30.0	2.92479E-01	2.50E-04
0.6	40.0	3.94913E-01	6.01E-04
0.6	50.0	5.00493E-01	1.18E-03
0.6	60.0	6.07080E-01	1.95E-03
0.6	70.0	7.05895E-01	2.51E-03
0.6	80.0	7.70069E-01	1.30E-03
0.6	90.0	7.77521E-01	1.47E-09
0.8	1.0	7.84233E-03	7.17E-09
0.8	2.0	1.56851E-02	5.87E-08
0.8	3.0	2.35289E-02	1.99E-07
0.8	4.0	3.13741E-02	4.71E-07
0.8	5.0	3.92212E-02	9.21E-07
0.8	6.0	4.70706E-02	1.59E-06
0.8	7.0	5.49228E-02	2.53E-06
0.8	8.0	6.27784E-02	3.77E-06
0.8	9.0	7.06375E-02	5.38E-06
0.8	10.0	7.85009E-02	7.37E-06
0.8	12.0	9.42416E-02	1.27E-05
0.8	14.0	1.10004E-01	2.02E-05
0.8	16.0	1.25790E-01	3.02E-05
0.8	18.0	1.41602E-01	4.30E-05
0.8	20.0	1.57443E-01	5.90E-05
0.8	30.0	2.37100E-01	1.99E-04
0.8	40.0	3.17290E-01	4.63E-04
0.8	50.0	3.96774E-01	8.62E-04
0.8	60.0	4.71845E-01	1.31E-03
0.8	70.0	5.33259E-01	1.40E-03
0.8	80.0	5.63499E-01	4.09E-04
0.8	90.0	5.65346E-01	5.15E-09

MODIFIED SECANT INTEGRAL

X	ANGLE	MSECI VALUE	ERROR
1.0	1.0	6.42069E-03	5.93E-09
1.0	2.0	1.28414E-02	4.81E-08
1.0	3.0	1.92621E-02	1.63E-07
1.0	4.0	2.56828E-02	3.86E-07
1.0	5.0	3.21034E-02	7.53E-07
1.0	6.0	3.85240E-02	1.30E-06
1.0	7.0	4.49446E-02	2.07E-06
1.0	8.0	5.13650E-02	3.08E-06
1.0	9.0	5.77853E-02	4.39E-06
1.0	10.0	6.42053E-02	6.02E-06
1.0	12.0	7.70444E-02	1.04E-05
1.0	14.0	8.98815E-02	1.65E-05
1.0	16.0	1.02715E-01	2.45E-05
1.0	18.0	1.15543E-01	3.49E-05
1.0	20.0	1.28364E-01	4.77E-05
1.0	30.0	1.92221E-01	1.58E-04
1.0	40.0	2.55003E-01	3.57E-04
1.0	50.0	3.14852E-01	6.32E-04
1.0	60.0	3.67759E-01	8.75E-04
1.0	70.0	4.06031E-01	7.80E-04
1.0	80.0	4.20543E-01	1.29E-04
1.0	90.0	4.21024E-01	5.89E-09
2.0	1.0	2.36192E-03	2.11E-09
2.0	2.0	4.72311E-03	1.75E-08
2.0	3.0	7.08286E-03	5.95E-08
2.0	4.0	9.44046E-03	1.41E-07
2.0	5.0	1.17952E-02	2.76E-07
2.0	6.0	1.41462E-02	4.76E-07
2.0	7.0	1.64929E-02	7.54E-07
2.0	8.0	1.88346E-02	1.12E-06
2.0	9.0	2.11703E-02	1.59E-06
2.0	10.0	2.34995E-02	2.18E-06
2.0	12.0	2.81349E-02	3.74E-06
2.0	14.0	3.27345E-02	5.88E-06
2.0	16.0	3.72918E-02	8.67E-06
2.0	18.0	4.18000E-02	1.22E-05
2.0	20.0	4.62521E-02	1.65E-05
2.0	30.0	6.74024E-02	4.97E-05
2.0	40.0	8.58898E-02	9.67E-05
2.0	50.0	1.00421E-01	1.33E-04
2.0	60.0	1.09708E-01	1.18E-04
2.0	70.0	1.13443E-01	4.19E-05
2.0	80.0	1.13892E-01	4.00E-07
2.0	90.0	1.13893E-01	6.62E-09

MODIFIED SECANT INTEGRAL

X	ANGLE	MSECI VALUE	ERROR
3.0	1.0	8.68853E-04	7.44E-10
3.0	2.0	1.73718E-03	6.36E-09
3.0	3.0	2.60444E-03	2.18E-08
3.0	4.0	3.47012E-03	5.17E-08
3.0	5.0	4.33368E-03	1.01E-07
3.0	6.0	5.19458E-03	1.74E-07
3.0	7.0	6.05232E-03	2.75E-07
3.0	8.0	6.90633E-03	4.09E-07
3.0	9.0	7.75610E-03	5.79E-07
3.0	10.0	8.60111E-03	7.89E-07
3.0	12.0	1.02747E-02	1.34E-06
3.0	14.0	1.19228E-02	2.10E-06
3.0	16.0	1.35411E-02	3.06E-06
3.0	18.0	1.51254E-02	4.26E-06
3.0	20.0	1.66715E-02	5.68E-06
3.0	30.0	2.36815E-02	1.56E-05
3.0	40.0	2.91357E-02	2.62E-05
3.0	50.0	3.26817E-02	2.81E-05
3.0	60.0	3.43370E-02	1.60E-05
3.0	70.0	3.47226E-02	2.25E-06
3.0	80.0	3.47395E-02	6.90E-10
3.0	90.0	3.47395E-02	6.44E-10
4.0	1.0	3.19619E-04	2.93E-10
4.0	2.0	6.38945E-04	2.38E-09
4.0	3.0	9.57688E-04	8.05E-09
4.0	4.0	1.27556E-03	1.91E-08
4.0	5.0	1.59226E-03	3.71E-08
4.0	6.0	1.90750E-03	6.38E-08
4.0	7.0	2.22101E-03	1.01E-07
4.0	8.0	2.53248E-03	1.49E-07
4.0	9.0	2.84164E-03	2.11E-07
4.0	10.0	3.14821E-03	2.86E-07
4.0	12.0	3.75244E-03	4.84E-07
4.0	14.0	4.34297E-03	7.48E-07
4.0	16.0	4.91767E-03	1.08E-06
4.0	18.0	5.47446E-03	1.49E-06
4.0	20.0	6.01136E-03	1.96E-06
4.0	30.0	8.33634E-03	4.93E-06
4.0	40.0	9.94841E-03	7.10E-06
4.0	50.0	1.08180E-02	5.94E-06
4.0	60.0	1.11173E-02	2.17E-06
4.0	70.0	1.11589E-02	1.20E-07
4.0	80.0	1.11596E-02	4.60E-10
4.0	90.0	1.11596E-02	5.52E-10

MODIFIED SECANT INTEGRAL

X	ANGLE	MSECI VALUE	ERROR
5.0	1.0	1.17575E-04	1.03E-10
5.0	2.0	2.35006E-04	8.66E-10
5.0	3.0	3.52152E-04	2.95E-09
5.0	4.0	4.68869E-04	6.98E-09
5.0	5.0	5.85015E-04	1.36E-08
5.0	6.0	7.00451E-04	2.33E-08
5.0	7.0	8.15038E-04	3.67E-08
5.0	8.0	9.28636E-04	5.43E-08
5.0	9.0	1.04111E-03	7.65E-08
5.0	10.0	1.15233E-03	1.04E-07
5.0	12.0	1.37048E-03	1.74E-07
5.0	14.0	1.58208E-03	2.67E-07
5.0	16.0	1.78617E-03	3.83E-07
5.0	18.0	1.98184E-03	5.20E-07
5.0	20.0	2.16829E-03	6.76E-07
5.0	30.0	2.93992E-03	1.55E-06
5.0	40.0	3.41726E-03	1.93E-06
5.0	50.0	3.63154E-03	1.25E-06
5.0	60.0	3.68639E-03	2.93E-07
5.0	70.0	3.69104E-03	6.21E-09
5.0	80.0	3.69108E-03	2.90E-10
5.0	90.0	3.69108E-03	2.53E-10
6.0	1.0	4.32511E-05	3.72E-11
6.0	2.0	8.64364E-05	3.18E-10
6.0	3.0	1.29490E-04	1.08E-09
6.0	4.0	1.72347E-04	2.56E-09
6.0	5.0	2.14942E-04	4.97E-09
6.0	6.0	2.57212E-04	8.52E-09
6.0	7.0	2.99094E-04	1.34E-08
6.0	8.0	3.40525E-04	1.98E-08
6.0	9.0	3.81445E-04	2.78E-08
6.0	10.0	4.21795E-04	3.75E-08
6.0	12.0	5.00558E-04	6.26E-08
6.0	14.0	5.76376E-04	9.52E-08
6.0	16.0	6.48851E-04	1.35E-07
6.0	18.0	7.17620E-04	1.82E-07
6.0	20.0	7.82372E-04	2.33E-07
6.0	30.0	1.03863E-03	4.90E-07
6.0	40.0	1.18023E-03	5.22E-07
6.0	50.0	1.23328E-03	2.64E-07
6.0	60.0	1.24345E-03	3.97E-08
6.0	70.0	1.24399E-03	3.08E-10
6.0	80.0	1.24399E-03	4.02E-11
6.0	90.0	1.24399E-03	4.31E-11

MODIFIED SECANT INTEGRAL

X	ANGLE	MSECI VALUE	ERROR
7.0	1.0	1.59104E-05	1.44E-11
7.0	2.0	3.17918E-05	1.18E-10
7.0	3.0	4.76152E-05	3.99E-10
7.0	4.0	6.33518E-05	9.41E-10
7.0	5.0	7.89733E-05	1.82E-09
7.0	6.0	9.44517E-05	3.12E-09
7.0	7.0	1.09760E-04	4.90E-09
7.0	8.0	1.24870E-04	7.21E-09
7.0	9.0	1.39757E-04	1.01E-08
7.0	10.0	1.54396E-04	1.36E-08
7.0	12.0	1.82833E-04	2.25E-08
7.0	14.0	2.10001E-04	3.40E-08
7.0	16.0	2.35738E-04	4.78E-08
7.0	18.0	2.59907E-04	6.35E-08
7.0	20.0	2.82394E-04	8.05E-08
7.0	30.0	3.67555E-04	1.54E-07
7.0	40.0	4.09631E-04	1.41E-07
7.0	50.0	4.22824E-04	5.58E-08
7.0	60.0	4.24731E-04	5.35E-09
7.0	70.0	4.24793E-04	1.15E-11
7.0	80.0	4.24794E-04	2.59E-11
7.0	90.0	4.24795E-04	2.30E-11
8.0	1.0	5.85281E-06	5.04E-12
8.0	2.0	1.16932E-05	4.30E-11
8.0	3.0	1.75086E-05	1.46E-10
8.0	4.0	2.32869E-05	3.45E-10
8.0	5.0	2.90159E-05	6.67E-10
8.0	6.0	3.46837E-05	1.14E-09
8.0	7.0	4.02788E-05	1.79E-09
8.0	8.0	4.57899E-05	2.62E-09
8.0	9.0	5.12060E-05	3.67E-09
8.0	10.0	5.65169E-05	4.92E-09
8.0	12.0	6.67840E-05	8.10E-09
8.0	14.0	7.65185E-05	1.21E-08
8.0	16.0	8.56584E-05	1.69E-08
8.0	18.0	9.41526E-05	2.22E-08
8.0	20.0	1.01962E-04	2.78E-08
8.0	30.0	1.30282E-04	4.86E-08
8.0	40.0	1.42806E-04	3.83E-08
8.0	50.0	1.46101E-04	1.18E-08
8.0	60.0	1.46462E-04	7.20E-10
8.0	70.0	1.46471E-04	4.31E-12
8.0	80.0	1.46471E-04	6.65E-12
8.0	90.0	1.46471E-04	9.70E-12

MODIFIED SECANT INTEGRAL

X	ANGLE	MSECI VALUE	ERROR
9.0	1.0	2.15303E-06	1.95E-12
9.0	2.0	4.30081E-06	1.60E-11
9.0	3.0	6.43815E-06	5.40E-11
9.0	4.0	8.55988E-06	1.27E-10
9.0	5.0	1.06609E-05	2.45E-10
9.0	6.0	1.27364E-05	4.18E-10
9.0	7.0	1.47814E-05	6.53E-10
9.0	8.0	1.67914E-05	9.56E-10
9.0	9.0	1.87618E-05	1.33E-09
9.0	10.0	2.06886E-05	1.78E-09
9.0	12.0	2.43956E-05	2.92E-09
9.0	14.0	2.78837E-05	4.33E-09
9.0	16.0	3.11296E-05	5.96E-09
9.0	18.0	3.41149E-05	7.75E-09
9.0	20.0	3.68271E-05	9.58E-09
9.0	30.0	4.62506E-05	1.53E-08
9.0	40.0	4.99852E-05	1.04E-08
9.0	50.0	5.08113E-05	2.48E-09
9.0	60.0	5.08803E-05	9.67E-11
9.0	70.0	5.08812E-05	2.52E-12
9.0	80.0	5.08812E-05	2.34E-12
9.0	90.0	5.08813E-05	1.98E-12
10.0	1.0	7.92014E-07	7.18E-13
10.0	2.0	1.58186E-06	5.87E-12
10.0	3.0	2.36738E-06	1.98E-11
10.0	4.0	3.14645E-06	4.65E-11
10.0	5.0	3.91699E-06	8.98E-11
10.0	6.0	4.67697E-06	1.53E-10
10.0	7.0	5.42443E-06	2.38E-10
10.0	8.0	6.15749E-06	3.48E-10
10.0	9.0	6.87438E-06	4.84E-10
10.0	10.0	7.57342E-06	6.46E-10
10.0	12.0	8.91180E-06	1.05E-09
10.0	14.0	1.01617E-05	1.54E-09
10.0	16.0	1.13144E-05	2.11E-09
10.0	18.0	1.23636E-05	2.71E-09
10.0	20.0	1.33055E-05	3.30E-09
10.0	30.0	1.64432E-05	4.83E-09
10.0	40.0	1.75586E-05	2.82E-09
10.0	50.0	1.77665E-05	5.23E-10
10.0	60.0	1.77799E-05	1.20E-11
10.0	70.0	1.77800E-05	1.62E-12
10.0	80.0	1.77800E-05	1.26E-12
10.0	90.0	1.77800E-05	1.62E-12

MODIFIED SECANT INTEGRAL

X	ANGLE	MSECI VALUE	ERROR
11.0	1.0	2.91350E-07	2.50E-13
11.0	2.0	5.81814E-07	2.14E-12
11.0	3.0	8.70510E-07	7.21E-12
11.0	4.0	1.15658E-06	1.70E-11
11.0	5.0	1.43916E-06	3.28E-11
11.0	6.0	1.71745E-06	5.58E-11
11.0	7.0	1.99065E-06	8.70E-11
11.0	8.0	2.25801E-06	1.27E-10
11.0	9.0	2.51882E-06	1.76E-10
11.0	10.0	2.77243E-06	2.34E-10
11.0	12.0	3.25565E-06	3.77E-10
11.0	14.0	3.70352E-06	5.50E-10
11.0	16.0	4.11288E-06	7.44E-10
11.0	18.0	4.48163E-06	9.46E-10
11.0	20.0	4.80878E-06	1.14E-09
11.0	30.0	5.85418E-06	1.52E-09
11.0	40.0	6.18786E-06	7.64E-10
11.0	50.0	6.24042E-06	1.11E-10
11.0	60.0	6.24300E-06	1.67E-12
11.0	70.0	6.24301E-06	2.36E-13
11.0	80.0	6.24302E-06	3.59E-13
11.0	90.0	6.24301E-06	3.48E-13
12.0	1.0	1.07177E-07	9.89E-14
12.0	2.0	2.13995E-07	7.98E-13
12.0	3.0	3.20099E-07	2.67E-12
12.0	4.0	4.25139E-07	6.27E-12
12.0	5.0	5.28775E-07	1.21E-11
12.0	6.0	6.30678E-07	2.05E-11
12.0	7.0	7.30534E-07	3.18E-11
12.0	8.0	8.28044E-07	4.62E-11
12.0	9.0	9.22932E-07	6.39E-11
12.0	10.0	1.01494E-06	8.48E-11
12.0	12.0	1.18941E-06	1.36E-10
12.0	14.0	1.34990E-06	1.96E-10
12.0	16.0	1.49528E-06	2.63E-10
12.0	18.0	1.62488E-06	3.31E-10
12.0	20.0	1.73850E-06	3.93E-10
12.0	30.0	2.08703E-06	4.80E-10
12.0	40.0	2.18700E-06	2.07E-10
12.0	50.0	2.20032E-06	2.33E-11
12.0	60.0	2.20082E-06	1.46E-13
12.0	70.0	2.20082E-06	1.24E-13
12.0	80.0	2.20082E-06	1.12E-13
12.0	90.0	2.20082E-06	1.35E-13

MODIFIED SECANT INTEGRAL

X	ANGLE	MSECI VALUE	ERROR
13.0	1.0	3.94260E-08	3.52E-14
13.0	2.0	7.87081E-08	2.91E-13
13.0	3.0	1.17704E-07	9.80E-13
13.0	4.0	1.56273E-07	2.30E-12
13.0	5.0	1.94281E-07	4.42E-12
13.0	6.0	2.31595E-07	7.48E-12
13.0	7.0	2.68093E-07	1.16E-11
13.0	8.0	3.03656E-07	1.68E-11
13.0	9.0	3.38177E-07	2.32E-11
13.0	10.0	3.71558E-07	3.07E-11
13.0	12.0	4.34551E-07	4.88E-11
13.0	14.0	4.92058E-07	7.01E-11
13.0	16.0	5.43688E-07	9.30E-11
13.0	18.0	5.89240E-07	1.16E-10
13.0	20.0	6.28701E-07	1.36E-10
13.0	30.0	7.44965E-07	1.51E-10
13.0	40.0	7.74965E-07	5.61E-11
13.0	50.0	7.78351E-07	4.87E-12
13.0	60.0	7.78450E-07	2.39E-14
13.0	70.0	7.78453E-07	5.47E-14
13.0	80.0	7.78452E-07	6.25E-14
13.0	90.0	7.78453E-07	5.26E-14
14.0	1.0	1.45032E-08	1.25E-14
14.0	2.0	2.89491E-08	1.06E-13
14.0	3.0	4.32810E-08	3.58E-13
14.0	4.0	5.74433E-08	8.42E-13
14.0	5.0	7.13820E-08	1.62E-12
14.0	6.0	8.50457E-08	2.73E-12
14.0	7.0	9.83856E-08	4.23E-12
14.0	8.0	1.11356E-07	6.13E-12
14.0	9.0	1.23915E-07	8.43E-12
14.0	10.0	1.36026E-07	1.11E-11
14.0	12.0	1.58769E-07	1.76E-11
14.0	14.0	1.79377E-07	2.50E-11
14.0	16.0	1.97712E-07	3.28E-11
14.0	18.0	2.13723E-07	4.04E-11
14.0	20.0	2.27428E-07	4.68E-11
14.0	30.0	2.66237E-07	4.77E-11
14.0	40.0	2.75254E-07	1.52E-11
14.0	50.0	2.76117E-07	1.03E-12
14.0	60.0	2.76137E-07	2.81E-15
14.0	70.0	2.76137E-07	7.02E-15
14.0	80.0	2.76137E-07	6.32E-15
14.0	90.0	2.76137E-07	7.02E-15

MODIFIED SECANT INTEGRAL

X	ANGLE	MSECI VALUE	ERROR
15.0	1.0	5.33520E-09	4.91E-15
15.0	2.0	1.06477E-08	3.97E-14
15.0	3.0	1.59150E-08	1.33E-13
15.0	4.0	2.11153E-08	3.10E-13
15.0	5.0	2.62272E-08	5.94E-13
15.0	6.0	3.12306E-08	1.00E-12
15.0	7.0	3.61064E-08	1.55E-12
15.0	8.0	4.08370E-08	2.24E-12
15.0	9.0	4.54062E-08	3.07E-12
15.0	10.0	4.97999E-08	4.03E-12
15.0	12.0	5.80118E-08	6.32E-12
15.0	14.0	6.53959E-08	8.92E-12
15.0	16.0	7.19078E-08	1.16E-11
15.0	18.0	7.75351E-08	1.41E-11
15.0	20.0	8.22953E-08	1.62E-11
15.0	30.0	9.52571E-08	1.50E-11
15.0	40.0	9.79704E-08	4.12E-12
15.0	50.0	9.81913E-08	2.15E-13
15.0	60.0	9.81952E-08	2.11E-15
15.0	70.0	9.81953E-08	2.11E-15
15.0	80.0	9.81953E-08	2.11E-15
15.0	90.0	9.81952E-08	4.91E-15
16.0	1.0	1.96262E-09	1.78E-15
16.0	2.0	3.91629E-09	1.48E-14
16.0	3.0	5.85217E-09	4.84E-14
16.0	4.0	7.76164E-09	1.14E-13
16.0	5.0	9.63640E-09	2.18E-13
16.0	6.0	1.14686E-08	3.67E-13
16.0	7.0	1.32507E-08	5.65E-13
16.0	8.0	1.49760E-08	8.14E-13
16.0	9.0	1.66384E-08	1.11E-12
16.0	10.0	1.82324E-08	1.46E-12
16.0	12.0	2.11974E-08	2.27E-12
16.0	14.0	2.38434E-08	3.18E-12
16.0	16.0	2.61561E-08	4.10E-12
16.0	18.0	2.81340E-08	4.93E-12
16.0	20.0	2.97873E-08	5.57E-12
16.0	30.0	3.41190E-08	4.73E-12
16.0	40.0	3.49367E-08	1.12E-12
16.0	50.0	3.49934E-08	4.78E-14
16.0	60.0	3.49942E-08	1.84E-15
16.0	70.0	3.49944E-08	4.52E-15
16.0	80.0	3.49943E-08	3.33E-15
16.0	90.0	3.49943E-08	2.54E-15

MODIFIED SECANT INTEGRAL

X	ANGLE	MSECI VALUE	ERROR
17.0	1.0	7.21967E-10	6.20E-16
17.0	2.0	1.44043E-09	5.39E-15
17.0	3.0	2.15191E-09	1.77E-14
17.0	4.0	2.85304E-09	4.16E-14
17.0	5.0	3.54058E-09	7.95E-14
17.0	6.0	4.21148E-09	1.34E-13
17.0	7.0	4.86285E-09	2.06E-13
17.0	8.0	5.49211E-09	2.96E-13
17.0	9.0	6.09691E-09	4.05E-13
17.0	10.0	6.67520E-09	5.29E-13
17.0	12.0	7.74575E-09	8.18E-13
17.0	14.0	8.69393E-09	1.14E-12
17.0	16.0	9.51528E-09	1.45E-12
17.0	18.0	1.02105E-08	1.72E-12
17.0	20.0	1.07847E-08	1.92E-12
17.0	30.0	1.22333E-08	1.49E-12
17.0	40.0	1.24800E-08	3.04E-13
17.0	50.0	1.24946E-08	1.06E-14
17.0	60.0	1.24947E-08	1.27E-15
17.0	70.0	1.24948E-08	2.54E-15
17.0	80.0	1.24947E-08	2.15E-15
17.0	90.0	1.24947E-08	1.93E-15
18.0	1.0	2.65585E-10	2.52E-16
18.0	2.0	5.29799E-10	2.01E-15
18.0	3.0	7.91287E-10	6.57E-15
18.0	4.0	1.04874E-09	1.54E-14
18.0	5.0	1.30089E-09	2.93E-14
18.0	6.0	1.54656E-09	4.91E-14
18.0	7.0	1.78464E-09	7.54E-14
18.0	8.0	2.01414E-09	1.08E-13
18.0	9.0	2.23417E-09	1.47E-13
18.0	10.0	2.44398E-09	1.92E-13
18.0	12.0	2.83051E-09	2.94E-13
18.0	14.0	3.17029E-09	4.05E-13
18.0	16.0	3.46200E-09	5.12E-13
18.0	18.0	3.70635E-09	6.02E-13
18.0	20.0	3.90580E-09	6.63E-13
18.0	30.0	4.39042E-09	4.70E-13
18.0	40.0	4.46498E-09	8.24E-14
18.0	50.0	4.46873E-09	2.28E-15
18.0	60.0	4.46876E-09	2.63E-16
18.0	70.0	4.46878E-09	7.89E-16
18.0	80.0	4.46877E-09	4.82E-16
18.0	90.0	4.46877E-09	8.33E-16

MODIFIED SECANT INTEGRAL

X	ANGLE	MSECI VALUE	ERROR
19.0	1.0	9.76980E-11	8.75E-17
19.0	2.0	1.94862E-10	7.11E-16
19.0	3.0	2.90965E-10	2.41E-15
19.0	4.0	3.85498E-10	5.63E-15
19.0	5.0	4.77972E-10	1.07E-14
19.0	6.0	5.67929E-10	1.79E-14
19.0	7.0	6.54949E-10	2.75E-14
19.0	8.0	7.38652E-10	3.94E-14
19.0	9.0	8.18705E-10	5.35E-14
19.0	10.0	8.94820E-10	6.94E-14
19.0	12.0	1.03438E-09	1.06E-13
19.0	14.0	1.15614E-09	1.45E-13
19.0	16.0	1.25974E-09	1.81E-13
19.0	18.0	1.34563E-09	2.10E-13
19.0	20.0	1.41490E-09	2.29E-13
19.0	30.0	1.57714E-09	1.48E-13
19.0	40.0	1.59970E-09	2.23E-14
19.0	50.0	1.60067E-09	5.92E-16
19.0	60.0	1.60068E-09	2.17E-16
19.0	70.0	1.60068E-09	1.15E-16
19.0	80.0	1.60068E-09	3.13E-16
19.0	90.0	1.60068E-09	2.44E-16
20.0	1.0	3.59393E-11	3.29E-17
20.0	2.0	7.16712E-11	2.64E-16
20.0	3.0	1.06992E-10	8.85E-16
20.0	4.0	1.41703E-10	2.06E-15
20.0	5.0	1.75616E-10	3.92E-15
20.0	6.0	2.08557E-10	6.57E-15
20.0	7.0	2.40363E-10	1.00E-14
20.0	8.0	2.70891E-10	1.44E-14
20.0	9.0	3.00015E-10	1.94E-14
20.0	10.0	3.27632E-10	2.52E-14
20.0	12.0	3.78023E-10	3.81E-14
20.0	14.0	4.21654E-10	5.16E-14
20.0	16.0	4.58448E-10	6.40E-14
20.0	18.0	4.88638E-10	7.35E-14
20.0	20.0	5.12701E-10	7.90E-14
20.0	30.0	5.67043E-10	4.68E-14
20.0	40.0	5.73874E-10	6.07E-15
20.0	50.0	5.74126E-10	1.56E-16
20.0	60.0	5.74127E-10	7.13E-17
20.0	70.0	5.74127E-10	6.03E-17
20.0	80.0	5.74127E-10	8.50E-17
20.0	90.0	5.74128E-10	1.51E-16

MODIFIED SECANT INTEGRAL

X	ANGLE	MSECI VALUE	ERROR
21.0	1.0	1.32207E-11	1.24E-17
21.0	2.0	2.63611E-11	9.71E-17
21.0	3.0	3.93422E-11	3.26E-16
21.0	4.0	5.20877E-11	7.56E-16
21.0	5.0	6.45254E-11	1.44E-15
21.0	6.0	7.65876E-11	2.40E-15
21.0	7.0	8.82130E-11	3.67E-15
21.0	8.0	9.93470E-11	5.23E-15
21.0	9.0	1.09943E-10	7.06E-15
21.0	10.0	1.19962E-10	9.11E-15
21.0	12.0	1.38156E-10	1.37E-14
21.0	14.0	1.53791E-10	1.84E-14
21.0	16.0	1.66859E-10	2.26E-14
21.0	18.0	1.77470E-10	2.57E-14
21.0	20.0	1.85829E-10	2.72E-14
21.0	30.0	2.04040E-10	1.47E-14
21.0	40.0	2.06112E-10	1.64E-15
21.0	50.0	2.06177E-10	2.64E-17
21.0	60.0	2.06178E-10	1.42E-17
21.0	70.0	2.06178E-10	2.35E-17
21.0	80.0	2.06178E-10	3.44E-17
21.0	90.0	2.06178E-10	2.36E-17
22.0	1.0	4.86335E-12	4.30E-18
22.0	2.0	9.69570E-12	3.54E-17
22.0	3.0	1.44666E-11	1.19E-16
22.0	4.0	1.91466E-11	2.77E-16
22.0	5.0	2.37079E-11	5.27E-16
22.0	6.0	2.81248E-11	8.78E-16
22.0	7.0	3.23739E-11	1.34E-15
22.0	8.0	3.64347E-11	1.90E-15
22.0	9.0	4.02896E-11	2.56E-15
22.0	10.0	4.39245E-11	3.30E-15
22.0	12.0	5.04938E-11	4.93E-15
22.0	14.0	5.60966E-11	6.57E-15
22.0	16.0	6.07379E-11	7.98E-15
22.0	18.0	6.44677E-11	8.97E-15
22.0	20.0	6.73712E-11	9.40E-15
22.0	30.0	7.34776E-11	4.64E-15
22.0	40.0	7.41071E-11	4.52E-16
22.0	50.0	7.41239E-11	1.32E-17
22.0	60.0	7.41240E-11	1.03E-17
22.0	70.0	7.41241E-11	1.44E-17
22.0	80.0	7.41240E-11	1.40E-17
22.0	90.0	7.41242E-11	1.99E-17

MODIFIED SECANT INTEGRAL

X	ANGLE	MSECI VALUE	ERROR
23.0	1.0	1.78905E-12	1.71E-18
23.0	2.0	3.56615E-12	1.33E-17
23.0	3.0	5.31957E-12	4.42E-17
23.0	4.0	7.03803E-12	1.02E-16
23.0	5.0	8.71087E-12	1.94E-16
23.0	6.0	1.03282E-11	3.22E-16
23.0	7.0	1.18813E-11	4.89E-16
23.0	8.0	1.33623E-11	6.94E-16
23.0	9.0	1.47648E-11	9.31E-16
23.0	10.0	1.60836E-11	1.20E-15
23.0	12.0	1.84556E-11	1.77E-15
23.0	14.0	2.04634E-11	2.34E-15
23.0	16.0	2.21118E-11	2.82E-15
23.0	18.0	2.34229E-11	3.14E-15
23.0	20.0	2.44314E-11	3.24E-15
23.0	30.0	2.64800E-11	1.46E-15
23.0	40.0	2.66712E-11	1.23E-16
23.0	50.0	2.66756E-11	4.28E-18
23.0	60.0	2.66756E-11	4.45E-18
23.0	70.0	2.66756E-11	4.45E-18
23.0	80.0	2.66756E-11	3.60E-18
23.0	90.0	2.66756E-11	5.31E-18
24.0	1.0	6.58120E-13	6.22E-19
24.0	2.0	1.31164E-12	4.87E-18
24.0	3.0	1.95607E-12	1.62E-17
24.0	4.0	2.58707E-12	3.74E-17
24.0	5.0	3.20057E-12	7.11E-17
24.0	6.0	3.79281E-12	1.18E-16
24.0	7.0	4.36047E-12	1.78E-16
24.0	8.0	4.90063E-12	2.53E-16
24.0	9.0	5.41C87E-12	3.38E-16
24.0	10.0	5.88931E-12	4.33E-16
24.0	12.0	6.74577E-12	6.38E-16
24.0	14.0	7.46527E-12	8.36E-16
24.0	16.0	8.05074E-12	9.97E-16
24.0	18.0	8.51158E-12	1.10E-15
24.0	20.0	8.86191E-12	1.12E-15
24.0	30.0	9.54954E-12	4.61E-16
24.0	40.0	9.60769E-12	3.31E-17
24.0	50.0	9.60886E-12	1.05E-18
24.0	60.0	9.60888E-12	1.17E-18
24.0	70.0	9.60888E-12	1.05E-18
24.0	80.0	9.60889E-12	1.55E-18
24.0	90.0	9.60887E-12	1.28E-18

MODIFIED SECANT INTEGRAL

X	ANGLE	MSECI VALUE	ERROR
25.0	1.0	2.42096E-13	2.21E-19
25.0	2.0	4.82427E-13	1.77E-18
25.0	3.0	7.19270E-13	5.95E-18
25.0	4.0	9.50964E-13	1.37E-17
25.0	5.0	1.17596E-12	2.59E-17
25.0	6.0	1.39282E-12	4.30E-17
25.0	7.0	1.60030E-12	6.52E-17
25.0	8.0	1.79731E-12	9.20E-17
25.0	9.0	1.98294E-12	1.23E-16
25.0	10.0	2.15652E-12	1.57E-16
25.0	12.0	2.46576E-12	2.29E-16
25.0	14.0	2.72360E-12	2.98E-16
25.0	16.0	2.93154E-12	3.52E-16
25.0	18.0	3.09354E-12	3.83E-16
25.0	20.0	3.21522E-12	3.86E-16
25.0	30.0	3.44617E-12	1.45E-16
25.0	40.0	3.46389E-12	9.24E-18
25.0	50.0	3.46418E-12	3.85E-19
25.0	60.0	3.46418E-12	4.39E-19
25.0	70.0	3.46418E-12	4.71E-19
25.0	80.0	3.46419E-12	7.50E-19
25.0	90.0	3.46418E-12	8.46E-19
26.0	1.0	8.90579E-14	8.63E-20
26.0	2.0	1.77440E-13	6.64E-19
26.0	3.0	2.64486E-13	2.20E-18
26.0	4.0	3.49563E-13	5.05E-18
26.0	5.0	4.32076E-13	9.52E-18
26.0	6.0	5.11490E-13	1.58E-17
26.0	7.0	5.87324E-13	2.38E-17
26.0	8.0	6.59177E-13	3.35E-17
26.0	9.0	7.26714E-13	4.47E-17
26.0	10.0	7.89689E-13	5.69E-17
26.0	12.0	9.01348E-13	8.26E-17
26.0	14.0	9.93746E-13	1.06E-16
26.0	16.0	1.06761E-12	1.25E-16
26.0	18.0	1.12455E-12	1.34E-16
26.0	20.0	1.16682E-12	1.33E-16
26.0	30.0	1.24440E-12	4.58E-17
26.0	40.0	1.24981E-12	2.54E-18
26.0	50.0	1.24988E-12	9.64E-20
26.0	60.0	1.24989E-12	2.03E-19
26.0	70.0	1.24988E-12	1.39E-19
26.0	80.0	1.24988E-12	2.14E-19
26.0	90.0	1.24988E-12	2.46E-19

MODIFIED SECANT INTEGRAL

X	ANGLE	MSECI VALUE	ERROR
27.0	1.0	3.27608E-14	3.06E-20
27.0	2.0	6.52633E-14	2.43E-19
27.0	3.0	9.72546E-14	8.05E-19
27.0	4.0	1.28494E-13	1.85E-18
27.0	5.0	1.58755E-13	3.49E-18
27.0	6.0	1.87834E-13	5.77E-18
27.0	7.0	2.15553E-13	8.70E-18
27.0	8.0	2.41758E-13	1.22E-17
27.0	9.0	2.66329E-13	1.62E-17
27.0	10.0	2.89176E-13	2.06E-17
27.0	12.0	3.29493E-13	2.97E-17
27.0	14.0	3.62605E-13	3.80E-17
27.0	16.0	3.88837E-13	4.40E-17
27.0	18.0	4.08854E-13	4.67E-17
27.0	20.0	4.23538E-13	4.59E-17
27.0	30.0	4.49619E-13	1.44E-17
27.0	40.0	4.51268E-13	6.88E-19
27.0	50.0	4.51289E-13	5.62E-20
27.0	60.0	4.51290E-13	7.50E-20
27.0	70.0	4.51291E-13	9.64E-20
27.0	80.0	4.51291E-13	9.97E-20
27.0	90.0	4.51290E-13	9.37E-20
28.0	1.0	1.20514E-14	1.07E-20
28.0	2.0	2.40041E-14	8.84E-20
28.0	3.0	3.57617E-14	2.95E-19
28.0	4.0	4.72322E-14	6.77E-19
28.0	5.0	5.83303E-14	1.28E-18
28.0	6.0	6.89784E-14	2.11E-18
28.0	7.0	7.91095E-14	3.17E-18
28.0	8.0	8.86674E-14	4.45E-18
28.0	9.0	9.76067E-14	5.89E-18
28.0	10.0	1.05895E-13	7.45E-18
28.0	12.0	1.20453E-13	1.07E-17
28.0	14.0	1.32319E-13	1.35E-17
28.0	16.0	1.41636E-13	1.55E-17
28.0	18.0	1.48673E-13	1.63E-17
28.0	20.0	1.53775E-13	1.59E-17
28.0	30.0	1.62546E-13	4.56E-18
28.0	40.0	1.63049E-13	1.93E-19
28.0	50.0	1.63055E-13	2.41E-20
28.0	60.0	1.63055E-13	2.88E-20
28.0	70.0	1.63055E-13	3.61E-20
28.0	80.0	1.63054E-13	2.54E-20
28.0	90.0	1.63055E-13	4.95E-20

MODIFIED SECANT INTEGRAL

X	ANGLE	MSECI VALUE	ERROR
29.0	1.0	4.43325E-15	4.27E-21
29.0	2.0	8.82886E-15	3.30E-20
29.0	3.0	1.31501E-14	1.09E-19
29.0	4.0	1.73620E-14	2.49E-19
29.0	5.0	2.14321E-14	4.69E-19
29.0	6.0	2.53313E-14	7.72E-19
29.0	7.0	2.90343E-14	1.16E-18
29.0	8.0	3.25201E-14	1.62E-18
29.0	9.0	3.57725E-14	2.14E-18
29.0	10.0	3.87797E-14	2.70E-18
29.0	12.0	4.40362E-14	3.85E-18
29.0	14.0	4.82884E-14	4.84E-18
29.0	16.0	5.15978E-14	5.49E-18
29.0	18.0	5.40712E-14	5.71E-18
29.0	20.0	5.58433E-14	5.47E-18
29.0	30.0	5.87944E-14	1.43E-18
29.0	40.0	5.89483E-14	5.22E-20
29.0	50.0	5.89498E-14	6.69E-21
29.0	60.0	5.89496E-14	2.01E-21
29.0	70.0	5.89498E-14	7.36E-21
29.0	80.0	5.89499E-14	1.07E-20
29.0	90.0	5.89499E-14	1.34E-20
30.0	1.0	1.63081E-15	1.51E-21
30.0	2.0	3.24729E-15	1.20E-20
30.0	3.0	4.83545E-15	4.00E-20
30.0	4.0	6.38200E-15	9.12E-20
30.0	5.0	7.87466E-15	1.72E-19
30.0	6.0	9.30246E-15	2.82E-19
30.0	7.0	1.06559E-14	4.23E-19
30.0	8.0	1.19273E-14	5.90E-19
30.0	9.0	1.31105E-14	7.78E-19
30.0	10.0	1.42015E-14	9.78E-19
30.0	12.0	1.60996E-14	1.38E-18
30.0	14.0	1.76234E-14	1.72E-18
30.0	16.0	1.87988E-14	1.94E-18
30.0	18.0	1.96684E-14	1.99E-18
30.0	20.0	2.02840E-14	1.89E-18
30.0	30.0	2.12774E-14	4.52E-19
30.0	40.0	2.13245E-14	1.49E-20
30.0	50.0	2.13249E-14	2.68E-21
30.0	60.0	2.13249E-14	3.76E-21
30.0	70.0	2.13249E-14	3.01E-21
30.0	80.0	2.13249E-14	5.48E-21
30.0	90.0	2.13249E-14	6.69E-21

MODIFIED SECANT INTEGRAL

X	ANGLE	MSECI VALUE	ERROR
31.0	1.0	5.99913E-16	5.59E-22
31.0	2.0	1.19437E-15	4.45E-21
31.0	3.0	1.77805E-15	1.46E-20
31.0	4.0	2.34593E-15	3.35E-20
31.0	5.0	2.89335E-15	6.29E-20
31.0	6.0	3.41618E-15	1.03E-19
31.0	7.0	3.91088E-15	1.54E-19
31.0	8.0	4.37458E-15	2.15E-19
31.0	9.0	4.80506E-15	2.83E-19
31.0	10.0	5.20089E-15	3.55E-19
31.0	12.0	5.88624E-15	4.98E-19
31.0	14.0	6.43236E-15	6.16E-19
31.0	16.0	6.84985E-15	6.86E-19
31.0	18.0	7.15550E-15	6.97E-19
31.0	20.0	7.36937E-15	6.52E-19
31.0	30.0	7.70393E-15	1.43E-19
31.0	40.0	7.71835E-15	4.73E-21
31.0	50.0	7.71841E-15	7.53E-22
31.0	60.0	7.71844E-15	1.55E-21
31.0	70.0	7.71842E-15	1.17E-21
31.0	80.0	7.71842E-15	1.46E-21
31.0	90.0	7.71842E-15	1.21E-21
32.0	1.0	2.20685E-16	2.11E-22
32.0	2.0	4.39296E-16	1.65E-21
32.0	3.0	6.53817E-16	5.36E-21
32.0	4.0	8.62335E-16	1.23E-20
32.0	5.0	1.06310E-15	2.31E-20
32.0	6.0	1.25455E-15	3.78E-20
32.0	7.0	1.43536E-15	5.65E-20
32.0	8.0	1.60448E-15	7.83E-20
32.0	9.0	1.76110E-15	1.03E-19
32.0	10.0	1.90470E-15	1.28E-19
32.0	12.0	2.15217E-15	1.79E-19
32.0	14.0	2.34788E-15	2.20E-19
32.0	16.0	2.49617E-15	2.42E-19
32.0	18.0	2.60362E-15	2.44E-19
32.0	20.0	2.67792E-15	2.25E-19
32.0	30.0	2.79063E-15	4.50E-20
32.0	40.0	2.79504E-15	1.18E-21
32.0	50.0	2.79508E-15	4.55E-22
32.0	60.0	2.79507E-15	2.20E-22
32.0	70.0	2.79508E-15	5.88E-22
32.0	80.0	2.79508E-15	4.68E-22
32.0	90.0	2.79507E-15	3.95E-22

MODIFIED SECANT INTEGRAL

X	ANGLE	MSECI VALUE	ERROR
33.0	1.0	8.11810E-17	7.39E-23
33.0	2.0	1.61575E-16	5.97E-22
33.0	3.0	2.40416E-16	1.96E-21
33.0	4.0	3.16982E-16	4.53E-21
33.0	5.0	3.90609E-16	8.46E-21
33.0	6.0	4.60715E-16	1.38E-20
33.0	7.0	5.26803E-16	2.06E-20
33.0	8.0	5.88482E-16	2.85E-20
33.0	9.0	6.45463E-16	3.73E-20
33.0	10.0	6.97564E-16	4.65E-20
33.0	12.0	7.86918E-16	6.44E-20
33.0	14.0	8.57055E-16	7.83E-20
33.0	16.0	9.09727E-16	8.56E-20
33.0	18.0	9.47500E-16	8.51E-20
33.0	20.0	9.73310E-16	7.75E-20
33.0	30.0	1.01131E-15	1.42E-20
33.0	40.0	1.01266E-15	4.37E-22
33.0	50.0	1.01267E-15	1.73E-22
33.0	60.0	1.01267E-15	1.91E-22
33.0	70.0	1.01267E-15	2.01E-22
33.0	80.0	1.01267E-15	2.80E-22
33.0	90.0	1.01267E-15	3.66E-22
34.0	1.0	2.98635E-17	2.91E-23
34.0	2.0	5.94285E-17	2.25E-22
34.0	3.0	8.84046E-17	7.24E-22
34.0	4.0	1.16519E-16	1.67E-21
34.0	5.0	1.43521E-16	3.10E-21
34.0	6.0	1.69192E-16	5.06E-21
34.0	7.0	1.93348E-16	7.52E-21
34.0	8.0	2.15844E-16	1.04E-20
34.0	9.0	2.36575E-16	1.36E-20
34.0	10.0	2.55478E-16	1.69E-20
34.0	12.0	2.87742E-16	2.32E-20
34.0	14.0	3.12878E-16	2.80E-20
34.0	16.0	3.31586E-16	3.03E-20
34.0	18.0	3.44866E-16	2.98E-20
34.0	20.0	3.53832E-16	2.68E-20
34.0	30.0	3.66643E-16	4.48E-21
34.0	40.0	3.67058E-16	1.18E-22
34.0	50.0	3.67059E-16	4.97E-23
34.0	60.0	3.67061E-16	8.63E-23
34.0	70.0	3.67061E-16	1.07E-22
34.0	80.0	3.67060E-16	1.02E-22
34.0	90.0	3.67060E-16	8.89E-23

MODIFIED SECANT INTEGRAL

X	ANGLE	MSECI VALUE	ERROR
35.0	1.0	1.09856E-17	1.05E-23
35.0	2.0	2.18580E-17	8.24E-23
35.0	3.0	3.25075E-17	2.66E-22
35.0	4.0	4.28307E-17	6.11E-22
35.0	5.0	5.27336E-17	1.14E-21
35.0	6.0	6.21338E-17	1.85E-21
35.0	7.0	7.09631E-17	2.75E-21
35.0	8.0	7.91675E-17	3.78E-21
35.0	9.0	8.67098E-17	4.93E-21
35.0	10.0	9.35679E-17	6.11E-21
35.0	12.0	1.05218E-16	8.33E-21
35.0	14.0	1.14226E-16	9.98E-21
35.0	16.0	1.20871E-16	1.07E-20
35.0	18.0	1.25539E-16	1.04E-20
35.0	20.0	1.28655E-16	9.23E-21
35.0	30.0	1.32976E-16	1.41E-21
35.0	40.0	1.33103E-16	2.91E-23
35.0	50.0	1.33104E-16	1.26E-23
35.0	60.0	1.33105E-16	2.19E-23
35.0	70.0	1.33105E-16	2.94E-23
35.0	80.0	1.33105E-16	2.45E-23
35.0	90.0	1.33104E-16	2.55E-23
36.0	1.0	4.04116E-18	3.77E-24
36.0	2.0	8.03948E-18	3.01E-23
36.0	3.0	1.19534E-17	9.73E-23
36.0	4.0	1.57440E-17	2.24E-22
36.0	5.0	1.93757E-17	4.16E-22
36.0	6.0	2.28179E-17	6.77E-22
36.0	7.0	2.60451E-17	1.00E-21
36.0	8.0	2.90373E-17	1.38E-21
36.0	9.0	3.17813E-17	1.79E-21
36.0	10.0	3.42694E-17	2.21E-21
36.0	12.0	3.84761E-17	3.00E-21
36.0	14.0	4.17044E-17	3.56E-21
36.0	16.0	4.40649E-17	3.78E-21
36.0	18.0	4.57060E-17	3.63E-21
36.0	20.0	4.67884E-17	3.18E-21
36.0	30.0	4.82469E-17	4.47E-22
36.0	40.0	4.82861E-17	1.29E-23
36.0	50.0	4.82861E-17	6.54E-24
36.0	60.0	4.82862E-17	9.80E-24
36.0	70.0	4.82862E-17	8.99E-24
36.0	80.0	4.82862E-17	1.03E-23
36.0	90.0	4.82862E-17	1.50E-23

MODIFIED SECANT INTEGRAL

X	ANGLE	MSECI VALUE	ERROR
37.0	1.0	1.48659E-18	1.46E-24
37.0	2.0	2.95697E-18	1.12E-23
37.0	3.0	4.39545E-18	3.61E-23
37.0	4.0	5.78731E-18	8.25E-23
37.0	5.0	7.11924E-18	1.53E-22
37.0	6.0	8.37970E-18	2.48E-22
37.0	7.0	9.55924E-18	3.66E-22
37.0	8.0	1.06506E-17	5.03E-22
37.0	9.0	1.16489E-17	6.51E-22
37.0	10.0	1.25516E-17	8.02E-22
37.0	12.0	1.40706E-17	1.08E-21
37.0	14.0	1.52276E-17	1.27E-21
37.0	16.0	1.60660E-17	1.34E-21
37.0	18.0	1.66430E-17	1.27E-21
37.0	20.0	1.70190E-17	1.10E-21
37.0	30.0	1.75113E-17	1.41E-22
37.0	40.0	1.75233E-17	3.43E-24
37.0	50.0	1.75234E-17	2.29E-24
37.0	60.0	1.75234E-17	2.78E-24
37.0	70.0	1.75234E-17	4.25E-24
37.0	80.0	1.75234E-17	4.90E-24
37.0	90.0	1.75234E-17	4.74E-24
38.0	1.0	5.46857E-19	5.25E-25
38.0	2.0	1.08759E-18	3.97E-24
38.0	3.0	1.61626E-18	1.32E-23
38.0	4.0	2.12734E-18	3.02E-23
38.0	5.0	2.61580E-18	5.58E-23
38.0	6.0	3.07736E-18	9.07E-23
38.0	7.0	3.50848E-18	1.34E-22
38.0	8.0	3.90654E-18	1.83E-22
38.0	9.0	4.26974E-18	2.36E-22
38.0	10.0	4.59724E-18	2.90E-22
38.0	12.0	5.14573E-18	3.88E-22
38.0	14.0	5.56038E-18	4.53E-22
38.0	16.0	5.85819E-18	4.72E-22
38.0	18.0	6.06101E-18	4.43E-22
38.0	20.0	6.19166E-18	3.79E-22
38.0	30.0	6.35792E-18	4.41E-23
38.0	40.0	6.36164E-18	1.14E-24
38.0	50.0	6.36166E-18	7.15E-25
38.0	60.0	6.36168E-18	1.35E-24
38.0	70.0	6.36166E-18	1.09E-24
38.0	80.0	6.36167E-18	2.30E-24
38.0	90.0	6.36165E-18	1.57E-24

MODIFIED SECANT INTEGRAL

X	ANGLE	MSECI VALUE	ERROR
39.0	1.0	2.01167E-19	1.87E-25
39.0	2.0	4.00019E-19	1.45E-24
39.0	3.0	5.94320E-19	4.84E-24
39.0	4.0	7.81980E-19	1.11E-23
39.0	5.0	9.61123E-19	2.05E-23
39.0	6.0	1.13014E-18	3.32E-23
39.0	7.0	1.28771E-18	4.88E-23
39.0	8.0	1.43289E-18	6.67E-23
39.0	9.0	1.56503E-18	8.58E-23
39.0	10.0	1.68385E-18	1.05E-22
39.0	12.0	1.88191E-18	1.40E-22
39.0	14.0	2.03050E-18	1.62E-22
39.0	16.0	2.13630E-18	1.67E-22
39.0	18.0	2.20761E-18	1.55E-22
39.0	20.0	2.25300E-18	1.31E-22
39.0	30.0	2.30918E-18	1.41E-23
39.0	40.0	2.31031E-18	4.19E-25
39.0	50.0	2.31032E-18	4.70E-25
39.0	60.0	2.31032E-18	5.82E-25
39.0	70.0	2.31032E-18	6.43E-25
39.0	80.0	2.31032E-18	6.64E-25
39.0	90.0	2.31032E-18	8.58E-25
40.0	1.0	7.40016E-20	7.34E-26
40.0	2.0	1.47130E-19	5.46E-25
40.0	3.0	2.18541E-19	1.79E-24
40.0	4.0	2.87448E-19	4.07E-24
40.0	5.0	3.53147E-19	7.52E-24
40.0	6.0	4.15036E-19	1.22E-23
40.0	7.0	4.72633E-19	1.78E-23
40.0	8.0	5.25582E-19	2.43E-23
40.0	9.0	5.73657E-19	3.12E-23
40.0	10.0	6.16765E-19	3.81E-23
40.0	12.0	6.88282E-19	5.02E-23
40.0	14.0	7.41538E-19	5.77E-23
40.0	16.0	7.79115E-19	5.89E-23
40.0	18.0	8.04184E-19	5.42E-23
40.0	20.0	8.19953E-19	4.51E-23
40.0	30.0	8.38939E-19	4.42E-24
40.0	40.0	8.39290E-19	1.35E-25
40.0	50.0	8.39294E-19	1.74E-25
40.0	60.0	8.39292E-19	1.66E-25
40.0	70.0	8.39291E-19	1.49E-25
40.0	80.0	8.39293E-19	2.43E-25
40.0	90.0	8.39292E-19	2.25E-25